SCHOOL *of*
GRADUATE STUDIES
EAST TENNESSEE STATE UNIVERSITY

Electronic Theses and Dissertations   Student Works

8-2022

Validation of the 40 Hz Auditory Steady State Response as a Pharmacodynamic Biomarker of Evoked Neural Synchrony

Muhammad Ummear Raza
East Tennessee State University

Follow this and additional works at: https://dc.etsu.edu/etd

Part of the Pharmacology Commons, and the Systems Neuroscience Commons

Recommended Citation

Validation of the 40 Hz Auditory Steady State Response as a Pharmacodynamic Biomarker of
Evoked Neural Synchrony

_____

A dissertation

presented to

the faculty of the Department of Biomedical Sciences

East Tennessee State University

In partial fulfillment

of the requirements for the degree

Doctor of Philosophy in Biomedical Sciences, Pharmacology Concentration

_____

by

Muhammad Ummear Raza

August 2022

_____

Dr. Siva Digavalli, Chair

Dr. Brooks Pond

Dr. David Roane

Dr. Gregory Ordway

Dr. Russell Brown

Keywords: Schizophrenia, Gamma oscillation, 40 Hz ASSR, NMDA, MK-801, Clozapine,
Neural Synchrony, Event Related, E/I, Pharmacodynamic Biomarker

ABSTRACT

Validation of the 40 Hz Auditory Steady State Response as a Pharmacodynamic Biomarker of

Evoked Neural Synchrony

by

Muhammad Ummear Raza

Schizophrenia is a troubling and severe mental illness that is only incompletely treated by

currently available drugs. New drug development is hindered by a scarcity of functionally

relevant pharmacodynamic biomarkers that are translatable across preclinical and human

subjects. Although psychosis is a major feature of schizophrenia, cognitive and negative

symptoms determine the long-term functional outcomes for patients. Stimulus-evoked neural

synchrony at gamma (~ 40 Hz) frequency plays an important role in the processing and

integration of sensory information. Not surprisingly, schizophrenia patients show deficits in

gamma oscillations. NMDA receptor (NMDAR) activation on fast-spiking parvalbumin-positive

interneurons is deemed important for the generation of gamma oscillations. NMDA hypofunction

has been proposed as an alternative hypothesis to the well-known dopamine dysregulation to

explain the neurochemical abnormalities associated with schizophrenia. For this dissertation, we

validated a preclinical model to pharmacologically probe NMDA-mediated gamma oscillations

by further characterizing the auditory-steady state response (ASSR) in female Sprague Dawley

rats. The ASSR is a measure of cortical neural synchrony evoked in response to periodic auditory

stimuli. ASSR at 40 Hz is consistently disrupted in patients. First, we established the reliability

of click train-evoked 40 Hz ASSR and tone-evoked gamma oscillations in 6 separate sessions,

spread over a 3-week period. Then we established the sensitivity of these neural synchrony

measures to acute NMDAR blockade using the high affinity NMDA channel blocker MK-801,

2

using a repeated measures design. Next, we compared the reliability and sensitivity of the 40 Hz ASSR from two distinct recording sites. Results from this study showed that as compared to vertex, temporal recording showed a greater gamma synchrony. However, the temporal recording had poor test-retest reliability and lower sensitivity to MK-801-induced disruption. Lastly, we characterized the dose-response profiles of an NMDA co-agonist D-serine, an atypical (clozapine) and a typical (haloperidol) antipsychotic, on the 40 Hz ASSR. Results from these studies showed that only clozapine was effective in robustly augmenting 40 Hz ASSR. Furthermore, only clozapine pretreatment had partial protective effect against MK-801 induced ASSR disruption. Overall, this work establishes that vertex recorded 40 Hz ASSR is a reliable neural synchrony biomarker in female SD rats that is amenable for *bidirectional* pharmacodynamic modulation.

DEDICATION

I would like to dedicate this dissertation to my younger brothers, Usman, and Noman Raza. They have always been a source of joy for me. I want to let you know that I always love you and miss you. I would also like to dedicate this dissertation to my parents for their love and support. Finally, I would like to dedicate this dissertation to myself for believing in me and staying consistent, and optimistic even in stressful situations.

ACKNOWLEDGEMENTS

First, I would like to acknowledge my dissertation advisor: Dr. Siva Digavalli. He took me under his supervision during an uncertain time in my PhD. He gave me a chance to learn and explore in a field I had no experience at all. He has been a true mentor to me during all these years. I want to let you know that your support has meant a lot to me, and I will remember your kindness for the rest of my life.

I would also like to thank my committee members, Dr. Brooks Pond, Dr. Gregory Ordway, Dr. David Roane, and Dr. Russell Brown for all their support and valuable input for my dissertation research. Additionally, I would also like to thank Dr. Hanley, Jennie, Marie, Antoinette, Priscilla, Robin, especially, and everyone else involved in DLAR. Moreover, I would like to thank Dr. Lana Cook in the Biomedical Sciences PhD program for her help.

This work was supported by funding from Bill Gatton College of Pharmacy, and a PhD dissertation award from the East Tennessee State University.

TABLE OF CONTENTS

9

LIST OF TABLES

LIST OF FIGURES

ABBREVIATIONS

5-HT	5-hydroxytryptamine/Serotonin
ABR	Auditory Brainstem Response
AER	Auditory-Evoked Response
ANOVA	Analysis of Variance
AP	Anterior-Posterior
ASSR	Auditory Steady-State Response
BIS	Bispectral Index
CR	Concordance Rate
CSPP	Limbic cortex, Striatum, Peduncle, Pontine tegmentum
CV	Coefficient of Variation
DSM	Diagnostic and Statistical Manual of Mental Disorders
DV	Dorsal-Ventral
EEG	Electroencephalography
EMG	Electromyography
ERP	Event Related Potential
FS	Fast Spiking
GABA	Gamma-Aminobutyric Acid
GMS	Glycine Modulatory Site
GWAS	Genome Wide Association Studies
ICC	Intraclass Correlation Coefficient
ICD	International Statistical Classification of Diseases
IIR	Infinite Impulse Response
ING	Interneuron Network Mediated Gamma
ISI	Inter-Stimulus Interval
ITC	Inter-Trail Coherence
ITI	Inter-Trial Interval
LFP	Local Field Potential

LLR	Late Latency Response
LORETA	Low-Resolution Electromagnetic Tomography Analysis
LPS	Lipopolysaccharide
MAM	Methylazoxymethanol Acetate
MEG	Magnetoencephalography
MGB	Medial Geniculate Body
ML	Medial-Lateral
MLR	Middle Latency Response
MMN	Mismatch Negativity
NMDA	N-Methyl-D-Aspartate
PCP	Phencyclidine
PFC	Prefrontal Cortex
PING	Pyramidal-interneuron Network Mediated Gamma
PPI	Prepulse Inhibition
PV	Parvalbumin
RMS	Root Mean Square
SC	Subcutaneous
SD	Sprague Dawley
SEM	The Standard Error of the Mean
SER	Stimulus-Evoked Response
SN	Substantia Nigra
SSR	Steady-State Response
TFA	Time Frequency Response
VTA	Ventral Tegmental Area

Overview

Schizophrenia is a debilitating psychiatric illness affecting nearly 1% of the world population (Ropper et al. 2019). People with schizophrenia experience distorted reality, altered perception, blunted sensory and emotional experiences, and exhibit poor social skills. In clinical parlance, patient experiences such as hallucinations, delusions, disorganized thinking, and speech are referred to as positive symptoms, while inability to experience normal emotions coupled with a flattened affect are referred to as negative symptoms. Social and/or neurocognitive deficits constitute the third core feature of this disease.

In 1911, Eugen Bleuler, a Swiss psychiatrist, coined the term schizophrenia (Bleuler 1911; Moskowitz and Heim 2011), which consists of two Greek words skhizein (to split) and phrēn (mind), referring to the fragmentation of psychological functioning that he observed in patients (Fusar-Poli and Politi 2008). Earlier, a German psychiatrist, Emil Kraepelin had described a distinct psychotic condition, different from other forms of psychosis, and named it "dementia praecox" (Kraepelin 1899; Falkai et al. 2015), which Bleuler challenged by calling it neither dementia, nor something precocious. The pioneering works of Kraeplin and, especially Bleuler, presented for the first time a diagnosis of mental illnesses based on psychology, which later influenced the symptoms-based classification of psychiatric disorders leading to the 1st edition of the Diagnostic and Statistical Manual of Mental Disorders (DSM-I) (Andreasen 1989).

Even after more than 100 years of treatment and research related to schizophrenia, diagnosis is still based on symptoms as defined in the latest edition of DSM (DSM-V) (American Psychiatric Association 2013). Pharmacotherapy involves the use of antipsychotics that show

partial efficacy against positive symptoms and fail to improve negative and cognitive symptoms to any substantive extent (Murphy et al. 2006; Tandon et al. 2009; Tandon et al. 2010). Moreover, most of the currently used antipsychotics fail to work in a significant fraction of patients (classified as treatment-resistant) and are associated with serious side effects (Miyamoto et al. 2012).

Unfortunately, there is no comprehensive understanding about the pathophysiology of schizophrenia. There is, however, a growing understanding that schizophrenia may be a neurodevelopmental disorder shaped by genetic and environmental factors (Lewis and Levitt 2002; Demjaha et al. 2012; Wahbeh and Avramopoulos 2021).

At present, there is a lack of objective biomarkers that can inform diagnosis or establish treatment efficacy (Weickert et al. 2013; García-Gutiérrez et al. 2020). In the last few decades, there has been a trend towards characterizing schizophrenia-associated neural processes for the development of reliable biomarkers, an approach to transition away from a symptoms-based heuristic. There is an expectation that the development of neural-based biomarkers will lead to a more specific targeting of biological abnormalities underlying schizophrenia (Abi-Dargham and Horga 2016; Light et al. 2020), leading to a more rational understanding and treatment of the disease. Additionally, disease-relevant neural circuit performance-based measures are critical for new drug development as they can highlight a particular abnormality objectively and attempt to correct it through pharmacological or other types of interventions.

Historically, a major focus of schizophrenia research has been to manage psychotic symptoms because of their overt and aversive nature, while the negative and cognitive symptoms have not been a center of attention. Yet, it is now widely accepted that both negative and

cognitive symptoms have a more profound bearing on long-term patient outcomes, such as how well they are able to be a part of a community and function with a degree of independence (Harvey et al. 2006; Yang et al. 2021). Availability of validated neural circuit function biomarkers that impact these hitherto neglected symptom domains may lead to the development of new and improved therapies (Spellman and Gordon 2015). More specifically, to address the negative and cognitive symptoms of schizophrenia that directly determine the overall functional outcomes of treatment (Fett et al. 2011; Green and Plaza 2016; Z. Yang et al. 2021).

Schizophrenia Symptoms

As outlined above, schizophrenia represents a complex mental illness exhibiting a spectrum of symptoms that are classified into three major domains, positive, negative, and cognitive. Positive symptoms refer to the most apparent mental dysfunction such as hallucinations (a tendency to misattribute perceptual experiences to the outside environment), and delusions, or strongly held beliefs that are not based in reality. Negative symptoms involve apathy/avolition (lack of motivation), anhedonia (inability to feel pleasure), social withdrawal, and flattened affect. Cognitive symptoms involve an inability to pay attention, disorganized thoughts (thought disorder), limited verbal fluency, and poor short/long term memory (Andreasen 1995; van Os and Kapur 2009; Ropper et al. 2019). The onset of the first episode of psychosis often happens between early adolescence to young adulthood, typically, with an earlier onset in males than in females (Ochoa et al. 2012). Around 75% of the individuals go through a prodromal phase and present psychotic symptoms at a subthreshold level for up to 1 year (Häfner et al. 2003; Sørensen et al. 2009), before they suffer an acute episode leading to a hospital admission and diagnosis. A significant body of data now indicates that cognitive symptoms

precede psychosis and represent a core feature of the disease (Kahn and Keefe 2013; Üçok et al. 2013; McCleery and Nuechterlein 2019). Moreover, psychotic symptoms flare up as acute episodes and subside, while negative and cognitive symptoms persist throughout the duration of the illness (Harvey et al. 2006).

Etiology

Genetic Factors

As stated earlier, both genetic and environmental factors contribute to the etiology of schizophrenia. Even though the rate of incidence is approximately 1% in the general population, the probability of occurrence of schizophrenia in a first-degree relative of a patient is 8-fold higher. This goes up to 11-fold, if two first-degree relatives are affected (Le et al. 2020). If one monozygotic twin develops schizophrenia, the other has a 50% overall likelihood of developing the same (an incidence rate of 41-65 %, measured as concordance rate), while in fraternal twins, this incidence can range between 0-28 %. Moreover, monozygotic twin studies report a genetic heritability for schizophrenia of up to 80-85% (i.e., genetic contribution explains 80% of the 50% overall likelihood) (Cardno and Gottesman 2000; Sullivan et al. 2003).

While epidemiological studies show a strong genetic component, no single allele/locus is known to markedly increase susceptibility. Genome-wide association studies (GWAS) have resulted in more than 100 loci associated with schizophrenia, with each locus having a minor contribution, thus further reinforcing the multifactorial and complex etiology of schizophrenia (Dennison et al. 2020). The only exception, however, is 22q11.2 deletion syndrome, which causes a ~25-fold increase in the risk of developing schizophrenia. That is, approximately 25%

of the individuals with the deletion ultimately develop schizophrenia symptoms (Cleynen et al. 2020). Other than genetic, environmental influence accounts for about 10-20% risk for schizophrenia (Cardno and Gottesman 2000), thus suggesting an important role for environment-mediation during perinatal development. Different environmental factors that have shown to be associated with schizophrenia include, but not limited to, obstetric complications (Cannon et al. 2002), prenatal infections (Cheslack-Postava and Brown 2021), adverse childhood experiences (Varese et al. 2012), migration (Henssler et al. 2020), and cannabis use (Wainberg et al. 2021).

Neurodevelopmental Factors

Both genetic and environmental factors may contribute to cause aberrant brain development. A meta-analysis of the neuroimaging data obtained from more than 5000 healthy controls and 4000 schizophrenia patients showed a significant reduction in the thickness and surface area of the temporal and frontal lobes in patients (van Erp et al. 2018). In the normally developing brain, there is a constant process of balanced synaptic growth and pruning. Through the first few decades of life, the white matter representing myelinated axons increases in volume, while there is a general reduction in gray matter representing the pruning of the dendritic processes and neuropil.

Another important aspect of normal development is the gradual increase in inhibitory synapses, that prevent runaway excitation in the cortical circuits and help maintain an optimal excitatory/inhibitory (E/I) balance. One theory posits that abnormal neurodevelopmental processes during childhood involving excessive pruning and a significant reduction in the number inhibitory synapses may result in the emergence of schizophrenia in adolescence (van Erp et al. 2018). Several genes associated with schizophrenia as reported by genome-wide

association studies (GWAS) play an important developmental role; for example, genes such as dysregulated in schizophrenia 1 (DISC1), neuregulin 1 (NRG1), and its receptor ErbB4 (ERBB4), dysbindin (DNTBP1), and reelin (RELN) are integral to synaptogenesis and plasticity (Harrison and Weinberger 2005) and get highlighted as variants in schizophrenia patients. Early exposure to environmental factors like stress and certain drugs can exacerbate the sensitivity of aberrant circuits to certain neurotransmitters, biasing towards psychosis (Niemelä et al. 2016; Popovic et al. 2019). Thus, it is thought that genetic and environmental factors interact to increase the susceptibility to schizophrenia by skewing a normal neurodevelopmental trajectory towards illness.

Neurochemical

On the other hand, the neurochemical imbalance hypothesis offers an explanation where regional alterations in key neurotransmitters' activity is implicated in the manifestation of schizophrenia symptoms, as proximate cause.

The dopamine hypothesis. Dopamine is one of the key neurotransmitters in the brain that regulate important behaviors like reward, motivation, executive function, and motor control (Robbins and Arnsten 2009; Bromberg-Martin et al. 2010). It is synthesized in the substantia nigra (SN) and ventral tegmental area (VTA) of the brain. Dopaminergic neurons from these two areas project to diverse brain regions principally through nigrostriatal, mesolimbic, and mesocortical projections. The dopamine hypothesis suggests that the positive symptoms arise due to dopamine *hyperactivity in the mesolimbic pathway*, while negative and cognitive symptoms arise due to *hypoactivity of dopamine in the mesocortical pathway* (Fabiana et al. 2008).

The dopamine hypothesis originated after the discovery of dopamine as a neurotransmitter by Arvid Carlsson in 1958 (Carlsson et al. 1958). Subsequently, Carlsson's group reported that the prototypical antipsychotics, chlorpromazine and haloperidol, block the dopamine (D2) receptors, a critical milestone in formulating the dopamine hypothesis (Carlsson and Lindqvist 1963). Subsequent studies established a correlation between the clinical efficacy of all the available antipsychotics to their D2 receptor binding (Creese et al. 1976; Seeman et al. 1976). Indeed, D2 receptor affinity and blockade of the D2 receptors at therapeutic concentrations is the most parsimonious explanation for the efficacy of all the clinically effective antipsychotic drugs to date. Moreover, dopamine-releasing drugs like amphetamine were shown to induce psychotomimetic effects in humans and primates (Bell 1973; Ellison et al. 1981), strengthening further the evidence for this hypothesis.

Further support comes from studies showing that schizophrenia patients show dopamine dysregulation in the mesolimbic and mesocortical areas (Perez-Costas et al. 2010; Lodge and Grace 2011; Yoon et al. 2013). While postmortem histopathological studies and antemortem neuroimaging studies have reported contradicting results regarding the density of dopamine receptors in schizophrenia patients (Farde et al. 1987; Lahti et al. 1996; Seeman et al. 1997; Seeman and Kapur 2000), imaging analyses of drug-naïve schizophrenia patients consistently show striatal dopaminergic hyperactivity (Abi-Dargham et al. 2000; Patel et al. 2010).

Notwithstanding the evidence summarized above, antipsychotics that block D2 receptors and blunt subcortical hyperdopaminergia, are only partially effective against schizophrenia symptoms (Gründer and Cumming 2016). One of the reasons for this is that dopamine dysregulation is not pathognomonic as schizophrenia patients show neurochemical heterogeneity. That is, imbalance may be noted with several neurotransmitters, not just dopamine

20

(Yang and Tsai 2017). This is further supported by the fact that one of the most effective antipsychotics, clozapine (or atypical antipsychotics in general), shows a relatively low affinity for D2 receptors (Seeman et al. 1997). Thus, there is a reason to explore other neurotransmitter systems that may be equally important in causing schizophrenia pathophysiology, one of which is glutamate (Kristiansen et al. 2007; Bubenikova-Valesova et al. 2008; Balu 2016).

The glutamate hypothesis. In the late 1950s and 60s, it was observed that certain drugs like phencyclidine (PCP) can induce schizophrenia-like symptoms in chronic users and aggravate schizophrenia symptoms in patients (Luby et al. 1959; Davies and Beech 1960; Cohen et al. 1962; Itil et al. 1967). PCP disrupts glutamate neurotransmission by blocking N-methyl-D-aspartate receptors (NMDAR). According to the glutamate hypothesis, NMDAR hypofunction leads to a disruption of glutamate signaling and results in schizophrenia symptoms. Non-competitive NMDAR inhibitors like PCP and ketamine not only induce positive symptoms but also negative and cognitive symptoms, which implicate glutamate transmission in phenotypes resistant to D2-based antipsychotics (Snyder 1980; Javitt and Zukin 1991; Carter et al. 1997). The NMDAR hypofunction also reconciles the dopaminergic dysregulation outlined above. For example, NMDAR dependent cortical activity inhibits dopamine release in the limbic regions while promoting its release in the cortical areas (Schwartz et al. 2012). Therefore, a reduced NMDAR tone in the cortical circuits has a disinhibitory effect on the dopamine neurotransmission in the mesolimbic circuit (*hyperdopaminergia*), and a net inhibition on the dopamine release in the mesocortical pathway (*hypodopaminergia*). Thus, according to the glutamate hypothesis of schizophrenia, the dopamine dysregulation is *secondary* to NMDAR hypofunction.

Postmortem examination of the dorsolateral prefrontal cortex region of the brain from schizophrenia patients has noted a reduced density of NR1 subunit, an obligatory component of the NMDAR channel (Vibeke et al. 2015; Vibeke et al. 2016). This evidence for reduced NMDA-dependent glutamate signaling was shown to correlate with cognitive deficits (Weickert et al. 2012). However, it must be noted that some studies have found no change or increased expression of NMDAR in the nucleus accumbens and dorsolateral prefrontal cortex, respectively, suggesting a brain region-specific alteration of glutamate signaling (Dracheva et al. 2001; Lum et al. 2018). The increase in NMDAR may be an adaptation secondary to reduced glutamate release. Indeed, genetic analysis has shown an association of single nucleotide polymorphisms (SNPs) in many genes associated with glutamate signaling (Kirov et al. 2011; Weickert et al. 2012; Fromer et al. 2014). These findings support an etiological role for region-specific dysregulation of NMDAR transmission in schizophrenia.

Even though NMDARs are expressed on both pyramidal and GABAergic interneurons, NMDAR antagonists at low concentrations seem to preferentially affect GABAergic interneurons, especially the parvalbumin (PV; a calcium-binding protein) expressing subtype (Lewis and Moghaddam 2006). This may be because the interneurons receive a higher number of glutamatergic inputs as compared to any other type. Furthermore, PV+ neurons show higher baseline activity and a relatively more depolarized membrane potential, as compared to pyramidal neurons. Thus, making them prone to the removal of Mg^{2+} "plug" from the NMDA channel pore, and therefore more susceptible to NMDA open channel blockers like MK801 (Lewis and Moghaddam 2006). Preferential inhibition of NMDAR on the GABAergic neurons, by NMDAR antagonists reduces inhibitory control or disinhibits the excitatory pyramidal neurons, leading to hyperexcitation of the cortical circuits and an increase in the E/I ratio

(Homayoun and Moghaddam 2007; Cohen et al. 2015; Zorumski et al. 2016). Modeling studies have illustrated how an overall increase in E/I ratio results in localized circuit dysfunction and an inability to integrate context-specific cues (Calvin and Redish 2021). In summary, according to the NMDAR hypofunction hypothesis, poor NMDA-based GABAergic activation leads to disinhibition of the pyramidal neurons and skews the E/I balance towards an increase resulting in disruption of cortical processing and schizophrenia symptoms.

Animal Models Of Schizophrenia

The development of suitable animal models for schizophrenia is essential to improve our current understanding of schizophrenia pathophysiology, as well as to enable novel drug development. Thoughtfully developed animal models can provide valuable information about the molecular, structural, and electrophysiological abnormalities relevant to schizophrenia leading to the identification of new drug targets and candidates. However, the development of animal models for schizophrenia also poses challenges due to the following reasons. 1. Schizophrenia is heterogeneous (i.e., clinical symptoms are diverse, genetic/epigenetic influences are manifold, and disease progression is uneven), and a complex (i.e., overlapping symptoms with other psychiatric conditions, significant comorbidities, many subtypes included under the same definition) human mental condition. 2. There is an incomplete understanding of the underlying neurobiological abnormalities (Powell and Miyakawa 2006).

A neurobiological approach to psychiatric conditions suggests that these are a result of a dysfunctional network response. Disrupted neural systems affect both human and animal behavior and share cross-species homology that may not be the case with overt behavior or symptoms. Thus, animal models may be developed that can mimic network dysfunction similar

23

to schizophrenia, even if they do not replicate the same symptoms or behavior. The human relevance of these animal models can be addressed through a validity analysis.

Three important types of validity are construct, predictive and face. The soundness of theoretical rationale for the interventions in animal models, which should be human disease-relevant, is addressed by construct validity. Predictive validity is concerned with how well the outcomes after intervention in animal models predict similar outcomes in human disease. Whereas face validity assesses the replication of biophysical and behavioral features of human disease in animal models (Marcotte et al. 2001; Jones et al. 2011). While modeling symptoms or behavior in animals, face validity may present a remarkable challenge vis-a-vis schizophrenia and other psychiatric diseases as well. For example, replication of cognitive symptoms in less cognitively developed animals, limits face validity. Similarly, animal models of depression like the forced swim test and tail suspension test have been criticized for questionable face validity (Cryan and Mombereau 2004; Slattery and Cryan 2014). On the other hand, certain elementary psychophysiological (e.g., startle) or neurophysiological responses (sensory gating) seen across species and believed to underlie a feeling of "sensory information overload" in patients, may be well suited for cross-species translation, especially if they have pathophysiological relevance (Swerdlow et al. 2008).

Animal models of schizophrenia have been created through genetic, pharmacological, physical, and neurodevelopmental interventions. As described previously, monozygotic twin studies show up to 80-85% heritability for schizophrenia, suggesting a strong genetic contribution (Cardno and Gottesman 2000). However, there are very few disease-associated alleles with high penetrance enough to cause illness in a predictive manner. GWAS have revealed several genes that interact to influence glutamatergic and dopaminergic pathways, as

well as affect processes like synaptogenesis, immune modulation, intracellular signaling, and neural plasticity. Some of the more common alleles include DAT, NR1, DISC1, NRG, ERBB4, DNTBP1, and RELN (Jones et al. 2011). Phospholipase C-β1 (PLC-β1) disruption is another genetic approach used in rodents to mimic schizophrenia-like phenotypes (Kim et al. 2015).

Neurodevelopmental disruption using physical, pharmacological, and behavioral interventions in rodents undergoing perinatal development has been an important approach for developing animal models. Behavioral interventions include causing maternal separation-related distress in neonates or their post-weaning social isolation (Jones et al. 2011). Developmental interventions that use neurotoxicants involve the injection of methylazoxymethanol acetate (MAM), an antimitotic agent, or the bacterial endotoxin lipopolysaccharide (LPS), or relatively large doses of the NMDA antagonists, administered to pregnant dams (du Bois and Huang 2007; Bubeníková-Valešová 2008; Lim et al. 2012). MAM specifically targets the neuroblast proliferation and migration in the CNS, which leads to anatomical and behavioral deficits (Jones et al. 2011). LPS induces immune activation in the maternal circulatory system that affects brain development. There is some evidence that maternal infection during pregnancy can be a risk factor for schizophrenia in the offspring (Brown and Derkits 2010; Brown 2011). Perinatal administration of quinpirole, a dopaminergic D2 agonist, has been reported to result in long-lasting D2 receptor sensitization and associated behaviors reminiscent of schizophrenia (Kostrzewa et al. 2016). Other models involve administering relatively large doses of NMDA antagonists to neonates during early development (e.g., postnatal days 7-15) (Plataki et al. 2021).

Acute pharmacological interventions rely on blocking glutamatergic transmission acutely through modest doses of the NMDAR antagonists like PCP, MK801, or ketamine. Other pharmacological models involve using dopamine agonists like amphetamine (Featherstone et al.

2008; Steeds et al. 2015). However, the amphetamine model has been criticized for its incompleteness as amphetamine-induced psychosis mimics the positive symptoms characteristic of schizophrenia, but not negative and cognitive symptoms (McCutcheon et al. 2020), a shortcoming not associated with acute NMDA antagonism, which replicates all three characteristic symptom domains (Krystal et al. 1994). Nearly all the above-reviewed approaches result in behavioral phenotypes that have some phenotypic relevance to schizophrenia and therefore have translational value (Steeds et al. 2015).

Biomarkers In Schizophrenia Research

A biomarker is "a defined characteristic that is measured as an indicator of normal biological processes, pathogenic processes, or biological responses to an exposure or intervention, including therapeutic interventions" (FDA-NIH Biomarker Working Group 2016). The biomarker working group excluded individual feeling, function, or survival from the definition of a biomarker. However, a biomarker can include "molecular, histologic, radiographic, or physiologic characteristics" (FDA-NIH Biomarker Working Group 2016). As described earlier, diagnosis of schizophrenia relies on either DSM-V or International Statistical Classification of Diseases and Related Health Problems, Eleventh Edition (ICD-11).

As mentioned earlier, schizophrenia presents a challenge for diagnosis, treatment, and drug development due to reliance on a symptoms-based approach and lack of etiological information underlying the disease. This is further complicated by the heterogeneous nature of the disease. Schizophrenia patients show a large degree of overlap in symptoms with patients of other mental illnesses and suffer with significant comorbidities (Buckley et al. 2009). These factors complicate diagnosis and pose a challenge to effective treatment development. There is a

need for biomarkers-based approach that can provide pathophysiological insight, can help in diagnosis, and in stratifying individuals based on the underlying pathophysiology for targeted treatment options.

Additionally, biomarkers are invaluable as critical goalposts to guide new drug development. They are needed for confirming target engagement, proof of concept studies as well as for dose selection during preclinical lead evaluation as well as during early-stage clinical development. *These drug development-related applications are the ones that are most pertinent to the current dissertation*.

Owing to the complex and heterogeneous nature of schizophrenia, individual schizophrenia symptoms are isolated and modeled in animals as simple, quantifiable, and singular behavioral measures. For example, hyperlocomotion in animals is proposed to replicate the condition of psychosis in humans, a reflection of the hyperdopaminergia in the mesolimbic circuit (Jones et al. 2011). Moreover, a subset of acutely ill patients does exhibit psychomotor agitation and stereotypy, justifying the use of hyperlocomotion as a behavioral measure (Powel and Miyakawa 2006). Sucrose preference is used to model negative symptoms like anhedonia (Muscat and Willner 1989), whereas tests of social interaction are used to model social withdrawal (Sams-Dodd 1998). Animal models are tested for working memory tasks or attention for cognitive deficit evaluation. Although the above behavioral measures are proposed to represent objective, quantifiable features replicating individual schizophrenia symptoms in animal models, it is unclear how well they represent these symptoms. For example, a lack of preference for a sweet treat is unlikely to be a specific, dependable, and accurate indicator of anhedonia. Besides, there are many confounding factors that can affect these measures, which

27

should be carefully controlled. For example, hyperlocomotion may have a non-specific effect on sucrose preference expression or a working memory performance.

More recently, there has been increased attention to develop and test schizophrenia-associated endophenotype responses, as an intermediate between a behavioral phenotype (disease symptom) and the underlying putative genotype and its cellular biochemical expression. An endophenotype is a hidden feature that is responsive to, and discoverable by testing. It is a quantitative measure of a heritable biological trait. It is stable and shows a close association to the underlying pathophysiology of the disease, unlike clinical symptoms that may wax and wane (Gottesman and Gould 2003). Widely used endophenotypes in schizophrenia research involve sensorimotor gating (pre-pulse inhibition of startle (PPI)), sensory gating response like P50 or N100, event-related potentials such as mismatch negativity (MMN), and P300 (ERP) (Gottesman and Gould 2003; Hamilton et al. 2018). Such endophenotypes reflect the function of discrete neural circuits. For example, PPI represents activation of the limbic cortex, striatum, pallidum, and pontine tegmentum (CSPP) regions (Swerdlow et al. 2001), while sensory gating reflects inhibitory neurotransmission in the hippocampus (Cromwell et al. 2008). More recently, researchers have focused on neural oscillations as an endophenotype to examine dysfunctional neural circuits in a layer-specific and cell-type-specific manner.

Neural Oscillations

The moment-to-moment neural activity in the cortical layers of the brain is reflected as the oscillatory electrical potential. Changes in electrical activity can be recorded through electroencephalography (EEG), while fluctuations in the magnetic field can be recorded through magnetoencephalography (MEG) (Beppi et al. 2021). EEG is the most widely used clinical tool

to probe the activity of cortical circuits in real time. It is non-invasive and provides temporal resolution in milliseconds. However, EEG has limited spatial resolution, which means relative to other imaging modalities like PET or fMRI, EEG is a poor indicator of the source of neural activity (Srinivasan 1999; Burle et al. 2015). This is especially the case when one or only a few scalp electrodes are used to record EEG. While it is challenging to decipher the spatial source of the electrical activity, methods such as low-resolution electromagnetic tomography or LORETA have been developed to compute neural sources from a large number of scalp electrodes (>64) through mathematical modeling (Pascaul Marqui et al. 1994). While it is possible to get excellent spatial resolution through an array of electrodes placed directly on the brain surface (e.g., electrocorticography or ECoG) or by recording local field potentials (LFPs) (Buzsáki et al. 2012), such methods are invasive and are viable only under some special conditions in humans.

Neural oscillations recorded through EEG reflect fluctuations in the electrical activity of a large population of cortical neurons. Hans Berger first developed the method to record EEG in humans in the 1920s. Transmembrane ion fluxes in large populations of cortical neurons result in real time changes in the extracellular field potential, which travel as a wave and can be recorded noninvasively from the scalp surface. Additionally, electrical activity produced by the synchronized firing of cortical neural populations is captured as periodic oscillations of the EEG (Buzsáki and Wang 2012).

Neural oscillations provide information regarding different vigilance states (e.g., alert or somnolent) of the brain and are consistent across mammalian species, making them ideal translational biomarkers (Buzsáki et al. 2013; Javitt et al. 2020). When considering a neural oscillatory signal (or any wave-like signal, for that matter), there are three important variables to consider: magnitude (or signal power), frequency, or number of cycles per second and phase of

the oscillation relative to some temporal event like stimulus onset. EEG oscillations are classified into canonical frequency bands called delta (0.5-4 Hz), theta (4-9 Hz), alpha (9-13 Hz), beta (13-30 Hz), gamma (30-90 Hz), and epsilon (> 90 Hz) (Buzsáki 2006; Freeman 2007; Keavy et al. 2016).

<p style="text-align:center">*Gamma Oscillations*</p>

Gamma oscillations have a frequency range of 30-90 Hz. They are thought to play an essential role in sensory processing, higher cognitive and behavioral processes (Buzsáki and Wang 2012). Over the years, studies on animals and humans have revealed a major role of gamma oscillations in bottom-up, top-down, and sideways information processing in the cortical circuits (Uhlhaas and Gray 2010). Gamma oscillations are especially important in cognitive functions. The so-called binding by synchrony theory explains the fundamental role of gamma oscillations in synchronizing activity across discrete brain regions involved in processing a common task (Gray et al. 1989; Singer and Gray 1995). Through gamma oscillations, distinct brain regions can integrate and coordinate information processing (Roelfsema et al. 1997; Tallon-Baudry and Bertrand 1999; Ghiani et al. 2021). For example, while traveling in a car, a flashing red light and a distant siren may immediately trigger the memory of an ambulance and make you move to the side. While each of these stimuli are processed by discrete cortical regions, the visual cortex for flashing light, auditory cortex for the sound, prefrontal cortex in deciding to move to the side, it is believed that they are processed as a common percept and gamma oscillations are critical for rapidly binding activity in spatially and functionally discrete regions of the brain, processing the same task (Carr et al. 2012). Another illustration of the role of gamma oscillations in cognitive processing has to do with working memory tasks. During a

working memory task, as an individual mentally holds a piece of information (e.g., a phone number or a house address) and recalls it after a brief delay, the brain regions involved in this process show gamma oscillatory activity. Moreover, the working memory performance correlates with the strength of the gamma signal over the delay phase (Howard et al. 2003). Such studies highlight the role of gamma oscillations in integrating perceptual experience as well as in enabling cognitive performance. Before moving forward, a brief description of the three important types of gamma oscillations is in order.

1: Spontaneous gamma. As the name suggests, these gamma oscillations are generated through the spontaneous activity of the neural populations. These oscillations are also called baseline or ongoing gamma and are generally independent of external stimuli. Typically, an increase in vigilance is associated with an increase in spontaneous gamma while slow-wave sleep correlates with low gamma activity (Amir et al. 2018).

2: Evoked gamma. This type of gamma oscillations are produced in response to an external (or an internal) event or stimulus. Evoked gamma oscillations show a time-locked relationship to the presented stimulus. For example, a brief auditory tone evokes a burst of gamma oscillatory activity, time-locked to the stimulus.

3: Induced gamma. This type of gamma oscillations are also dependent on external or internal stimuli. However, while induced gamma oscillations are temporally related to the stimulus, they are not strictly time locked in the way the evoked oscillations are. For example, when a brief tone elicits evoked gamma as above, it is accompanied by a different kind of gamma oscillations that are triggered by the tone but are not time-locked to it. Thus, in repeated trials, induced gamma appears around the time of the tone but are not strictly time-locked to it and tend to get diminished with averaging.

Generation Of Gamma Oscillations

Two models have been proposed to explain the generation of gamma oscillations: these are the interneuron network mediated gamma (ING) and pyramidal-interneuron network mediated gamma (PING) models. A schematic of both ING and PING model-based neural interactions are depicted in fig. 1.1.

In the ING model, gamma oscillations are generated through the interaction of two reciprocally connected interneuron populations (fig. 1.1-A). In this arrangement, when one interneuron population depolarizes as a result of an excitatory input, it feed-forwards inhibitory impulses to the second population, which undergoes hyperpolarization. When the second population depolarizes, the first group is inhibited. It takes ~25 milliseconds (ms) for the inhibited interneurons to recover due to the decay time constant of GABAA receptors. Thus, these interconnected neurons fire at a ~25 ms interval, giving rise to gamma oscillations (Wang and Buzsáki 1996; Buzsáki and Wang 2012).

The ING model was developed after studies showed that the power of gamma oscillations was associated with the firing rate of hippocampal interneurons, and tonic depolarization of interneuron populations in the hippocampus and cortex resulted in the generation of gamma oscillations (Buzsáki et al. 1983: Whittington et al. 1995). Later, optogenetic studies have confirmed that depolarization of fast-spiking (FS) interneurons is sufficient to generate gamma oscillations, while their prolonged hyperpolarization attenuates gamma oscillations (Sohal et al. 2009). Further support comes from *in vitro* studies that show, reciprocal inhibitory interaction between interneurons, through the GABAA receptor, are sufficient for the generation of gamma oscillations (Whittington et al. 1995).

32

The PING model on the other hand generates gamma oscillations because of interaction between the excitatory pyramidal neurons and the inhibitory interneurons (fig. 1.1-B). Thus, while pyramidal neurons feed-forward excitatory inputs to the interneurons, the interneurons impinge inhibition on the perisomatic segments of the same pyramidal neurons. Thus, in effect, the activated interneurons restrict the pyramidal cells to fire only when there is a near complete decay of the inhibitory input (~25 ms), leading to regular oscillations at the gamma frequency. Therefore, in PING networks, interneurons make it less likely for pyramidal neurons to fire randomly. Moreover, through this interaction, interneurons maintain the E/I balance in the cortical circuits. The PING model is supported by gene mutation and optogenetic studies in animals.
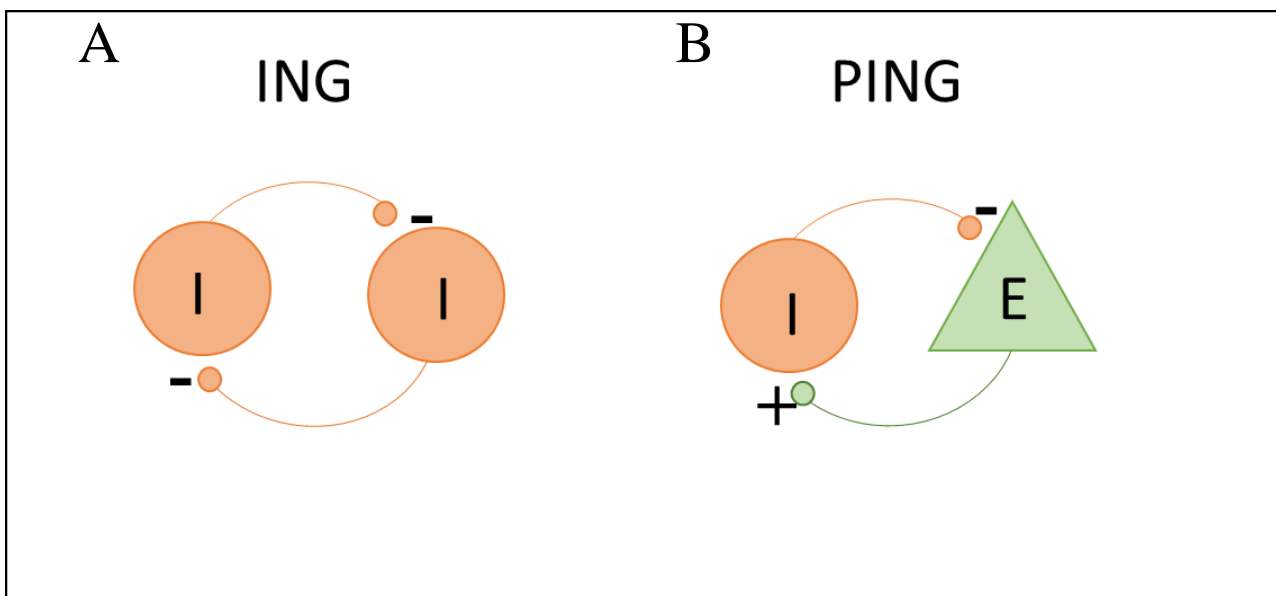
Figure 1.1. ING and PING models for the generation of gamma oscillations. In the Interneuron Network Gamma (ING) model (A), the interneurons spontaneously fire periodically at ~ 40 Hz (i.e., due to GABAA decay time constant of ~25 ms). The reciprocal inhibitory feedback between these interneurons shunts any random activity and thus results in a synchronized firing giving rise to gamma oscillations. In the Pyramidal Interneuron Network Gamma (PING) model (B), gamma oscillations arise due to the interaction between glutamatergic pyramidal neurons and GABAergic interneurons via excitatory and inhibitory interaction. Interneurons are driven by

excitatory inputs from the pyramidal neurons, which in return are synchronized by perisomatic feedback inhibition by the interneurons. (I) Inhibitory GABAergic neuron, (E) excitatory pyramidal neuron.

Depolarization of pyramidal neurons in the cortical circuits through optogenetic stimulation induces gamma oscillations (Yizhar et al. 2011; Lu et al. 2015; Bitzenhofer et al. 2017). Moreover, gamma oscillations can also be induced by stimulating NMDAR specifically on the interneurons (Mann and Mody 2009). Genetic ablation of the NR1, an obligatory subunit of the tetrameric NMDA receptor complex, results in entrainment deficit at gamma frequencies (Carlén et al. 2012). These findings suggest a vital role of NMDAR- dependent excitatory stimulation from the pyramidal neurons in generating gamma oscillations and provide support for the PING model.

There is a diverse variety of fast spiking (FS) interneurons based on electrophysiological, neurochemical, and morphological properties (Tremblay et al. 2016). Among the FS interneurons, basket cells that project onto the perisomatic region of the pyramidal neurons in cortical layers 2/3 are important for the generation of gamma oscillations. Specifically, the basket cells that are PV+ have been shown to be strongly associated with the generation of gamma oscillations (Buzsáki and Wang 2012). Recent optogenetic studies have shown that depolarization of PV+ interneurons facilitates gamma oscillations, while hyperpolarization of PV+ neurons results in a reduction in gamma power (Cardin et al. 2009). Moreover, phasic stimulation of PV+ neurons in the cortical layers 2/3 by light pulses at gamma frequencies evoked a faithful field gamma response at that frequency, suggesting that these neurons are also the most likely target for entrainment with rhythmic sensory input, such as an auditory click train. The importance of PV+ interneurons is further highlighted by the fact that schizophrenia

patients consistently show a reduction in PV+ cells in the layers 2/3 of the cerebral cortex, which is associated with gamma deficits (Gonzalez-Burgos et al. 2015), as described below.

Gamma Oscillations In Schizophrenia

Cognitive deficits represent one of the major symptom domains in schizophrenia (Heinrichs and Zakzanis 1998; Bora et al. 2009; Tripathin et al. 2018; Mascio et al. 2021). As outlined above, gamma oscillations correlate with cognitive functions such as processing of sensory input, working memory, and attention (Tallon-Baudry and Bertrand 1999; Singer 2004; Tallon-Baudry 2009). If gamma oscillations are causally linked to cognitive function, it is reasonable to hypothesize that schizophrenia patients with cognitive deficits will have abnormalities in gamma oscillations. Indeed, studies using visual or auditory stimulus paradigms have shown that schizophrenia patients indeed exhibit deficits in synchrony and power of gamma oscillations (Spencer et al. 2003; Spencer et al. 2008). Moreover, schizophrenia patients show reduced gamma activity during cognitive tasks (e.g., working memory) as compared to healthy controls (Basar-Eroglu et al. 2007; Karch et al. 2009; Minzenberg et al. 2010). There have also been studies showing the correlation of gamma deficits in schizophrenia patients with real-world functional outcomes (Cho et al. 2006; Shin et al. 2011; Keil et al. 2016; Zhou et al. 2018; Koshiyama et al. 2020; Molina et al. 2020). Thus, these studies point to the clinical and functional consequence of gamma deficits.

As described previously, PV+ neurons play an important role in generating gamma oscillations. PV+ interneurons, and glutamic acid decarboxylase (GAD67), an enzyme important for GABA synthesis, show reduced immunoreactivity in specific cortical regions in the postmortem brain of schizophrenia patients (Beasley and Reynolds 1997; Beasley et al. 2002;

Reynolds et al. 2002). Notably, this loss is lamina specific with layer 2/3 of the supragranular cortex being the most affected (Beneyto and Lewis 2019). Other studies, however, have shown that patient brains may have reduced immunoreactivity for PV protein while not affecting the cellular density (Hashimoto et al. 2003; Woo et al. 2006; Enwright et al. 2018). For example, Hashimoto and colleagues (2003) showed that when compared to healthy subjects, the PFC of schizophrenia patients have reduced mRNA levels of PV protein per cell, which was highly associated with reduced expression of GAD67, while there was no significant reduction in the total number of PV+ neurons (Hashimoto et al. 2003). Overall, there is substantial evidence that supports that the functioning of PV+ neurons is reduced in schizophrenia in a laminar-specific manner (Kaar et al. 2019). PV+ neurons express NMDAR, making them susceptible to NMDAR antagonists. Studies have shown that administration of NMDAR antagonists in awake rats results in the reduced firing of fast-spiking interneurons (Homayoun and Moghaddam 2007). Genetic ablation of NR1 subunit, an obligatory subunit of NMDAR, specifically on the PV+ neurons, results in the reduction of locally generated gamma oscillations (Carlén et al. 2012) as well as reduced entrainment to rhythmic stimuli. Furthermore, schizophrenia patients show reduced expression of the NR1 mRNA and protein in their brains (Catts et al. 2016). Other studies have shown that sustained NMDAR antagonism in rodents attenuates PV mRNA and GAD67 expression (Cochran et al. 2003; Behrens et al. 2007), mimicking PV and GAD67 reductions seen in schizophrenia (Lewis et al. 2005). Thus, the NMDAR hypofunction hypothesis links the disruption of NMDAR on PV+ neurons to gamma deficits seen in schizophrenia.

Stimulus-Evoked Response (SER)

When a discrete stimulus, either as a somatosensory, visual, or auditory event is repeatedly presented as trials to a human or animal subject, an EEG response, called stimulus-evoked response (SER) is obtained by averaging such trials (Sörnmo and Laguna 2005). Averaging of the EEG response trials ensures canceling out of the background electrical activity unrelated to the stimulus, and only the consistent stimulus-dependent, time-locked response remains. SER represents the sensory processing of the stimulus information in the neural circuits; thus, it is a valuable tool to measure the structural and functional integrity of these pathways (Brenner et al. 2009). EEG response to a stimulus can be classified into two categories: transient response and steady-state response (SSR). Transient response results after the presentation of a transient stimulus like a brief tone or a single click. Whereas presentation of periodic or rhythmic stimuli like a click train results in an SSR. Unlike the transient response, which is short-lived, SSR shows a sustained response to the periodic/isochronic stimuli that is constant in amplitude and phase for the duration of the stimulus, a so-called steady-state response (Brenner et al. 2009).

Auditory-Evoked Response (AER)

Evoked response in the form of a time-locked change in EEG that remains after averaging a number of trials in response to auditory stimulation is called auditory-evoked response, or potential (AER/P). AER can be a transient response or auditory steady-state response (ASSR) that lasts as long as the train stimuli. In humans, the transient response shows several peaks and troughs over a duration of 300 milliseconds (fig. 1.2). It includes auditory-brain stem response (ABR; occurs with 2-10 ms latency), middle latency response (MLR; 15-60 ms), and late latency response (LLR; 50-300 ms), following the onset of the auditory stimulus

(Melcher 2009). ABR is generated by the electrical activity in the auditory nerve and the brain stem auditory nuclei like the superior olives and the inferior colliculus. MLR represents the activity of thalamocortical pathways whereas the LLR captures the activity of primary and secondary auditory cortices, as well as association and frontal cortices (Moore 1987; McGee et al. 1991). Thus, the ABR, MLR, and LLR with different latencies, show the ascending transmission of auditory signals from the inner ear to the cortical regions.

ABR consists of seven positive peaks (I-VII) with different latencies depending on the auditory stimulus and mammalian species (Jewett and Williston 1971; Stapellst et al. 1984). ABR is independent of the arousal state and thus, it is not affected by sleep or anesthesia. It is used to measure the hearing threshold in infants, ascertain neurological problems in the auditory pathway like lesions or tumors, and for diagnosing hearing disorders (Young et al. 2022). ABRs are generally well preserved in schizophrenia patients, suggesting that infra thalamic auditory pathway function is not affected by this condition. MLR has two positive and two negative peaks named as Na-Pa and Nb-Pb. MLR is influenced by the state of arousal, and thus, under anesthesia, shows higher latencies and lower peak amplitudes. MLR is also used to ascertain hearing threshold, determine the depth of anesthesia, assess the postoperative integrity and function of cochlear implants, and localize lesions in the auditory pathway (Kraus et al. 1982; Özdamar and Kraus 1983). Lastly, LLR show positive and negative peaks named P1, N1, P2, and N2 (Backer et al. 2019). P1 is often interchanged with Pb component of the MLR due to time overlap, however different neural generators are responsible for Pb and P1, and they show different developmental trajectories. This suggests that P1 and Pb components may indicate different attributes of auditory processing (Ponton et al. 2002). Mammals like cats, rats, and guinea pigs show AERs similar to humans, with a proportional change in latency due to the size

38

and length of the conduction pathways. For example, the P1 latency is around 50 ms after tone

onset in humans and its equivalent in rodents tends to be around 20 ms. Similarly, the prominent

negative deflection called N1 happens in humans around 100 ms after stimulus onset while it

happens around 40-50 ms after tone onset in rodents (Umbricht et al. 2004) (fig. 1.3). From the

foregoing, it is apparent that given the similar sensory processing across mammals and the

morphological similarities of the AERs, they are reasonable measures to study stimulus-evoked

auditory event processing in humans and rodents.
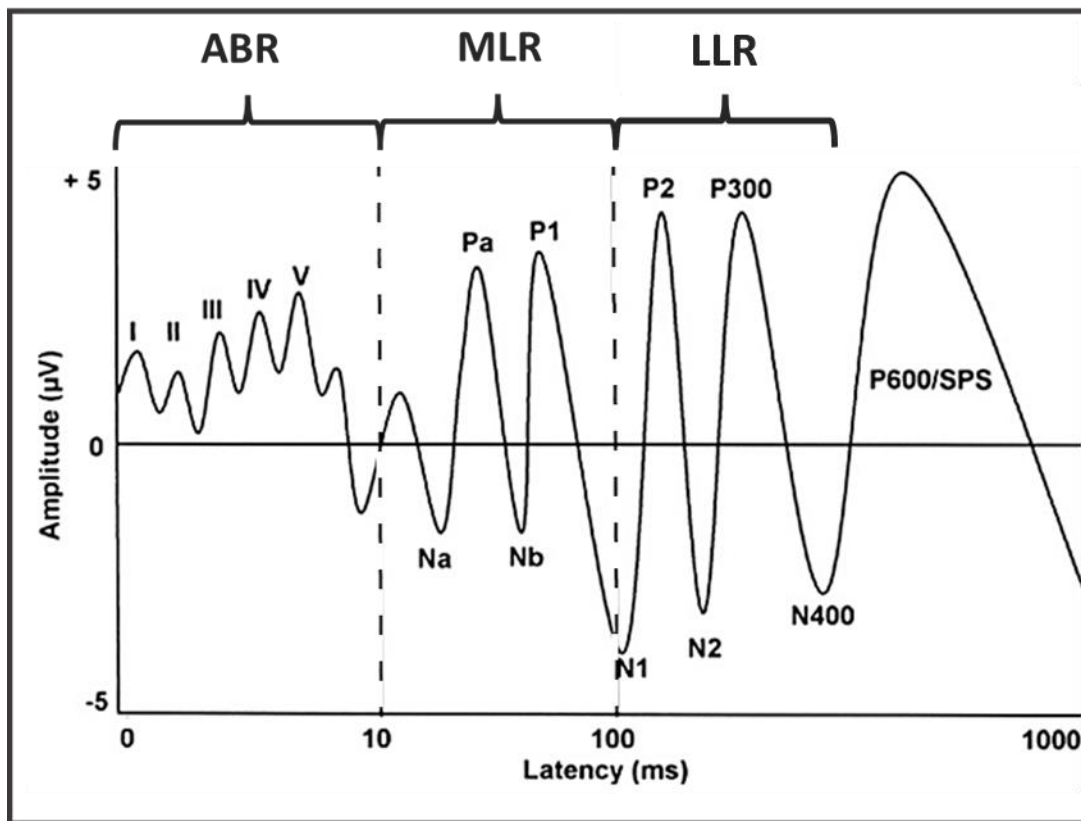
Figure 1.2. Diagram of the auditory-evoked response in humans recorded at electrode Cz.
Adapted from Folmer et al.*, 2011.
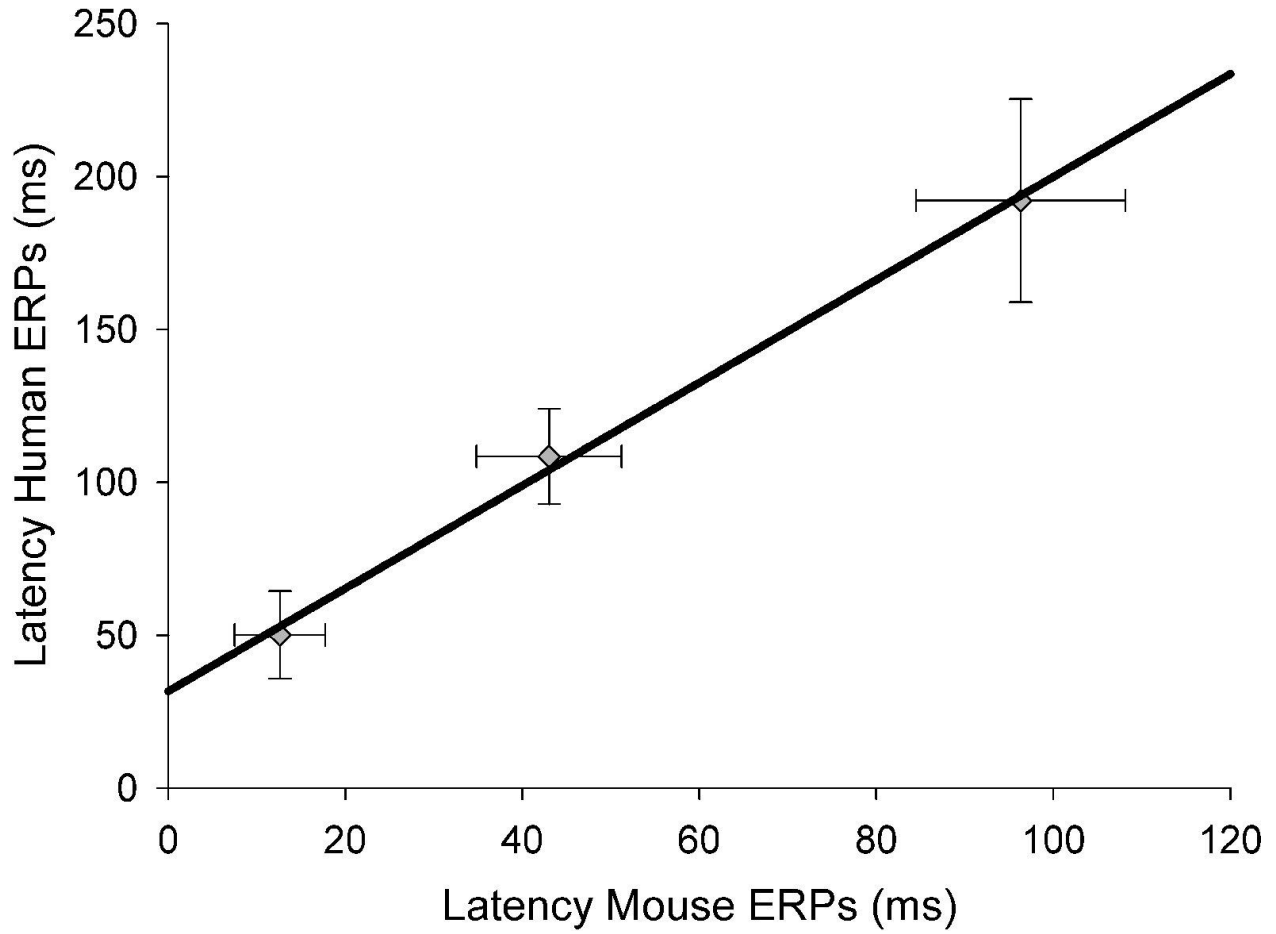
Figure 1.3. Comparison of latencies of AER's P1, N1 and P2 in mice and in human subjects. Reproduced with permission from Umbricht et al., 2004.

Auditory Steady-State Response (ASSR)

A single click or tone stimulus elicits a transient EEG response, as outlined above, that is comparable across human and preclinical species. This response happens as momentary deflections in the EEG potential. However, when this response is analyzed for spectral content through signal processing techniques such as fast Fourier transforms or wavelet-based time-frequency analysis (Markovic et al. 2012), one can isolate many distinct canonical oscillatory frequencies (e.g., delta, theta, alpha etc.) that underlie the response. Owing to this frequency content, the AER is considered as a broadband signal. In contrast to the AER, a train of discrete clicks presented at a given frequency and duration elicit a response that is constant in amplitude and phase and reflects the driving frequency and its duration (Regan 1989; Brenner et al. 2009). Additionally, ASSR starts off with a transient broadband oscillatory signal, much like a response from a single click. However, this is followed by a gradual buildup of an entrainment response that is limited to a narrow driving frequency and lasts as long as the train stimuli. Thus, an ASSR, once established, has a signal/noise (S/N) ratio advantage over transient stimulus-evoked responses like single clicks or pips since the transient responses are broadband and so is the background EEG signal or "noise". In contrast, the ASSR signal is narrowband and mimics the driving frequency even as the background "noise" continues to be broadband. The ASSR has been interpreted as the linear superposition of transient AERs evoked by individual click stimuli, as explained by the linear superposition theory of ASSR generation (Galambos et al. 1981; Bohórquez and Özdamar 2008; Presacco et al. 2010; Capilla et al. 2011). However, several studies have raised questions about the superposition theory by showing that simple superposition did not account for the observed ASSR accurately (Suzuki et al. 1994; Azzena et al. 1995; Conti et al. 1999).

An alternative mechanism called the entrainment theory suggests that phase synchronization and resetting of the ongoing oscillating neural field potential to match the driving frequency of the steady-state stimuli is the basis for the ASSR (Ross et al. 2005; Thut et al. 2011; Lütkenhöner and Patterson 2015). According to the entrainment theory, cortical circuits have a preferred resonance frequency, and auditory stimulation induces the most synchronization/entrainment at that frequency (Galambos 1982; Başar et al. 1987). Recent studies give strong support to the entrainment/phase synchronization hypothesis (Light et al. 2006; Presacco et al. 2010; Capilla et al. 2011; Koenig et al. 2012; Griskova-Bulanova et al. 2014; Tada et al. 2016).

40 Hz ASSR As A Biomarker In Schizophrenia

ASSR, especially at gamma frequency (~40 Hz), shows the highest magnitude and is consistently reduced in schizophrenia (Spencer et al. 2008; Hamm et al. 2011; Rass et al. 2012; Picton 2013; Thuné et al. 2016), and in people at risk for schizophrenia (Rass et al. 2012; Tada et al. 2016). Thus, the 40 Hz ASSR is regarded as both a *schizophrenia state* as well as a *schizophrenia trait* marker. Through 40 Hz ASSR, cortical neural circuits can be activated to generate gamma oscillations, and thus, 40 Hz ASSR is a tool to probe not only the integrity of the auditory sensory processing, but also the synchronization of the cortical neural circuits to a gamma driving frequency (Teale et al. 2003; Light et al. 2006; Brenner et al. 2009; Spencer et al. 2009; Koenig et al. 2012; Tada et al. 2016). Within the cortical lamina, the 40 Hz ASSR sources seem to be located principally in the thalamorecipient layer (layer 4) and layers 2/3 of the supragranular cortex (Cardin et al. 2009; Javitt and Sweet 2015; Welle and Contreras 2016). Deep layer 3 is the layer frequently associated with deficiency in the GABAergic cellular

machinery important for gamma oscillatory function, as outlined above (Lewis et al. 2005).

Thus, 40 Hz ASSR deficits in patients may reflect the layer-specific alterations of inhibitory

function. Since gamma oscillations play an essential role in sensory and cognitive processing, 40

Hz ASSR presents an opportune biomarker specifically to examine cortical function relevant to

gamma frequency. Deficits in 40 Hz have been extensively shown to correlate with cognitive

dysfunction in schizophrenia (Light et al. 2006; Rass et al. 2012; Tada et al. 2016; Puvvada et al.

2018; Sun et al. 2018; Leonhardt et al. 2020). Furthermore, 40 Hz ASSR deficits have been

shown to correlate with the severity of schizophrenia symptoms in general (Zhou et al. 2018).

40 Hz ASSR is routinely used as a measure of hearing acuity in audiometry tests (Picton

2010). More recently, 40 Hz ASSR features have been used to develop an index to monitor the

depth of anesthesia during the induction phase, which is faster and more reliable than the

traditionally used EEG based bispectral (BIS) index (Haghighi et al. 2018). Similarly, a 40 Hz

ASSR based classification system has been reported to show a very high accuracy in identifying

sleep states (Khuwaja et al. 2015). As compared to other EEG measures (i.e., transient AER),

ASSR shows a better signal to noise ratio (S/N), making it a superior measure for circuit-level

function (Reijden et al. 2004; Ross et al. 2005; Yokota and Naruse 2015; Christensen et al. 2018;

Prado-Gutierrez et al. 2019). The 40 Hz ASSR has been reported to show a dose-dependent

attenuation in response to NMDA blockade, thus making it a relevant biomarker for drug

engagement studies involving NMDA transmission (Raza and Sivarao 2021). Schizophrenia

patients, and people at high risk, show a strong association of 40 Hz ASSR with treatment

outcomes (Molina et al. 2020; Grent- 't-Jong et al. 2021). In animal models, NMDAR

antagonist-induced deficits in 40 Hz ASSR mimic ASSR disruption seen in schizophrenia

patients (Sivarao et al. 2013; Thuné et al. 2016; Raza and Sivarao 2021). These findings point to

encouraging predictive, construct and face validity features for testing 40 Hz ASSR in animal models for studying NMDAR transmission.

Furthermore, 40 Hz ASSR is considered here as an endophenotype that reflects the function of a discrete cortical circuit. LFP studies have shown layers 2/3 and 4 as the generators of 40 Hz ASSR (Nakao and Nakazawa 2014; Javitt and Sweet 2015; Funk et al. 2020). These are the regions associated with the generation of evoked gamma oscillations (Cardin et al. 2009; Welle and Contreras 2016). The superficial cortical layers also play an essential role in sensory processing (Quiquempoix et al. 2018) and cognitive function (e.g., working memory), processes affected in schizophrenia. Moreover, cortical layers 2/3 have centrifugal projections, which play an important role in integrating sensory information across different brain regions (Yamashita et al. 2018). Thus, 40 Hz ASSR can be used as a biomarker to probe the structural and functional integrity of superficial cortical layers associated with gamma oscillations.

Specific Aims

Schizophrenia is a severely debilitating mental illness affecting millions worldwide. Current medications are at best only partially effective. Yet, there has been a scale back in the pharma industry's investment in developing new treatments, in part due to a lack of reliable and disease-relevant biomarkers that can guide drug development (Weickert et al. 2013). Functional markers are required for preclinical lead selection and to demonstrate target engagement. In early-stage clinical drug development, biomarkers are critical for dose selection, proof of concept evaluation and patient stratification. Absence of such process goal posts makes drug development risky and discourages investment in psychiatric drug development.

Cutting across species, neural networks in the brain synchronize to discrete sounds such as a brief tone or a rhythmic click train. The ensuing oscillatory activity can be captured in real time using the technique of electroencephalography (EEG). Cutting-edge signal processing reveals robust synchrony measures that are highly relevant to sensory and cognitive information processing (Koshiyama et al. 2021). For example, clicks delivered at gamma frequency (~40 Hz), called the 40 Hz ASSR, evoke neural oscillations with high signal to noise ratio (McFadden et al. 2014). Gamma oscillations are a product of NMDA-mediated activation of the parvalbumin (PV) containing GABAergic interneurons and their modulation of the pyramidal neuron firing, particularly in the superficial layers of the cortex (Cardin et al. 2009; Sohal et al. 2009). Interestingly, schizophrenia patients show consistent deficits in transient gamma as well as 40 Hz ASSR (Kwon et al. 1999; Shin et al. 2011; Thuné et al. 2016), while postmortem studies have identified reduced GABAergic and glutamatergic markers in these layers (Hashimoto et al. 2003; Catts et al. 2016). In healthy human subjects as well as in rodents, acute pharmacological blockade of NMDA receptors results in gamma oscillatory deficits (Sivarao et al. 2013; Curic et al. 2019). Thus, pharmacological modulation of gamma oscillatory response constitutes a potential cortical layer-specific translational biomarker.

Yet, several aspects of the rodent assay remain unknown, limiting its potential for use in drug development studies. For example, inter subject variability in drug response is a significant challenge in neuropsychiatric drug testing. While within subject crossover design is a way to minimize this variability, it is predicated on the assay being stable over an extended period of time, to complete the crossover. While 40 Hz ASSR is disrupted by NMDA antagonism, we do not know if positive modulators of the NMDA receptor like D-serine would improve it. Furthermore, while rodent literature suggests several sites on the cortical mantle that are suitable

for 40 Hz ASSR, we do not know if these are distinct or redundant measures of synchrony or if one is preferable over the other. Answering these and other questions will fortify the rodent version of the 40 Hz ASSR as a reliable tool for psychiatric drug development.

Specific Aim 1a. Evaluate the psychometric performance of the rodent 40 Hz ASSR assay and the transient gamma oscillations over an extended period and demonstrate its suitability for crossover designs (addressed in Chapter 2). **Aim 1b**. Demonstrate responsivity of the assay measures to acute NMDA receptor blockade (Chapter 2).

Specific Aim 2a. Compare psychometric stability of 40 Hz ASSR from two discrete cortical regions, the temporal cortex, and the vertex (chapter 3). **Aim 2b**. Evaluate if the 40 Hz ASSR sensitivity to pharmacological intervention is different between these two regions (Chapter 3).

Specific Aim 3a. Using a range of doses, evaluate if D-serine, a co-agonist at NMDA receptor, can augment the gamma oscillatory response (Chapter 4). **Aim 3b**. Evaluate the 40 Hz ASSR responsivity to acute dosing with a typical and atypical antipsychotic drug (Chapter 4)

Expected outcomes. By establishing robust psychometric properties of the 40 Hz ASSR, and by demonstrating bidirectional modulation by pharmacological manipulations, we will reveal a reliable cross-species CNS assay for the drug development pipeline.

CHAPTER 2. TEST-RETEST RELIABILITY OF TONE- AND 40 HZ TRAIN-EVOKED GAMMA OSCILLATIONS IN FEMALE RATS AND THEIR SENSITIVITY TO LOW-DOSE NMDA CHANNEL BLOCKADE

Muhammad Ummear Raza and Digavalli V. Sivarao*

Department of Pharmaceutical Sciences, Bill Gatton College of Pharmacy, East Tennessee State

University, VA Building 7, Room 324, Maple Ave, Johnson City, TN 37604, USA

*Corresponding Author

Abstract

Rationale. Schizophrenia patients consistently show deficits in sensory-evoked broadband gamma oscillations and click-evoked entrainment at 40 Hz, called the 40-Hz auditory steady-state response (ASSR). Since such evoked oscillations depend on cortical N-methyl D-aspartic acid (NMDA)-mediated network activity, they can serve as pharmacodynamic biomarkers in the preclinical and clinical development of drug candidates engaging these circuits. However, there are few test-retest reliability data in preclinical species, a prerequisite for within-subject testing paradigms.

Objective. We investigated the long-term psychometric stability of these measures in a rodent model.

Methods. Female rats with chronic epidural implants were used to record tone- and 40 Hz click-evoked responses at multiple time points and across six sessions, spread over 3 weeks. We assessed reliability using intraclass correlation coefficients (ICC). Separately, we used mixed-effects ANOVA to examine time and session effects. Individual subject variability was determined using the coefficient of variation (CV). Lastly, to illustrate the importance of long-term measure stability for within-subject testing design, we used low to moderate doses of an NMDA antagonist MK801 (0.025–0.15 mg/kg) to disrupt the evoked response.

Results. We found that 40-Hz ASSR showed good reliability (ICC=0.60–0.75), while the reliability of tone-evoked gamma ranged from poor to good (0.33–0.67). We noted time but no session effects. Subjects showed a lower variance for ASSR over tone-evoked gamma. Both measures were dose-dependently attenuated by NMDA antagonism.

Conclusion. Overall, while both evoked gamma measures use NMDA transmission, 40-Hz ASSR showed superior psychometric properties of higher ICC and lower CV, relative to tone-evoked gamma.

Introduction

Schizophrenia is a disorder in which information processing is abnormal at multiple
levels, from distorted transmission to impaired perception (Javitt, 2009a, 2009b; Krishnan et al.,
2011; Silverstein and Keane, 2011). Sensory-evoked neural responses in patients tend to be
smaller and less synchronized across many paradigms (Javitt, 2009a; Luck et al., 2011; Rissling
and Light, 2010), suggesting an abnormal registration and/or processing. Specifically, discrete
auditory stimulus-evoked oscillations in the gamma frequency range (30–100 Hz) are
consistently abnormal in schizophrenia as well as in other neuropsychiatric conditions like
autism and bipolar disorder. The local interactions between parvalbumin-positive GABAergic
basket cells and pyramidal cells are important for the generation of gamma oscillations
(Gonzalez-Burgos and Lewis, 2008; Tiesinga and Sejnowski, 2009). Specifically, pyramidal
neuron feed-forward activation of the N-methyl D-aspartic acid (NMDA) receptors on the basket
cells and their feedback inhibition of the pyramidal cells is critical for the emergence of these
oscillations (Buzsáki and Wang, 2012; Cardin et al., 2009; Gonzalez-Burgos and Lewis, 2012).

Principally, two types of gamma oscillations are evoked by auditory stimuli like tones
and clicks. A transient burst of broadband gamma oscillatory activity (~ 30 to 100 Hz) that is
coincident with the auditory-evoked P1-N1-P2 potential (Javitt and Sweet, 2015; Ross et al.,
2010) is observed in response to a discrete tone or click stimulus. A second type of response,
called the auditory steady-state response (ASSR), is an electroencephalographic (EEG)

entrainment reflecting the driving frequency of periodic auditory stimuli such as clicks or amplitude-modulated tones, lasting as long as the train stimulus, and typically elicited at 40 Hz (Brenner et al., 2009). Both these responses are deficient in not only schizophrenia patients but also in individuals that are at high risk for the disease (Leicht et al., 2011, 2016; Oribe et al., 2019; Perez et al., 2013), making them state and trait markers. Moreover, an attenuation in tone-evoked gamma is frequently associated with cognitive and negative symptoms (Curic et al., 2019; Leicht et al., 2015). Offering a window to view such observations, Koshiyama et al., using structural equation modeling, established a framework through which "bottom-up" sensory measures like 40-Hz ASSR can influence clinical outcomes (Koshiyama et al., 2021). Moreover, evoked gamma output before a therapeutic intervention predicted the degree of improvement post-intervention, indicating a prognostic potential for circuit-level gamma response (Molina et al., 2020). Thus, gamma markers are emerging as versatile tools with growing applications in neuropsychiatric therapeutics (Kozono et al., 2019; Light et al., 2020; Luck et al., 2011; Sivarao, 2015; Sivarao et al., 2016).

In psychiatric drug development, there is now a greater appreciation for how patient heterogeneity leads to high odds ratios for many clinically efficacious drugs (Stroup et al., 2007). Clinical trials that use "within-subject" designs tend to better control such heterogeneity over "between-subject" designs (Salkind, 2010). Moreover, within-subject designs involving the so-called N=1 trials are emerging as a sensitive means for identifying the most effective treatment for an individual patient, taking into account his or her unique genetic/epigenetic background (Lauschke et al., 2019). Stable, objective, circuit-level biomarkers can de-risk or accelerate such fledgling efforts, by demonstrating neurophysiological engagement and guiding dose selection. In preclinical discovery too, biomarkers are critical to demonstrate circuit engagement and

enable prioritization of lead molecules for further development. Here too, within-subject crossover designs are more sensitive to pharmacological treatment, yielding typically better effect sizes over between-subject designs and requiring smaller group sizes to demonstrate treatment effect (Cleophas and De Vogel, 1998; Guo et al., 2013).

However, the use of biomarkers in within-subject design studies is predicated on their temporal stability to support multiple levels of drug treatment lasting weeks, if not months. Several recent studies have reported on the stability of 40-Hz ASSR measures in healthy human subjects (McFadden et al., 2014) as well as in schizophrenia patients (Cervenka et al., 2013; Ip et al. 2018; Legget et al., 2017; McFadden et al., 2014; Roach et al., 2019). Overwhelmingly though, such reports are limited to testing either a couple of times within one session (e.g., Ip et al) or only across a couple of discrete sessions (e.g., Cervenka et al., 2013; Legget et al., 2017; McFadden et al., 2014). Yet, to demonstrate target engagement, within the context of a repeated measures design testing several dose levels of an experimental drug, one needs to show not only temporal reliability within each session (for time-course) but also across several sessions (to accomodate cross-over treatments). However, to the best of our knowledge, such studies, clinical or preclinical, are largely missing.

In the current study, we tested the stability of tone-evoked broadband gamma (30–100 Hz) and 40 Hz click train-evoked narrowband gamma (35–45 Hz) activity in a group of female rats, in six sessions, spread over a 3-week period. We investigated the test-retest reliability using the intraclass correlation coefficients (ICC) at five discrete time points within each session. To rule out carryover effects of repeated testing, we used mixed-effects ANOVA, using test sessions and time of testing as fixed effects and subjects as a random effect. To estimate the individual subject variability, we calculated coefficients of variation (CV). Lastly, to illustrate the

52

importance of stability to pharmacological testing, we used a repeated measures design to test

low to moderate doses of the high affinity, open NMDA channel blocker MK-801, to disrupt

evoked gamma oscillations.

Methods

General

The Institutional Animal Care and Use Committee of the East Tennessee State University

approved all experimental procedures involving animal subjects. Female Sprague Dawley rats

(6–8-week-old; 200–250 g) were obtained from Envigo (Indianapolis, IN) and group housed

until surgery, with free access to food and water.

Surgical

Surgeries were performed under isoflurane anesthesia (5% induction: ~2% maintenance,

in oxygen, 1 L/min). The head was secured in a stereotaxic frame, and core temperature was

maintained at 36 ± 1 °C. Head was shaved and disinfected with alcohol and povidone-iodine

swabs. Bupivacaine (0.25 %, sc) was used for a local nerve block and ketoprofen (5 mg/kg, sc)

was used for perioperative analgesia. Atropine sulfate (0.05 mg/kg, sc) was given to limit

respiratory secretions. Skull was exposed through a midline incision, followed by blunt

dissection. A solution of 3% hydrogen peroxide was used to disinfect and dry the skull. An

aseptic drill bit was used to drill four burr holes into the skull, and epidural electrodes with

attached wires were screwed in, avoiding damage to underlying dura. Electrode coordinates were

as follows: frontal, 1 mm anterior to bregma and 1 mm lateral to midline; vertex, 4.5 mm caudal

to bregma and 1 mm lateral to midline; reference, 2 mm caudal to lambda and 2 mm lateral (left

side); and ground, 2 mm caudal to lambda and 2 mm lateral (right side). Dental cement slurry was poured over the electrodes and allowed to set. Electrode wires were soldered to the recording head mount (Pinnacle Technology, Lawrence, KS). For EMG, two wires from the head mount were sutured to the nuchal muscle (however, EMG data was not used in this study). The area was covered with a second layer of dental cement and, after curing, was closed using silk sutures. Rats were allowed to recover from surgery for at least 10 days and were later handled and acclimated extensively to the recording set up before use.

EEG Recording

Rats were placed in Plexiglas cylinders (Pinnacle Technology, Lawrence, KS) equipped with a video camera and a house speaker (DROK, B00LSEVA8I). They were tethered to the setup through a shielded preamplifier cable and a commutator for continuous EEG recording while permitting free access to explore within the chamber. The acquisition system (CED Power 1401; Cambridge Electronics Design (CED), Cambridge, UK) produced the auditory stimuli, as well as acquired the EEG (Signal v7); data were acquired as 5-s sequential sweeps (1 KHz sample rate). A tone stimulus (1 KHz, 2mV sinusoidal wave, 50-ms duration, 65 dB) was presented 1 s after sweep initiation. A click train (5 mV monophasic, 1-ms long square waves, 20/0.5 s, ~ 65 dB) was presented 2 s following the tone stimulus. Interval between the end of the click train and the beginning of the next tone was 2.5 s. Evoked responses were averaged from ~ 75 consecutive trials. For the ICC study, data were acquired at 0 (i.e., immediately after the animals were tethered), 30, 60, 90 and 120 min. The 0 min time point was omitted in the pharmacology study. Six sessions, each separated by at least 3 days, were used for the reliability study, whereas pharmacology study was carried out in four sessions (vehicle plus 3 dose levels

of MK801). EEG data discussed here were obtained from the vertex electrode. A schematic of the two studies (A and C) along with the Latin square (B) used in the pharmacology study are shown in fig. 2.1.

EEG Data Analysis

While all EEG data were evaluated for movement artifacts, very few frames (<3%) needed exclusion. Animal movement by and large did not affect the EEG. However, occasional chewing-related movements were noted and excluded if such movements were coincident with the auditory response. Thus, ~75 artifact-free frames were averaged per subject per time point, to generate an evoked response. Evoked response was band-pass filtered (30–100 Hz for tone and 35–45 Hz for the click train, using a second order Hanning infinite impulse response (IIR) filter; Signal v7). Root mean square (RMS) amplitudes were computed for tone-evoked (0–150 ms from onset) and ASSR (0-500 ms from onset), for each subject, at each time point. These were further averaged to summarize group responses.

Pharmacology

MK801 maleate (MW 337.4 g/mol) was obtained from Sigma-Aldrich. Free base mass was used to make 0.15 mg/ml stock solution, and this was diluted to make 0.025 and 0.05 mg/ml. MK801 doses were chosen to capture a wide range of NMDA channel occupancy (Fernandes et al. 2015). Rats were given intraperitoneal (IP) injection of either vehicle or MK-801 (1 ml/kg,
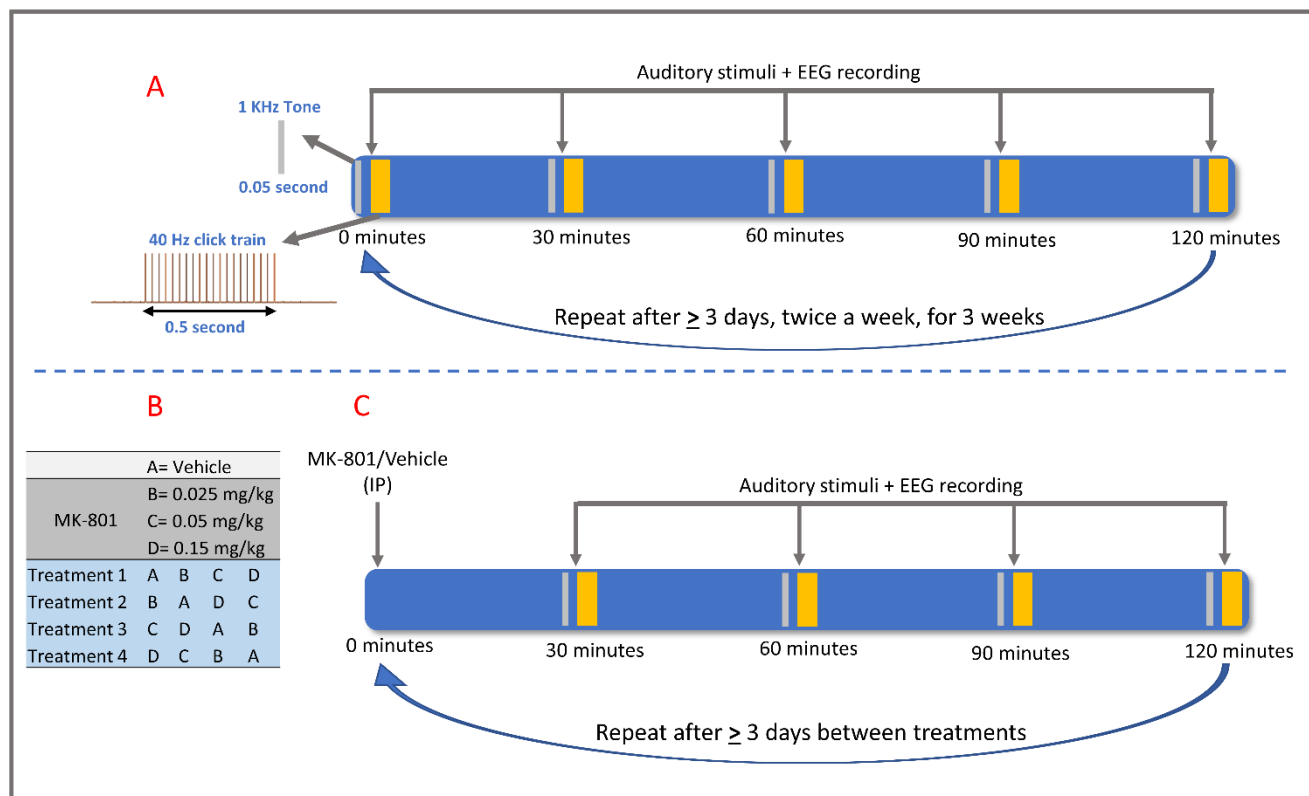
Figure 2.1. Schematic representations of the study design for the test-retest reliability (A), the Latin square treatment (B), and the MK-801 pharmacology study (C).

volume) at the start of experiment in a Latin-square design (fig. 2.1-B) and were then placed in the recording chamber. At least a 3-day period was allowed for washout, between treatments. Animals were monitored for carryover effects and weight fluctuations, but none were noted.

Statistics

Since a key goal of this work was to evaluate the suitability of evoked gamma oscillations as biomarkers in a repeated measures design, we wanted to know if there were any systemic effects of repeated testing. For this, we used a mixed-effects ANOVA (restricted maximum likelihood estimation as implemented in GraphPad Prism v8.4.3). Time of testing within a session was designated as a row factor, while multiple sessions were designated as a column factor. Data normality was assessed using quantile-quantile (q-q) plots. Sphericity was not assumed, and Greenhouse-Geisser correction was used. Where appropriate, Dunnett's tests were used to evaluate within session significance, using time-zero response as a comparator. For pharmacology studies, vehicle group at each time point was used as the comparator.

Reliability was measured by calculating the intraclass correlation coefficients (ICC). Defined as the ratio of subject variance to total (subject + error) variance, ICC assesses the reliability of an evoked response by comparing the between-measures variability of each subject to the total variation across all measures and all subjects (Koo and Li 2016; Tan et al. 2015). Unlike Pearson's correlation coefficient, which detects the linear association between two measures, irrespective of their absolute values, ICCs reflect the agreement of a subject's evoked power from one session to another, accounting for the variances (Tan et al., 2015).

There are many types of ICC reported in the literature. We implemented the two -way mixed-effects, absolute agreement, and single measurement formula, as discussed by Koo and Li

(2016). ICC estimates along with their 95% confidence intervals were calculated using SPSS

statistical package (SPSS v26, Chicago, IL). We used a qualitative interpretation of the ICC

values as reported recently by Ip et al., (2018). Thus, an ICC less than 0.39 was considered to be

an indicator of poor test-retest reliability, while ICC ranges between 0.40–0.59, 0.60–0.75 and

0.76, and above were considered respectively to be fair, good, or excellent (Ip et al., 2018).

Results

Auditory stimuli comprising of tone and click trains evoked robust broadband gamma

and steady-state entrainment respectively, in all subjects. An overlay in fig. 2.2. shows the grand

averaged RMS amplitude data from six sessions, corresponding to discrete time points (0 to 120

min) from a group of 12 rats; panel A summarizes tone-evoked gamma band activity while panel

B shows the ASSR. Individual subject averages for each session for both measures are shown in

a supplementary figure (fig. 1 supp).

For tone-evoked γ, a linear Q-Q plot confirmed normal distribution (data not shown).

Mixed-effects ANOVA showed a highly significant effect of time on group means ($p<0.0001$; F

(2.580, 28.38) = 13.91; epsilon = 0.6449). However, no significant session effect ($p=0.2195$; F

(2.458, 27.04) = 1.590; epsilon = 0.4917) or interaction of time $\times$ session ($p=0.1896$; F (5.319,

55.85) = 1.538; epsilon = 0.2659) were noted. Examining the mean response across time

indicated a pattern of smaller average responses at time zero relative to other times points (fig.

2.2-A). Confirming this, post hoc analysis showed that the time-zero response was smaller than

several other time points within each session ($p<0.05$; Dunnett's tests). Such differences were
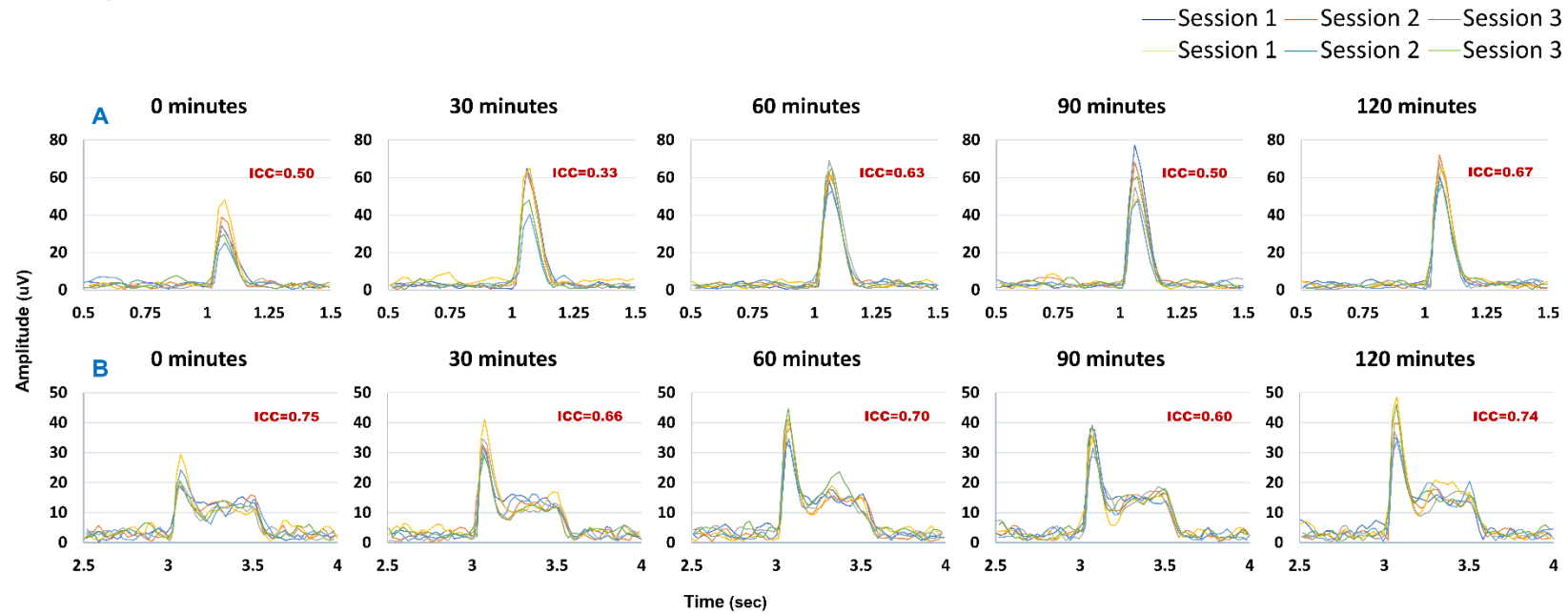
Figure 2.2. Overlay of the RMS amplitude measures of 1 KHz tone-evoked broadband gamma (30–100 Hz; A) and 40 Hz click-evoked narrowband steady-state response (35–45 Hz; B) at 0–120-min time points across 6 discrete sessions, spread over a 3-week period. Data were from a group of 12 rats.

noted in session 1 (p<0.05; 0 min vs. 30, 60, and 90 min), session 2 (0 min vs. 30, 60, 90, and 120 min), session 3 (0 min vs. 30, 60, and 120 min), and session 5 (0 min vs. 120 min).

The 40-Hz ASSR data too were normally distributed, based on a linear Q-Q plot (not shown). As with the tone-evoked gamma, mixed-effects analysis of 40-Hz ASSR showed a highly significant effect of time (p=0.0001; $F (3.1, 34.10) = 8.956$; epsilon = 0.7751) but no session effect (p=0.3021; $F (2.5, 27.5) = 1.268$; epsilon = 0.5) or interaction of time $\times$ session (p=0.6067; $F (3.916, 41.12) = 0.6802$; epsilon = 0.1958). As with transient gamma, mean ASSR at time zero tended to be smaller than responses at other time points (fig. 2.2-B). Within session Dunnett's tests revealed following contrasts to be significant (p<0.05): session 2 (0 min vs. 120 min), session 3 (0 min vs 60 min), session 4 (0 min vs. 60 min and 120 min), session 5 (0 min vs. 60 and 120 min), and session 6 (0 min vs. 60 and 120 min).

We next calculated the ICCs for each time point across sessions using a two-way mixed-effects model using single measurement, absolute agreement criteria as discussed elsewhere (Koo and Li 2016). The ICCs along with their 95% CIs, at designated time points and across 6 sessions, are shown in Table 1. Tone-evoked gamma, with the exception of one time point, showed an ICC that had a fair measure of reliability (0.33–0.67). On the other hand, ICC for 40-Hz ASSR showed good (0.60–0.75) reliability. Although we did not do a pair-wise statistical comparison between the two, it is apparent from the data summarized in Table 1 that for the same group of subjects, in each instance, 40-Hz ASSR had higher ICCs compared to tone-evoked gamma.

Table 2.1. Intraclass Correlation Coefficients (ICC) Across Time Points From Six Sessions. ICC were calculated using a two-way mixed-effects model, single measurement, and absolute agreement criteria (Koo and Li, 2016).

	Tone-evoked γ		40 Hz ASSR	
Time	ICC	95% CI	ICC	95% CI
0 min	0.50	0.22-0.83	0.75	0.51-0.93
30 min	0.33	0.09-0.72	0.66	0.39-0.90
60 min	0.63	0.37-0.86	0.70	0.47-0.89
90 min	0.50	0.27-0.77	0.60	0.37-0.83
120 min	0.67	0.45-87	0.74	0.54-0.90

Since the same group of 12 rats was repeatedly tested ~30 times, spread over 3 weeks, we had an opportunity to calculate % coefficient of variation (CV) as a measure of individual subject's response precision. Mean CV for tone-evoked gamma was 31.6%. In contrast, the mean CV for 40-Hz ASSR was markedly lower at 20.9. Fig. 2.3 summarizes these data as a violin plot, highlighting the difference between the two measures (p=0.0001; paired t-test).
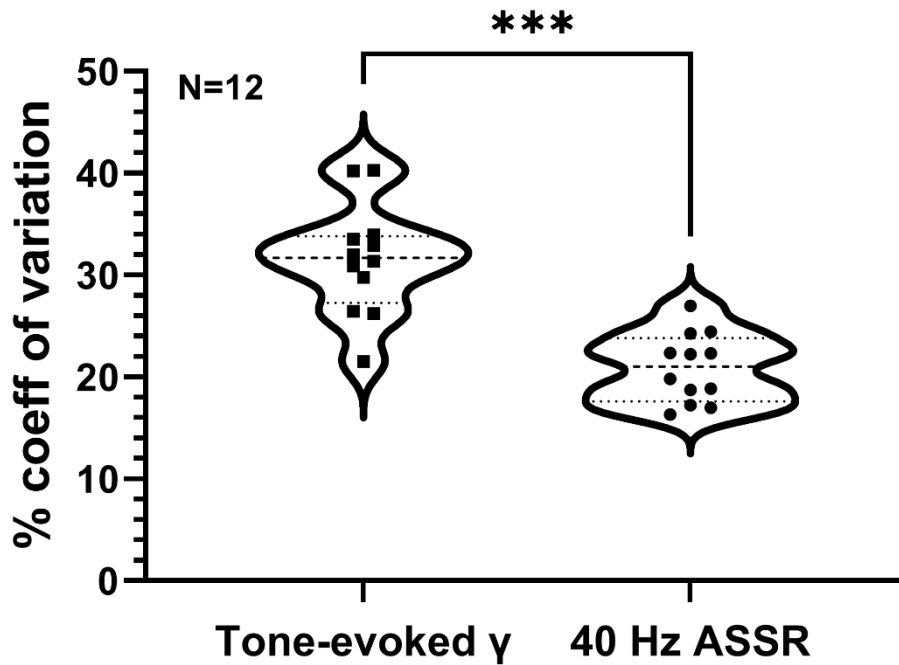
Figure 2.3. Summary of coefficient of variations (CV) of tone-evoked and 40 Hz click train-evoked responses from a group of 12 rats. Individual subject CVs are indicated within the violin plots. Significant difference between the two groups is indicated by asterisks (p = 0.0001; paired t-test).

In the second part of the study, we illustrated the utility of temporal stability of these measures by carrying out a dose-response with the NMDA channel blocker MK801, using a repeated measures design. We chose to omit testing at time zero but tested at other time points (30–120 min) post-dose. The dose of 0.15 mg/kg dose of MK-801 induced hyperactivity,
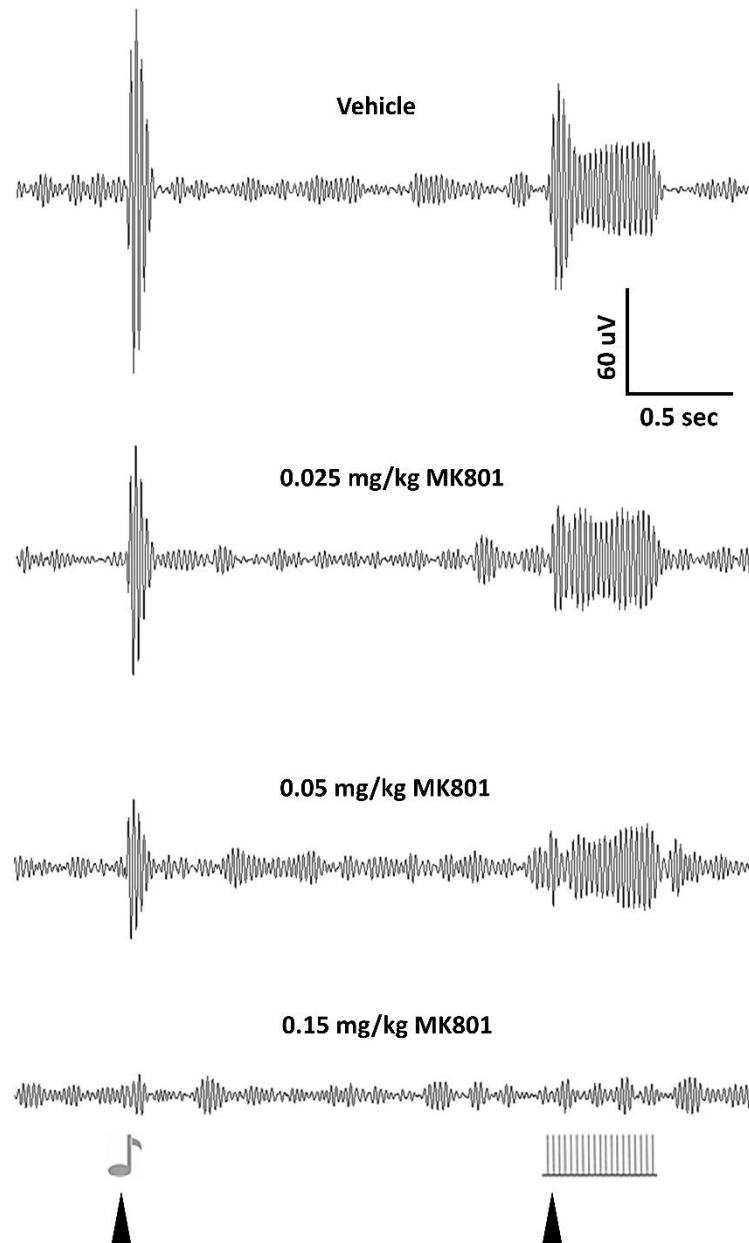
Figure 2.4. A compilation of grand average of narrow band gamma (35–45 Hz) activity in response to auditory tone (1 KHz) and 40-Hz click stimuli, 120 min after vehicle or MK801 (0.025, 0.05, or 0.15 mg/kg, ip) treatment. Data represents a grand average from 10 subjects. Note that the actual tone-evoked data were computed over a broadband of 30–100 Hz.

circumambulation along with stereotypic head movements that persisted for 3–4 h post-injection. However, no behavioral changes were noted at 0.025 or 0.05 mg/kg doses.

MK801 disrupted tone-evoked gamma in a highly dose-dependent and time-dependent manner. Fig. 2.5 summarizes the grand averaged evoked responses for all treatments, across all subjects, 60 min post-treatment. Fig. 2.5 (top panel) summarizes tone-evoked gamma after vehicle or MK801 treatments, along with individual RMS values. Normal distribution of the data was first ascertained through a Q-Q plot (not shown). Mixed-effects ANOVA showed a robust treatment effect ($p < 0.0001$; $F_{(1.574, 14.16)} = 25.98$; epsilon = 0.5246) but no time effect ($p = 0.4709$; $F_{(2.280, 20.25)} = 0.8149$; epsilon = 0.7600) or time $\times$ treatment interaction ($p = 0.2007$; $F_{(2.245, 20.21)} = 1.728$; epsilon = 0.2495). Post hoc comparisons using Dunnett's test showed that only 0.05 and 0.15 mg/kg doses of MK801 significantly ($p < 0.05$) attenuated tone-evoked gamma at multiple time-points, relative to vehicle treatment.

ASSR data too were normally distributed, based on a Q-Q plot (not shown). The 40-Hz ASSR responses from each subject along with group mean for each treatment condition are summarized in fig. 2.5, bottom panel. MK801 dose- and time-dependently disrupted 40 Hz train-evoked gamma. Robust treatment effect was noted ($p < 0.0001$; $F_{(1.884, 16.95)} = 31.39$; epsilon = 0.6279). However, neither time ($p = 0.4365$; $F_{(2.679, 24.11)} = 0.9208$; epsilon = 0.8930) nor time $\times$ treatment ($p = 0.5328$; $F_{(3.800, 34.20)} = 0.7922$; epsilon = 0.4222) were significant. Post hoc testing showed that all three doses were effective ($p < 0.05$) at one or more time points, in reducing 40-Hz ASSR response, using vehicle treatment as a comparator.

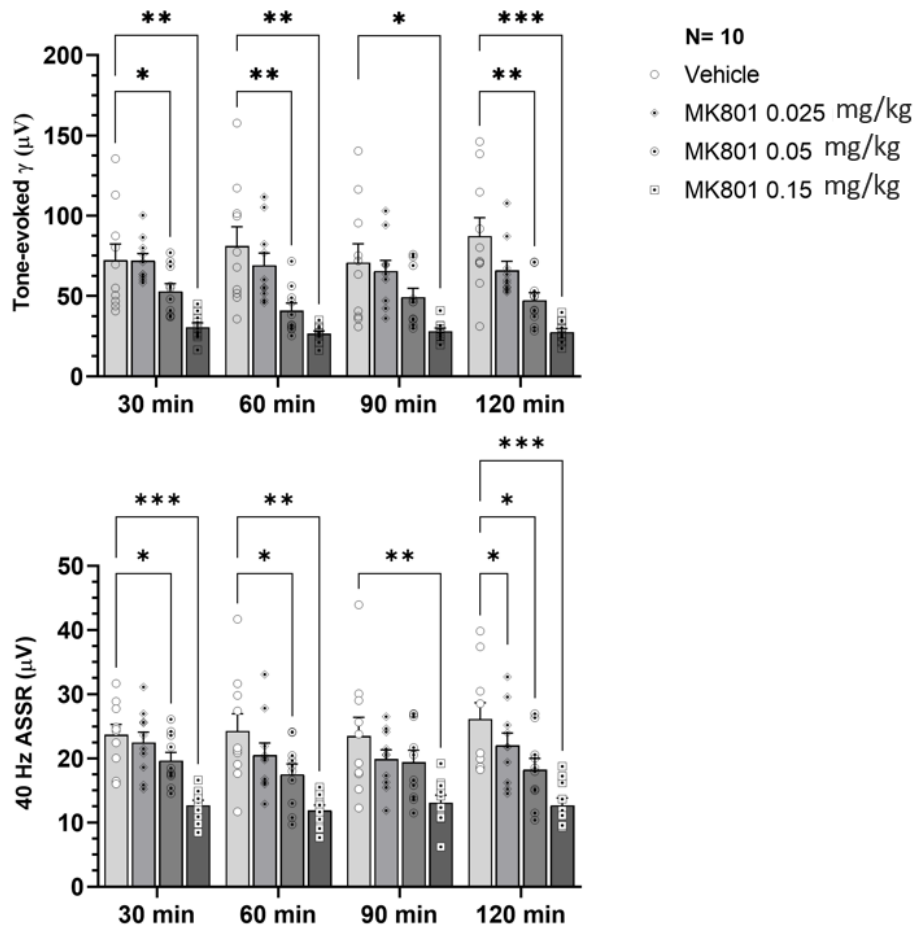**Figure 2.5.** Compilation of RMS data of tone-evoked gamma (top panel) and 40-Hz ASSR (bottom panel) in a group of rats treated with vehicle or MK801 (0.025, 0.05, or 0.15 mg/kg sc), at discrete time points (30, 60, 90, and 120 min). Significant differences between vehicle treatment and MK801 treatment are indicated by asterisks (*/**/***indicates $p < 0.05/0.01/0.001$; Dunnett's post hoc tests). Data are from a group of 10 rats.

Discussion

Circuit-based functional biomarkers are critical for early phase drug development; for prioritizing lead candidates in preclinical species and in the clinic for dose selection, proof of concept, and patient stratification (Light et al., 2020; Spellman and Gordon, 2015). While there are several recent clinical reports that show test-retest reliability for tone- and train-evoked gamma oscillations (Cervenka et al., 2013; Legget et al. 2017; McFadden et al., 2014; Tan et al., 2015), such findings only infrequently extend beyond a few test sessions (Ip et al., 2018; Roach et al., 2019). To date, complementary reliability studies of evoked gamma in preclinical species are unavailable. Thus, our current report addresses an important translational knowledge gap by establishing test-retest reliability of tone- and 40 Hz-train-evoked gamma oscillations across multiple sessions and time points, spread over a 3-week period.

Since our interest is in using these EEG measures for pharmacological testing using repeated measures design, we evaluated time and session effects (fixed variables) with subjects modeled as random effect, using a mixed-effects analysis. We found a robust time effect with time-zero response tending to be smaller in comparison to all other time points. Although rats were extensively acclimated, transfer from home cage to the recording chamber triggered an arousal response that may have affected the initial time point (Griskova-Bulanova et al., 2011; Griskova et al., 2007). Indeed, this period is often coincident with increased exploration of the recording chamber and whisking that dwindles over the following 30-min period (Drake et al. 1991).

We used female rats but did not monitor the estrous cycle during the study. While there was some session-to-session variability, it was not significant at the group level. It is however

not possible to conclude that estrous cycling did not affect the measures in question. This is something that needs studying in future along with determining psychometric reliability in males. There was no effect of session or session × time on the EEG measures. Since exploratory analysis suggested that response at time zero drove the time effect, we decided to omit sampling at time zero in the pharmacological study, to simplify data interpretation. This appeared to have removed time as a significant factor.

Our results indicate that while tone-evoked gamma and 40 Hz train-evoked gamma responses show acceptable reliability, 40-Hz ASSR is superior. Thus, at the group level, 40-Hz ASSR had a lower re-test related variance, compared to tone-evoked gamma. Since the same group of rats were repeatedly tested, we had an opportunity to evaluate if for a given subject, one measure evoked a more consistent response. We found that across ~30 test occasions conducted with the same 12 subjects, ASSR showed a consistently smaller CV than tone-evoked gamma, suggesting that the ASSR measure is less variable.

For testing the effect of the open channel blocker MK801 on gamma oscillations, we chose to include a range of doses that spanned an estimated occupancy of ~20 to 70% of the NMDA receptor pool (Fernandes et al., 2015). MK801 showed robust suppression of both the evoked measures at 0.05 mg/kg and 0.15 mg/kg doses. However, 0.025 mg/kg of MK801 was effective only against 40-Hz ASSR. The lower variance in the ASSR may have helped reveal the low dose effect.

In summary, we report the test-retest reliability of two frequently used response markers of sensory cortical circuit function that lend themselves for use as pharmacodynamic biomarkers. While both display acceptable psychometric properties for use in preclinical drug discovery and

are sensitive to disruption of NMDA neurotransmission, particularly in the context of within

subject repeated measures, 40-Hz ASSR has a quantitative edge over tone-evoked gamma.

References

Brenner, C. A., Krishnan, G. P., Vohs, J. L., Ahn, W. Y., Hetrick, W. P., Morzorati, S. L., & O'Donnell, B. F. (2009). Steady state responses: Electrophysiological assessment of sensory function in schizophrenia. In Schizophrenia Bulletin (Vol. 35, Issue 6, pp. 1065–1077). Oxford Academic. https://doi.org/10.1093/schbul/sbp091

Buzsáki, G., & Wang, X.-J. (2012). Mechanisms of Gamma Oscillations. Annual Review of Neuroscience, 35(1), 203–225. https://doi.org/10.1146/annurev-neuro-062111-150444

Cardin, J. A., Carlén, M., Meletis, K., Knoblich, U., Zhang, F., Deisseroth, K., Tsai, L. H., & Moore, C. I. (2009). Driving fast-spiking cells induces gamma rhythm and controls sensory responses. Nature, 459(7247), 663–667. https://doi.org/10.1038/nature08002

Cervenka, M. C., Franaszczuk, P. J., Crone, N. E., Hong, B., Caffo, B. S., Bhatt, P., Lenz, F. A., & Boatman-Reich, D. (2013). Reliability of early cortical auditory gamma-band responses. Clinical Neurophysiology, 124(1), 70–82. https://doi.org/10.1016/j.clinph.2012.06.003

Cleophas, T. J. M., & De Vogel, E. M. (1998). Crossover studies are a better format for comparing equivalent treatments than parallel-group studies. Pharmacy World and Science, 20(3), 113–117. https://doi.org/10.1023/A:1008626002664

Drake, M. E., Pakalnis, A., Phillips, B., Padamadan, H., & Hietter, S. A. (1991). Auditory Evoked Potentials in Anxiety Disorder. Clinical EEG and Neuroscience, 22(2), 97–101. https://doi.org/10.1177/155005949102200209

Fernandes, A., Wojcik, T., Baireddy, P., Pieschl, R., Newton, A., Tian, Y., Hong, Y., Bristow, L., & Li, Y. W. (2015). Inhibition of in vivo [3H]MK-801 binding by NMDA receptor open channel blockers and GluN2B antagonists in rats and mice. European Journal of Pharmacology, 766, 1–8. https://doi.org/10.1016/j.ejphar.2015.08.044

Gonzalez-Burgos, G., & Lewis, D. A. (2008). GABA Neurons and the Mechanisms of Network Oscillations: Implications for Understanding Cortical Dysfunction in Schizophrenia. Schizophrenia Bulletin, 34(5), 944–961. https://doi.org/10.1093/schbul/sbn070

Gonzalez-Burgos, Guillermo, & Lewis, D. A. (2012). NMDA receptor hypofunction, parvalbumin-positive neurons, and cortical gamma oscillations in schizophrenia. Schizophrenia Bulletin, 38(5), 950–957. https://doi.org/10.1093/schbul/sbs010

Griskova-Bulanova, I., Ruksenas, O., Dapsys, K., Maciulis, V., & Arnfred, S. M. H. (2011). Distraction task rather than focal attention modulates gamma activity associated with auditory steady-state responses (ASSRs). Clinical Neurophysiology, 122(8), 1541–1548. https://doi.org/10.1016/j.clinph.2011.02.005

Griskova, I., Morup, M., Parnas, J., Ruksenas, O., & Arnfred, S. M. (2007). The amplitude and phase precision of 40 Hz auditory steady-state response depend on the level of arousal. Experimental Brain Research, 183(1), 133–138. https://doi.org/10.1007/s00221-007-1111-0

Guo, Y., Logan, H. L., Glueck, D. H., & Muller, K. E. (2013). Selecting a sample size for studies with repeated measures. BMC Medical Research Methodology, 13(1), 100.

https://doi.org/10.1186/1471-2288-13-100

Ip, C. T., Ganz, M., Ozenne, B., Sluth, L. B., Gram, M., Viardot, G., l'Hostis, P., Danjou, P., Knudsen, G. M., & Christensen, S. R. (2018). Pre-intervention test-retest reliability of EEG and ERP over four recording intervals. International Journal of Psychophysiology, 134, 30–43. https://doi.org/10.1016/j.ijpsycho.2018.09.007

Javitt, D. C. (2009a). When doors of perception close: bottom-up models of disrupted cognition in schizophrenia. Annual Review of Clinical Psychology, 5, 249–275. https://doi.org/10.1146/annurev.clinpsy.032408.153502

Javitt, D. C. (2009b). Sensory processing in schizophrenia: Neither simple nor intact. In Schizophrenia Bulletin (Vol. 35, Issue 6, pp. 1059–1064). Oxford Academic. https://doi.org/10.1093/schbul/sbp110

Javitt, D. C., & Sweet, R. A. (2015). Auditory dysfunction in schizophrenia: Integrating clinical and basic features. In Nature Reviews Neuroscience (Vol. 16, Issue 9, pp. 535–550). Nature Publishing Group. https://doi.org/10.1038/nrn4002

Koo, T. K., & Li, M. Y. (2016). A Guideline of Selecting and Reporting Intraclass Correlation Coefficients for Reliability Research. Journal of Chiropractic Medicine, 15(2), 155. https://doi.org/10.1016/J.JCM.2016.02.012

Kozono, N., Honda, S., Tada, M., Kirihara, K., Zhao, Z., Jinde, S., Uka, T., Yamada, H., Matsumoto, M., Kasai, K., & Mihara, T. (2019). Auditory Steady State Response; nature and utility as a translational science tool. Scientific Reports, 9(1), 8454. https://doi.org/10.1038/s41598-019-44936-3

Krishnan, R. R., Kraus, M. S., & Keefe, R. S. E. (2011). Comprehensive model of how reality distortion and symptoms occur in schizophrenia: Could impairment in learning-dependent predictive perception account for the manifestations of schizophrenia? Psychiatry and Clinical Neurosciences, 65(4), 305–317. https://doi.org/10.1111/j.1440-1819.2011.02203.x

Lauschke, V. M., Zhou, Y., & Ingelman-Sundberg, M. (2019). Novel genetic and epigenetic factors of importance for inter-individual differences in drug disposition, response and toxicity. In Pharmacology and Therapeutics (Vol. 197, pp. 122–152). Elsevier Inc. https://doi.org/10.1016/j.pharmthera.2019.01.002

Legget, K. T., Hild, A. K., Steinmetz, S. E., Simon, S. T., & Rojas, D. C. (2017). MEG and EEG demonstrate similar test-retest reliability of the 40 Hz auditory steady-state response. International Journal of Psychophysiology, 114, 16–23. https://doi.org/10.1016/j.ijpsycho.2017.01.013

Leicht, G., Karch, S., Karamatskos, E., Giegling, I., Möller, H. J., Hegerl, U., Pogarell, O., Rujescu, D., & Mulert, C. (2011). Alterations of the early auditory evoked gamma-band response in first-degree relatives of patients with schizophrenia: Hints to a new intermediate phenotype. Journal of Psychiatric Research, 45(5), 699–705. https://doi.org/10.1016/j.jpsychires.2010.10.002

Leicht, G., Vauth, S., Polomac, N., Andreou, C., Rauh, J., Mußmann, M., Karow, A., & Mulert, C. (2016). EEG-Informed fMRI Reveals a Disturbed Gamma-Band-Specific Network in

Subjects at High Risk for Psychosis. Schizophrenia Bulletin, 42(1), 239–249. https://doi.org/10.1093/schbul/sbv092

Light, G. A., Joshi, Y. B., Molina, J. L., Bhakta, S. G., Nungaray, J. A., Cardoso, L., Kotz, J. E., Thomas, M. L., & Swerdlow, N. R. (2020). Neurophysiological biomarkers for schizophrenia therapeutics. Biomarkers in Neuropsychiatry, 2, 100012. https://doi.org/10.1016/j.bionps.2020.100012

Luck, S. J., Mathalon, D. H., O'Donnell, B. F., Hmlinen, M. S., Spencer, K. M., Javitt, D. C., & Uhlhaas, P. J. (2011). A roadmap for the development and validation of event-related potential biomarkers in schizophrenia research. In Biological Psychiatry (Vol. 70, Issue 1, pp. 28–34). Elsevier USA. https://doi.org/10.1016/j.biopsych.2010.09.021

McFadden, K. L., Steinmetz, S. E., Carroll, A. M., Simon, S. T., Wallace, A., & Rojas, D. C. (2014). Test-Retest Reliability of the 40 Hz EEG Auditory Steady-State Response. PLoS ONE, 9(1), e85748. https://doi.org/10.1371/journal.pone.0085748

Oribe, N., Hirano, Y., del Re, E., Seidman, L. J., Mesholam-Gately, R. I., Woodberry, K. A., Wojcik, J. D., Ueno, T., Kanba, S., Onitsuka, T., Shenton, M. E., Goldstein, J. M., Niznikiewicz, M. A., McCarley, R. W., & Spencer, K. M. (2019). Progressive reduction of auditory evoked gamma in first episode schizophrenia but not clinical high risk individuals. Schizophrenia Research, 208, 145–152. https://doi.org/10.1016/j.schres.2019.03.025

Perez, V. B., Roach, B. J., Woods, S. W., Srihari, V. H., McGlashan, T. H., Ford, J. M., & Mathalon, D. H. (2013). Early auditory gamma-band responses in patients at clinical high risk for schizophrenia. In Supplements to Clinical Neurophysiology (Vol. 62, pp. 147–162). Elsevier B.V. https://doi.org/10.1016/B978-0-7020-5307-8.00010-7

Rissling, A. J., & Light, G. A. (2010). Neurophysiological measures of sensory registration, stimulus discrimination, and selection in schizophrenia patients. In Current Topics in Behavioral Neurosciences (Vol. 4, pp. 283–309). Springer Verlag. https://doi.org/10.1007/7854_2010_59

Roach, B. J., D'Souza, D. C., Ford, J. M., & Mathalon, D. H. (2019). Test-retest reliability of time-frequency measures of auditory steady-state responses in patients with schizophrenia and healthy controls. NeuroImage: Clinical, 23, 101878. https://doi.org/10.1016/j.nicl.2019.101878

Roach, B. J., Ford, J. M., & Mathalon, D. H. (2019). Gamma Band Phase Delay in Schizophrenia. Biological Psychiatry: Cognitive Neuroscience and Neuroimaging, 4(2), 131–139. https://doi.org/10.1016/j.bpsc.2018.08.011

Ross, B., Schneider, B., Snyder, J. S., & Alain, C. (2010). Biological markers of auditory gap detection in young, middle-aged, and older adults. PLoS ONE, 5(4), 10101. https://doi.org/10.1371/journal.pone.0010101

Silverstein, S. M., & Keane, B. P. (2011). Vision science and schizophrenia research: Toward a re-view of the disorder editors' introduction to special section. In Schizophrenia Bulletin (Vol. 37, Issue 4, pp. 681–689). Schizophr Bull. https://doi.org/10.1093/schbul/sbr053

Sivarao, D. V. (2015). The 40-Hz auditory steady-state response: A selective biomarker for

cortical NMDA function. Annals of the New York Academy of Sciences, 1344(1), 27–36. https://doi.org/10.1111/nyas.12739

Sivarao, D. V, Chen, P., Senapati, A., Yang, Y., Fernandes, A., Benitex, Y., Whiterock, V., Li, Y.-W., & Ahlijanian, M. K. (2016). 40 Hz Auditory Steady-State Response Is a Pharmacodynamic Biomarker for Cortical NMDA Receptors. Neuropsychopharmacology, 41(9), 2232. https://doi.org/10.1038/NPP.2016.17

Spellman, T. J., & Gordon, J. A. (2015). Synchrony in schizophrenia: A window into circuit-level pathophysiology. In Current Opinion in Neurobiology (Vol. 30, pp. 17–23). Elsevier Ltd. https://doi.org/10.1016/j.conb.2014.08.009

Stroup, T. S., Lieberman, J. A., McEvoy, J. P., Swartz, M. S., Davis, S. M., Capuano, G. A., Rosenheck, R. A., Keefe, R. S. E., Miller, A. L., Belz, I., & Hsiao, J. K. (2007). Effectiveness of olanzapine, quetiapine, and risperidone in patients with chronic schizophrenia after discontinuing perphenazine: A CATIE study. American Journal of Psychiatry, 164(3), 415–427. https://doi.org/10.1176/ajp.2007.164.3.415

Tan, H. R. M., Gross, J., & Uhlhaas, P. J. (2015). MEG-measured auditory steady-state oscillations show high test-retest reliability: A sensor and source-space analysis. NeuroImage, 122, 417–426. https://doi.org/10.1016/j.neuroimage.2015.07.055

Tiesinga, P., & Sejnowski, T. J. (2009). Cortical Enlightenment: Are Attentional Gamma Oscillations Driven by ING or PING? In Neuron (Vol. 63, Issue 6, pp. 727–732). Neuron. https://doi.org/10.1016/j.neuron.2009.09.009

CHAPTER 3. THE 40 HZ ASSR RECORDED FROM THE VERTEX AND THE TEMPORAL REGIONS REPRESENT DISTINCT AND NOT REDUNDANT RESPONSES

Abstract

Rationale. Clinical literature indicates multiple cortical sources for the ASSR (Tada et al., 2019; Farahani et al., 2017). There have been at least eight cortical and subcortical primary generators of ASSR reported in previous studies (e.g., Farahani et al., 2019, 2021). However, recordings from the temporal region (targeting the primary auditory cortex) show the highest ASSR amplitude. Preclinically, epidural recording electrode positions are not standardized. ASSRs have been previously recorded from electrodes placed frontally, temporally or from the parietal cortex (Leishman et al., 2015; Sivarao et al., 2016; Kozono et al., 2019; Wang et al., 2020). Since the general practice has been to use one or the other but not all at the same time, it is unclear if any one position is more reliable than the others or if they all yield comparable results. To date, there have not been many studies that have made a head-to-head comparison between discrete regions to determine if: (1) one region is better than others or they have comparable reliability and (2) if they have comparable pharmacological sensitivity to test compounds.

Objective. We investigated the long-term stability and pharmacological sensitivity of 40 Hz ASSR recorded from vertex and temporal regions.

Methods. In the current study, we simultaneously recorded 40 Hz ASSR from the vertex and temporal electrodes in freely moving female rats, in four different sessions spanning a period of two weeks. Then, we evaluated the test-retest reliability of the measure through an intraclass correlation coefficient (ICC). Furthermore, we tested the effect of an open-channel NMDA receptor blocker MK-801 (0.025-0.1 mg/kg, SC) on the 40 Hz ASSR recorded from these two electrodes.

Results. We found that the 40 Hz ASSR obtained from the vertex region (overlying the retrosplenial cortex, a region implicated in episodic memory, navigation, and planning), while showing a smaller amplitude, had a good test-retest reliability, whereas the temporal 40 Hz ASSR, despite having a large amplitude and strong intertrial coherence, showed a relatively poor test-retest reliability. In the pharmacology study, vertex showed a strong dose-dependent reduction in 40 Hz ASSR in response to MK801, as demonstrated previously (Raza and Sivarao 2021). However, temporal 40 Hz ASSR did not show a comparable disruption. In a follow up study, we evaluated if a 3-fold higher dose of MK801 (0.3 mg/kg) would engender a reduction on the temporal cortex derived 40 Hz ASSR. Indeed, this higher dose of MK801 did strongly disrupt the temporal response.

Conclusion. These results show marked regional differences in the properties of the 40 Hz ASSR. Our results also highlight the observation that an identical stimulus paradigm can yield circuit responses with differing psychometric properties. Moreover, it is critical to understand these differences before pursuing pharmacology studies in preclinical species, especially when repeated measures design, rather than parallel groups is employed. Our results further indicate that the vertex region which involves the retrosplenial cortex, a region that is increasingly recognized to be involved in a range of cognitive functions like learning, spatial navigation, and episodic memory (Vann et al., 2009; Stacho and Manahan-Vaughan, 2022), is highly sensitive to NMDA blockade. On the other hand, the 40 Hz ASSR response from the temporal cortex seems less sensitive to NMDAR blockade.

Introduction

Auditory steady-state response (ASSR) is an entrained response of cortical neural populations synchronized to short trains of auditory click stimuli (Brenner et al., 2009). The evoked response recorded through EEG or MEG shows neural activity which is time and phase-locked to the driving stimulus frequency. ASSR has utility in audiometry and for monitoring the state of arousal under anesthesia (Draganova et al., 2008; Borck et al., 2011; Haghighi et al., 2018). ASSR, especially at gamma frequency (~ 40 Hz), is disrupted in schizophrenia (Thuné et al., 2016; Brenner et al., 2009), as well as in other psychiatric conditions such as bipolar depression (Rass et al., 2010) and autism (Seymour et al., 2020).

Due to the translational replicability of EEG across mammalian species, EEG-based biomarkers, in principle, provide an excellent tool to probe not only circuit function but also test promising therapeutic approaches for psychiatric illnesses. Studies have shown robust deficits in ASSR measures like evoked power and inter-trial coherence in schizophrenia patients (Brenner et al., 2009; Thuné et al., 2016). This has led to the development of pre-clinical animal models mimicking 40 Hz ASSR deficits as seen in human psychiatric subjects. Pharmacological manipulation in the form of acute dosing with NMDA receptor (NMDAR) antagonists like PCP (Leishman et al., 2015), Ketamine (Plourde et al., 1997; Sivarao et al., 2016), or MK-801 (Wang et al., 2020; Sivarao et al., 2013) disrupt 40 Hz ASSR synchrony. Moreover, genetic ablation of the NR1 subunit of NMDAR complex also demonstrated a selective entrainment deficit at gamma frequencies (Carlén et al., 2012; Nakai and Nakazawa 2014). Thus, 40 Hz ASSR has been proposed as a pharmacodynamic biomarker to investigate NMDAR-associated pathophysiology in schizophrenia and facilitate NMDAR-focused antipsychotic development (Sivarao, 2015).

Modeling schizophrenia, an essentially human malady in animals, poses a formidable challenge (Weickert et al., 2013). The use of circuit-based markers like 40 Hz ASSR as an intermediate phenotype may prove to be a more translatable and therefore viable proposition. At present, however, there is no uniformity of protocols for ASSR recording in preclinical species. Different studies have reported ASSR results by recording EEG from different cortical regions (Conti et al., 1999; Sivarao et al., 2016; Kozono et al., 2019; Wang et al., 2018). Moreover, there is only one study that we are aware of, that compared how a particular intervention (anesthesia) affected the same measure recorded concurrently from two or more anatomically discrete regions (Wang et al., 2018). This is an important question as we know that there are multiple generators in the brain for the 40 Hz ASSR (Farahani et al., 2019, 2021). However, it is unclear if they represent redundant or independent processes. Where there are multiple sources, it remains to be established if each of them are equally reliable or if some are more stable than others. This is an especially pertinent question when crossover designs are used to limit individual subject variability, as the same subject gets tested on different occasions, over a significant period. At the same time, it also remains to be established if such multiple sources are equally sensitive to pharmacological intervention.

In the current study, we implanted female Sprague Dawley (SD) rats with temporal and vertex electrodes for simultaneous recording of 40 Hz ASSR, while unrestrained. These two sites ostensibly represent electrical activity from the underlying regions, the primary auditory cortex, and the retrosplenial cortex, respectively. In the first experiment, we compared not only the stimulus-evoked responses but also their test-retest reliability across vertex and temporal electrodes. Furthermore, we compared the effect of the non-selective NMDAR inhibitor MK-801 on 40 Hz ASSR from the vertex and temporal recordings in a cross-over study design. We tested

76

three different doses of MK-801 (i.e., 0.025, 0.05, and 0.1 mg/kg), which show a wide range of

NMDAR occupancy to compare the sensitivity of 40 Hz ASSR recorded form vertex and

temporal regions to NMDAR inhibition. The current study provides important insight into the

recording-site specific test-retest reliability, and sensitivity of 40 Hz ASSR to NMDAR

inhibition. Studies like this are a crucial step in establishing 40 Hz ASSR as a translational

biomarker in psychiatric research.

Methods

General

The Institutional Animal Care and use Committee of the East Tennessee State University

approved all experimental procedures involving animal subjects. Female Sprague Dawley rats

(6-8-week-old; 200-250 g) were obtained from Envigo (Indianapolis, IN) and group housed until

surgery, with free access to food and water.

Surgery

Each rat was implanted with epidermal electrodes through stereotaxic surgery. Isoflurane

(5%) was used to induce anesthesia and the head was fixed in the stereotaxis frame. Anesthesia

was maintained with 2% isoflurane during surgery. Aseptic techniques were strictly followed to

avoid contamination and infection. The surgery area was cleaned with alcohol and iodine swabs.

Bupivacaine was infiltrated under the skin above the skull as field anesthesia. Meloxicam (1

mg/kg, sc) was given as part of perioperative analgesia. The skull was exposed through a single

midline incision on the scalp. A blunt instrument was used to scrape the tissue off the skull and

hydrogen peroxide (H_2O_2) was used to disinfect and dry the exposed bone. A 4 mm exposed

area was created by bisecting and removing the temporalis muscle to expose the temporal ridge as described previously (Kozono, et. al., 2019). Any bleeding was stopped though a cauterizer. A handheld drill bit was used to drill four holes in the skull at the following coordinates: from bregma, -4mm AP/ -1mm ML (vertex electrode; overlying the retrosplenial cortex); from bregma, -4 mm AP, 7.5 lateral to the sagittal suture, and -4 mm DV (temporal electrode; overlying the primary auditory cortex); from lambda, -2 mm AP, ±2 mm bilaterally (ground and reference electrodes, overlying the cerebellum). The electrode positions are marked in fig. 3.1-A. The stainless-steel electrodes with attached wires were gently screwed into the holes without causing any damage to dura mater. Dental cement slurry was used to cover the electrodes and the free ends of the electrode wires were fused to the EEG head mount through a solder. All the exposed wires were covered with another layer of dental cement. Nylon sutures were used to stitch the area and the wound was covered with a topical antibiotic ointment. A single tablet of Baytril (2mg/tab) was given for 7 days post-surgery to prevent postoperative infection.

Experimental Protocol

40 Hz ASSR recordings were carried out as described previously (Raza and Sivarao, 2021). Briefly, each rat was placed in the recording chamber and the headpiece was connected to the recording setup through a preamplifier cable. Auditory stimuli were presented, and EEG was simultaneously recorded through an acquisition device (CED Micro 1401-3; Cambridge Electronics Design (CED), Cambridge, UK)). Signal software was used to acquire EEG data at a sampling rate of 1000 Hz. Auditory stimuli consisted of a 1-second long 40 Hz click train (square wave, 65dB intensity, and 50 msec click duration) in a 3.5 second trial, which was repeated in rapid succession, 75 times. Each recording session started after a 10-minute

acclimation period. For the test-retest reliability study, rats were recorded for a 120-minute period, at 30 minutes intervals (i.e., 30, 60, 90 and 120 minutes) in a single session. Recordings were repeated for four sessions spanning a period of two weeks with a three-day interval between each recording session. In the MK-801 pharmacology study, a crossover study design was followed, where each rat received a different treatment as per a Latin square design, on different recording sessions. The washout period between sessions was at least 3 days and the study was completed in two weeks. MK-801 (as maleate salt from Sigma-Aldrich) was dissolved in 0.9% saline to prepare a stock solution of 0.1 mg/ml (based on free base mass), which was aliquoted and kept at -200C. Serial dilutions were made before dosing to appropriate concentrations.

EEG Data Analysis

The acquired EEG data was screened for chewing associated artifacts and only artifact free trials were selected for analysis (~70). Time-frequency analysis (TFA) was performed in the EMSE data editor software v5.6.1 (Cortech solutions, Wilmington, NC). Signal software v7.1 was used to first record the raw data, which were then exported as text files. The text files were then imported into EMSE v5.X software (Cortech Solutions Inc., Wilmington, NC). Morlet transformation was applied for TFA to obtain evoked power and inter-trial phase coherence (ITC). TFA involves convolution of the Morlet wavelet with EEG waveform to obtain time-varying wavelet transform coefficients (complex valued). Information about the amplitude (M) and phase (φ) are extracted from these complex valued coefficients (Morales and Bowers, 2022). ITC value represent trial-to-trial phase consistency, while evoked power is the measure of averaged 40 Hz ASSR power. Both ITC and evoked power measure 40 Hz ASSR signal, which

is time-locked to stimulus onset (Brian J. Roach and Mathalon, 2008). Peak and area

measurements of 40 Hz ASSR for ITC and evoked power were obtained to perform statistical
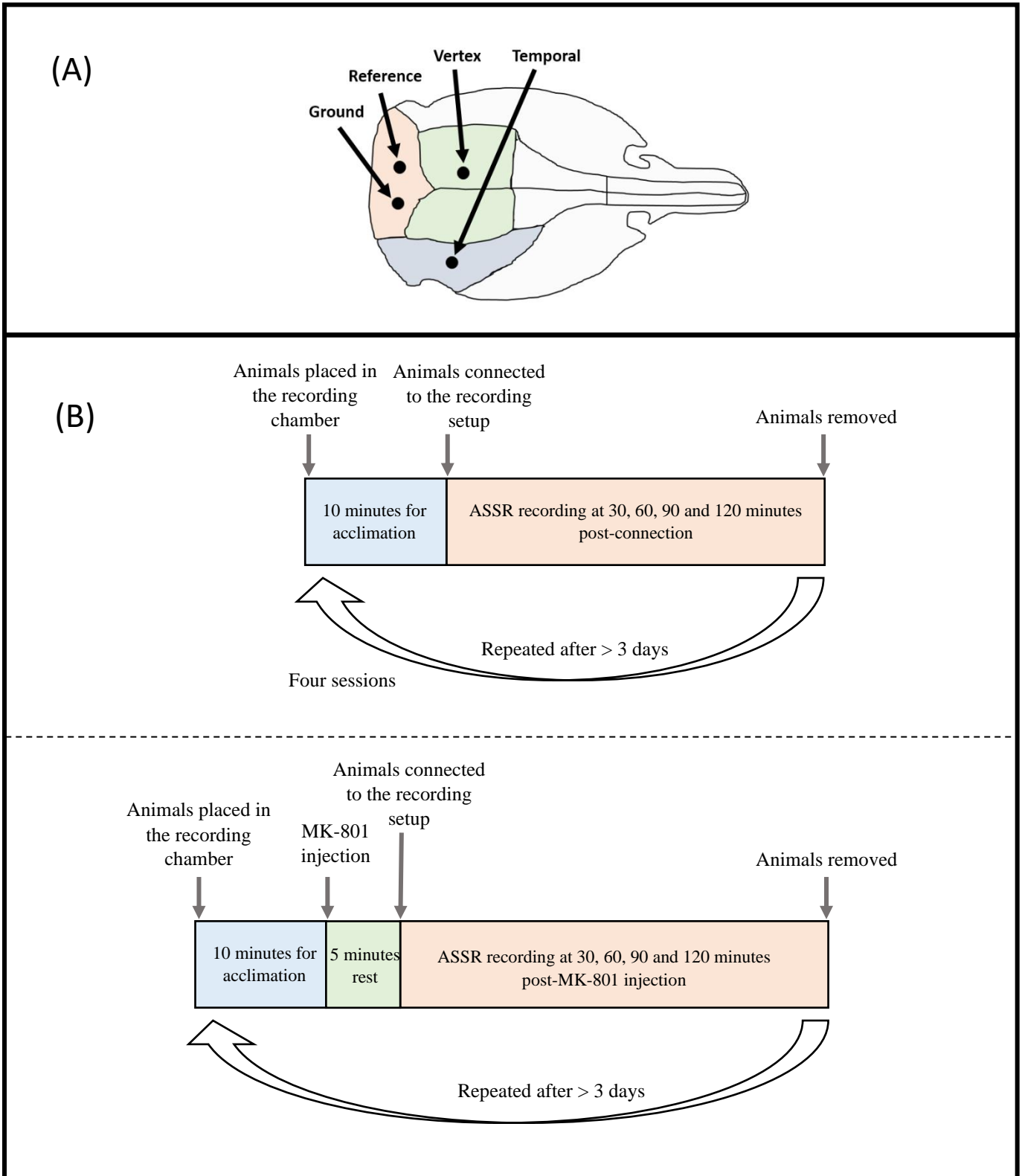
Figure 3.1. Schematic representations of the electrode placement (A), and study design for test-retest reliability and pharmacology studies (B). (sc) indicates subcutaneous dosing.

analysis. TFA was also performed on the concatenated data from each group to obtain summary results for representation.

Statistical Analysis

The key objective for the current study was to determine the suitability of vertex and temporal regions for 40 Hz ASSR recording in a repeated measures design. We first analyzed the effect of brain regions on 40 Hz ASSR recording. Then we examined the systematic effect of repeated testing on 40 Hz ASSR recorded from vertex and temporal regions simultaneously. We also compared the pharmacological effects of MK-801 treatment on vertex and temporal 40 Hz ASSR. We used a mixed-effects ANOVA (restricted maximum likelihood estimation as applied in GraphPad Prism v9.3.1 software) to determine the effect of brain region, repeated testing, and MK-801 treatment on 40 Hz ASSR. Time of recording was always selected as a row factor, while brain region, recording sessions, or pharmacological treatment were selected as a column factor. Data normality was ensured through Quantile-quantile (q-q) plot. In case the data were non-linear, we log transformed the data first to confirm linearity and then, parametric statistics were applied. Greenhouse-Geisser correction was implemented without assuming sphericity. Where appropriate, Bonferroni or Dunnett's post hoc analysis were used to measure between regions, sessions or treatment significance. In reliability study, session 1 was selected as comparator to measure between sessions significance, while 30 minutes timepoint was selected as comparator to measures within session significance, In the MK-801 pharmacology study,

vehicle group was selected as a comparator. Data are represented as group mean along with the SEM.

Test-retest reliability of the 40 Hz recording from the vertex and temporal electrodes was measured through the intra-class correlation coefficient. We chose mixed-effects, absolute agreement, and single measurement model for consistency with the previous studies as discussed previously (Koo and Li, 2016; Raza and Sivarao, 2021). Test-retest reliability between 4 sessions was measured for each of the four time-intervals (30-120 min). Sessions were selected as column factor and rats were selected as row factors for each time-intervals. SPSS statistical package (SPSS v26, Chicago, IL) was used to estimate ICC along with 95% confidence interval. ICC values were categorized as poor (<0.39), fair (0.40-0.59), good (0.60-0.75), and excellent (>0.76) (Ip et al., 2018; Raza and Sivarao, 2021). The variability of 40 Hz ASSR was measured through % coefficient of variation (% CV).

Results

Temporal Recordings Showed A Significantly Higher 40 Hz ASSR As Compared To Vertex

Clear evoked responses in the form of a large registration potential (P1-N1-P2) followed by visible entrainment of the click stimuli were recorded from both vertex and the temporal cortex. However, the recordings from the temporal cortex tended to be several fold larger than the vertex response (fig. 3.2-A). Filtered and unfiltered grand average compilation of vertex and temporal 40 Hz ASSR recordings are shown in fig. 3.2-A. Mixed-effects ANOVA with repeated measures design showed a highly significant effect of recording sites on ITC (p<0.0001; $F_{(1, 9)}$ = 80.40; epsilon = 1). However, there was no significant time effect (p=0.3319; $F_{(2.065, 18.58)}$

= 1.176; epsilon = 0.6883) or significant interaction between time and recording sites (p=0.1972; F (1.762, 15.85) = 1.813; epsilon = 0.5872). Further post hoc analysis showed a significantly higher 40 Hz ASSR ITC recorded from temporal region, as compared to vertex across at all time points (p<0.01-p<0.0001)

Evoked power also showed a highly significant effect of recording sites (p<0.0001; F (1, 9) = 89.93; epsilon = 1). However, there was no significant time effect (p=0.5350; F (1.586, 14.27) = 0.5793; epsilon = 0.5287) or significant interaction between time and recording sites (p=0.3619; F (2.010, 18.09) = 1.077; epsilon = 0.67). Multiple comparison revealed significantly higher evoked power of temporal 40 Hz ASSR, relative to vertex 40 Hz ASSR (p<0.001-(p<0.0001). Group mean summaries for ITC and evoked power of 40 Hz ASSR recorded from vertex and temporal regions are summarized in fig. 3.2 (B and C).
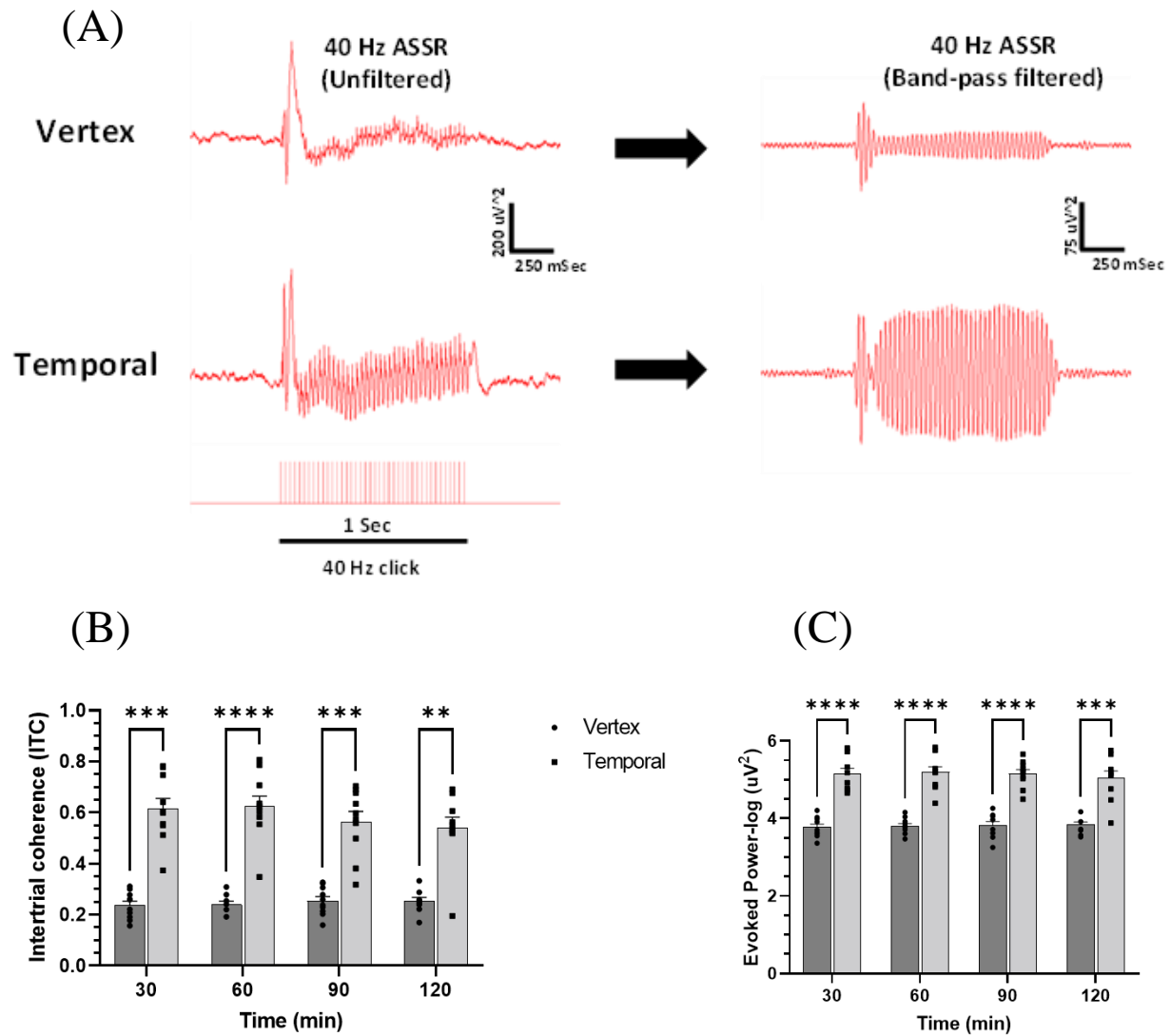
Figure 3.2. Comparison of 40 Hz ASSR recorded from vertex and temporal regions. A compilation of grand average (n=12) of unfiltered and narrow-band filtered (35–45 Hz) 40 Hz ASSR recorded from vertex and temporal regions (A) at 60 minutes time point. Time frequency analysis (TFA) was performed to calculate ITC (A), and evoked power (B) for vertex and temporal 40 Hz ASSR. The data represent group summaries from 12 rats, across 30, 60, 90, and 120 minutes from session 1. Significant differences between vertex and temporal 40 Hz ASSR are indicated by asterisks (**/***/****indicates $p<0.01$/$p<0.001$/0.0001; Bonferroni post hoc test).

40 Hz ASSR Recording From Vertex Showed Good Test-Retest Reliability, While Reliability Of Temporal 40 Hz ASSR Was Poor

In order for 40 Hz ASSR to be a translational biomarker, it must have good reliability. We tested the consistency of 40 Hz ASSR evoked power over a period of two weeks spanning four sessions. We performed repeated measures ANOVA on the evoked power data obtained from vertex and temporal recording sites to calculate between sessions and within session differences. Evoked power for vertex 40 Hz ASSR showed a significant session effect ($p < 0.05$; $F_{(2.689, 26.89)} = 4.726$; epsilon = 0.8963) on group means. However, there was no effect of time ($p = 0.6533$; $F_{(1.933, 19.33)} = 0.4247$; epsilon = 0.6445) or time x session interaction ($p = 0.4024$; $F_{(4.194, 41.94)} = 1.035$; epsilon = 0.4660). Dunnett's post hoc analysis, with session 1 as a comparator showed a significant difference with session 4 ($P < 0.05$) at only 30 minutes.

Then, we then analyzed the systematic effect of repeated testing on temporal 40 Hz ASSR evoked power. Repeated measures ANOVA showed a highly significant time effect ($p < 0.001$; $F_{(2.46, 24.59)} = 8.60$; epsilon = 0.82) but no session effect ($p > 0.05$; $F_{(1.99, 19.92)} = 2.23$; epsilon = 0.66) or time x session interaction ($p > 0.05$; $F_{(3.89, 38.86)} = 2.25$; epsilon = 0.43). Post hoc multiple comparisons (Dunnett's) showed that group means at 30 minutes time-point were significantly different from 90 and 120 minutes in session 1 ($p < 0.05$), and from 90 ($p < 0.05$), 60 and 120 ($p < 0.01$) minutes in session 2, 3 and 4, respectively.

Intraclass correlation coefficient (ICC) was measured to calculate reliability of 40 Hz ASSR recordings from the vertex and temporal regions. Vertex showed good test-retest reliability (ICC = 0.6-0.75) except at 30 minutes (ICC = 0.40-0.59). Whereas the test-retest reliability of temporal 40 Hz ASSR was poor (ICC = 0-0.14) across all sessions for all time

points. The ICC values for each time point across 4 sessions, along with their 95% CIs, are

shown in Table 1. We did not perform pairwise comparisons of ICCs for vertex and temporal 40

Hz ASSR, as the difference in ICCs between the two groups is noticeable from table 1.

Table 3.1. ICC For 40 Hz ASSR Evoked Power From Vertex And Temporal Recording. ICC
values for four sessions across time points (i.e., 30, 60, 90 and 120 minutes) were calculated
using a two-way mixed-effects model, single measurement, and absolute agreement criteria (Koo
and Li 2016). The data are from a group of 12 rats.

Time	Vertex		Temporal	
	ICC	95% CI	ICC	95% CI
30	0.5	0.21-0.79	0	0-0.34
60	0.67	0.40-0.88	0.14	0-0.51
90	0.67	0.40-0.88	0.07	0-0.44
120	0.65	0.38-0.87	0.06	0-0.41

We also performed Pearson's correlation analysis for each time points between session 1 and the

rest of the sessions (i.e., sessions 2-4). Vertex recordings of 40 Hz ASSR showed a moderate

correlation across sessions (r = 0.53-0.87), whereas there was no correlation across sessions for

temporal recordings. Table 3.2 shows Pearson's correlation coefficient (r) values for vertex and

temporal 40 Hz ASSR recordings.

Table 3.2. Pearson's Correlation Coefficient (R) Values For Vertex And Temporal Recording Of 40 Hz ASSR. Vertex data showed moderate correlation between session 1 and other sessions (r>0.5), whereas temporal lead showed a poor and variable correlation. The data are from a group of 12 rats.

Time	Sessions	Session 2		Session 3		Session 4	
		Vertex	Temporal	Vertex	Temporal	Vertex	Temporal
30 Minutes	Session 1	0.5314	-0.1373	0.6292	-0.5094	0.5312	0.1935
60 Minutes	Session 1	0.6371	-0.169	0.6029	-0.1893	0.6707	0.1453
90 Minutes	Session 1	0.7012	-0.03128	0.8724	-0.005014	0.5823	0.2794
120 Minutes	Session 1	0.5818	-0.009851	0.6371	0.5857	0.5184	-0.05542

Then, we calculated CV, as a measure of individual animal's response precision for 16 recordings (i.e., 4-time points x 4 sessions). Vertex 40 Hz ASSR showed a markedly lower mean CV at 29.3 %. Whereas temporal 40 Hz ASSR showed a significantly higher mean CV at 71.2%. Fig. 3.3 highlights the differences between these two measures as a violin plot (p=0.0001; paired t-test).
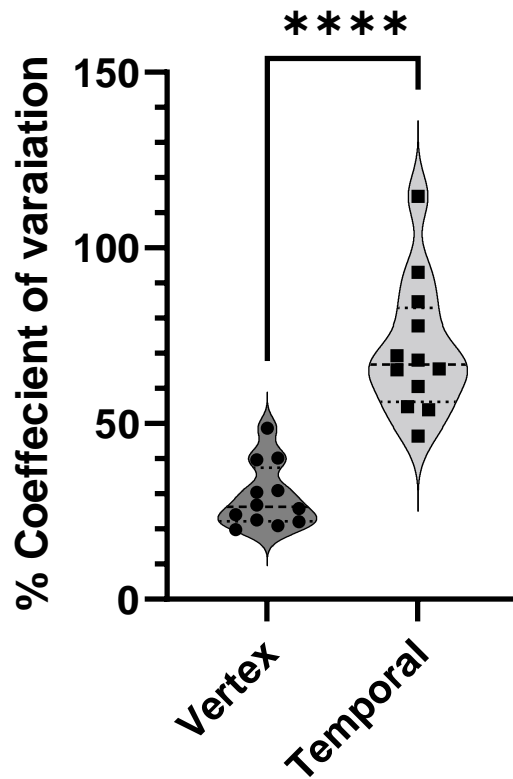
Figure 3.3. Summary of % CV of vertex and temporal 40 Hz ASSR evoked power from a group of 12 rats. Dots and squares represent individual animals within the violin plots. Asterisks indicate significant difference between the two groups (p <0.0001; paired t-test).

Next, we compared the sensitivity of vertex and temporal 40 Hz ASSR to open channel NMDA blocker MK-801. We selected three doses of 0.025, 0.05 and 0.1 mg/kg MK-801 to represent a range of NMDA channel blockade (Fernandes et al., 2015). Rats showed a stereotyped behavior with head weaving and circumambulation after 0.1 mg/kg MK-801 that lasted for up to 3 hours, whereas 0.025 or 0.05 mg/kg MK—801 did not induce any discernible behavioral changes.

Vertex 40 Hz ASSR showed a highly dose-dependent reduction in ITC and evoked power by MK-801. Mixed-effects ANOVA for ITC showed a robust treatment effect ($p<0.0001$; $F_{(2.214, 19.92)} = 48.62$; epsilon = 0.7379) but no time effect ($p=0.3345$; $F_{(1.881, 16.93)} = 1.159$; epsilon = 0.6271). However, there was a significant time $\times$ treatment interaction ($p<0.05$; $F_{(3.556, 30.02)} = 3.648$; epsilon = 0.3951). Post hoc comparisons using Dunnett's test showed that 0.05 and 0.1 mg/kg doses of MK801 significantly ($p<0.01$) attenuated vertex 40 Hz ASSR ITC at multiple time-points, as compared to vehicle treatment (fig. 3.4-B).

Evoked power also showed a highly significant treatment effect ($p<0.0001$; $F_{(2.004, 18.04)} = 38.66$; epsilon = 0.6680) but no time effect ($p= 0.3191$; $F_{(2.085, 18.77)} = 1.220$; epsilon = 0.6951) or time $\times$ treatment interaction ($p=0.1120$; $F_{(2.245, 20.21)} = 1.728$; epsilon = 0.4858). Post hoc analysis showed significant reduction ($p<0.01$) by only 0.05 and 0.1 mg/kg doses of MK801 at multiple time-points, as compared to vehicle treatment (fig. 3.4-C). Fig. 3.4-A shows the group summary of ITC, and evoked power, at the 60 minutes-post vehicle or MK-801 injection, represented as heat maps.
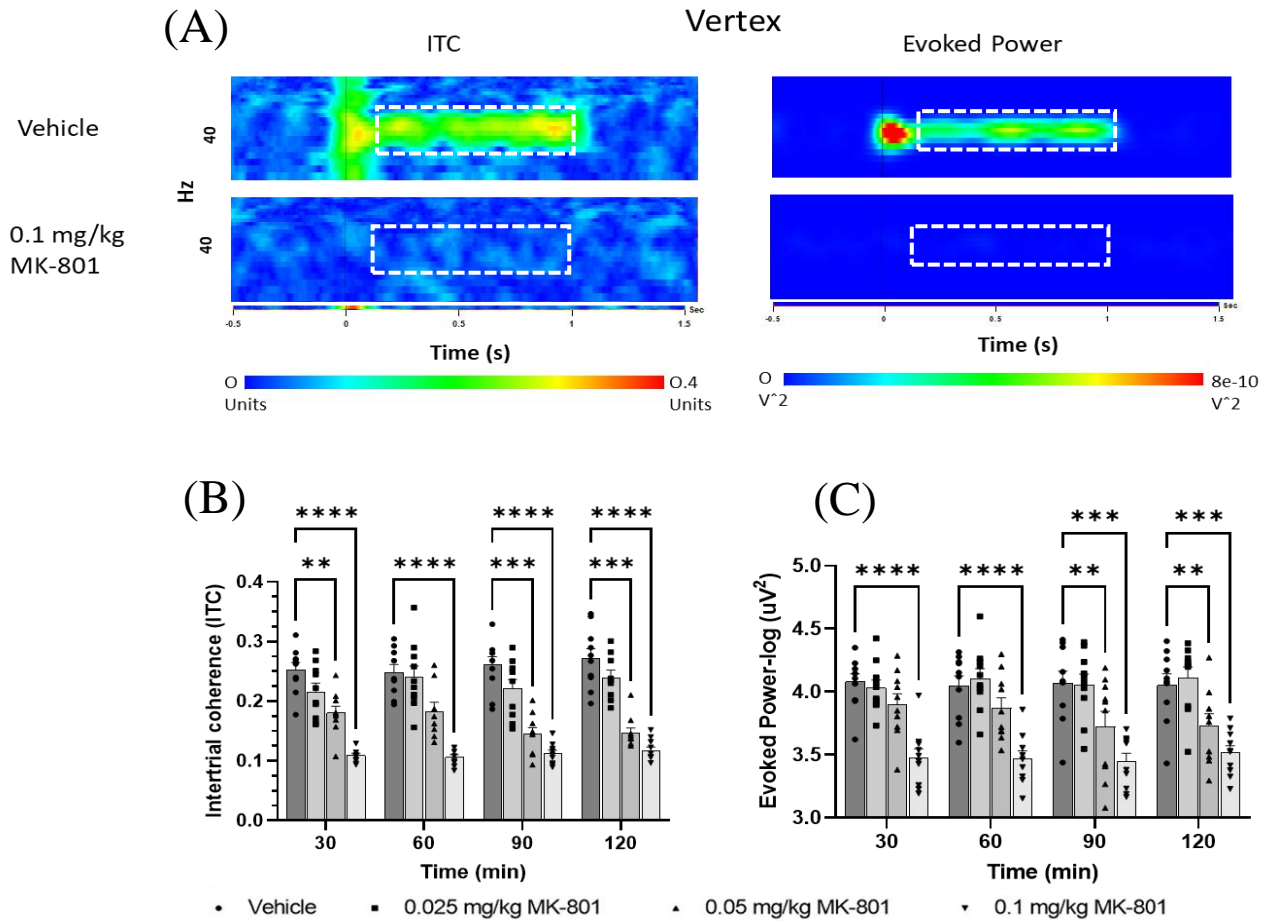
Figure 3.4. Effect of MK-801 on vertex 40 Hz ASSR. Heat-map summaries of ITC and evoked power (A) at 60 minutes after vehicle or 0.1 mg/kg MK-801 (sc) treatment. Group summaries of ITC (B) and evoked power (C) data at 30, 60, 90 and 120 minutes after vehicle or MK-801 (0.025, 0.05, or 0.1 mg/kg, sc) treatment. Data are from a group of 10 rats. (**p<0.01, ***p<0.001, ****p<0.0001; Dunnett's post hoc).

MK-801 Did Not Cause A Significant Attenuation In Temporal 40 Hz ASSR

In contrast to vertex, MK-801 did not show any significant effect on temporal 40 Hz ASSR ITC and evoked power. Mixed-effects ANOVA for ITC showed no treatment effect (p=0.1189; $F_{(2.181, 19.63)} = 2.342$; epsilon = 0.7269). However, there was a significant time

effect (p<0.0001; F (2.283, 20.54) = 2.342; epsilon = 0.7609), and a significant time × treatment

interaction (p<0.01; F (4.056, 36.05) = 5.353; epsilon = 0.4507). Post hoc comparisons using

Dunnett's test showed that only 0.025 mg/kg MK801 significantly (p<0.05) increased temporal

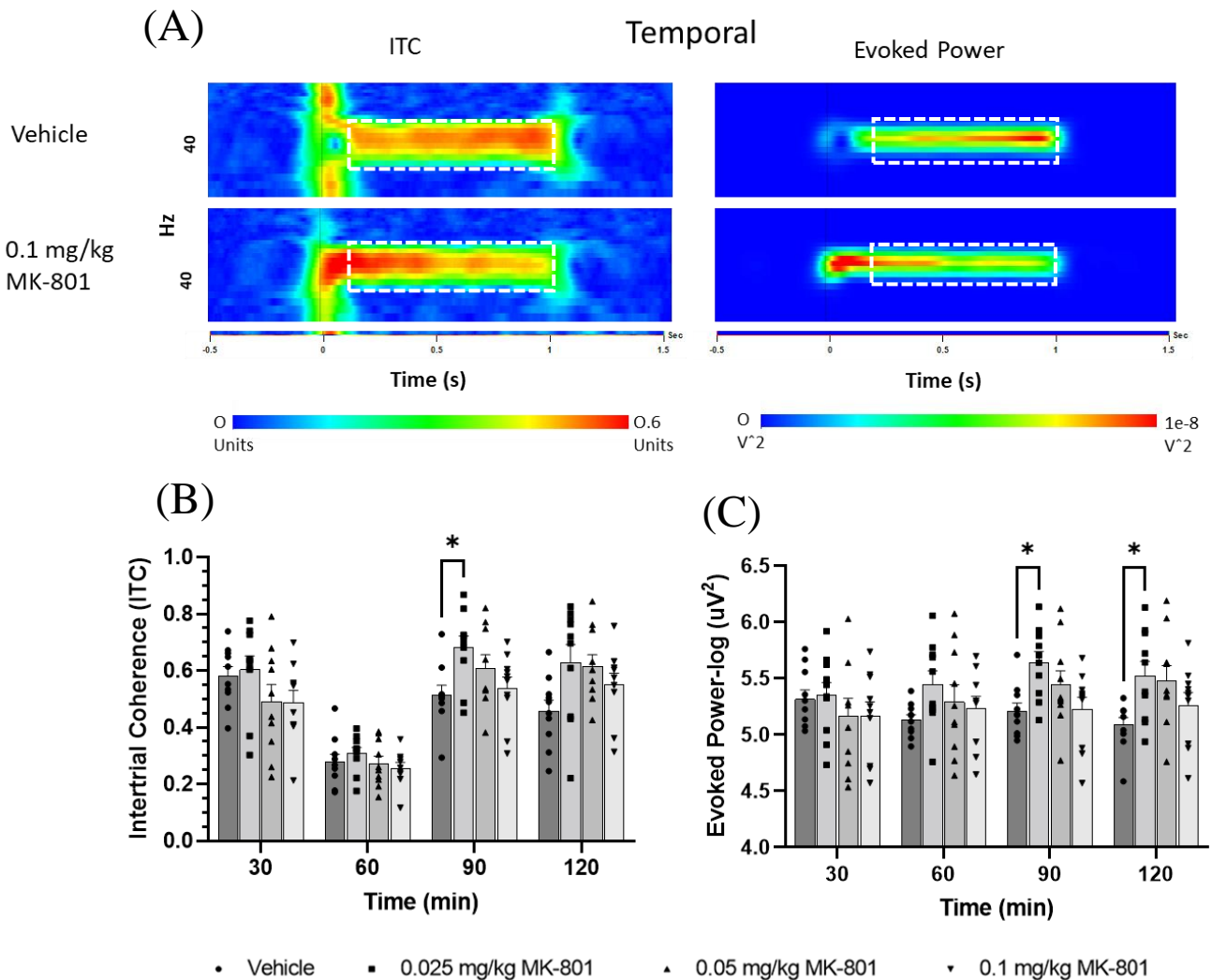40 Hz ASSR ITC only at 90 minutes time point, relative to vehicle treatment (fig. 3.5-B).

Figure 3.5. Effect of MK-801 on temporal 40 Hz ASSR. Heat-map summaries of ITC and
evoked power (A) at 60 minutes after vehicle or 0.1 mg/kg MK-801 (sc) treatment. Group

summaries of ITC (B) and evoked power (C) data at 30, 60, 90 and 120 minutes after vehicle or MK-801 (0.025, 0.05, or 0.1 mg/kg, sc) treatment. Data are from a group of 10 rats. (*p<0.05; Dunnett's post hoc).

Temporal 40 Hz ASSR evoked power also showed no treatment effect (p=0.0859; F (1.915, 17.24) = 2.867; epsilon = 0.6385) with repeated measures ANOVA. Again, there was a significant time effect (p<0.05; F (1.962, 17.66) = 4.585; epsilon = 0.6539), and a significant time × treatment interaction (p<0.01; F (3.567, 32.91) = 5.339; epsilon = 0.4069). Post hoc comparisons using Dunnett's test showed that only 0.025 mg/kg MK801 significantly (p<0.05) increased temporal 40 Hz ASSR evoked power at 90-, and 120-minutes time points, relative to vehicle treatment (fig. 3.5-C). Fig. 3.5-A shows the group summary of ITC and evoked power at the 60 minutes-post vehicle or MK-801 injection, represented as heat maps.

0.3 mg/kg Dose Of MK-801 Significantly Reduced 40 Hz ASSR From Both Vertex And Temporal Recordings

In a follow up study, we administered a higher dose of MK-801 (0.3 mg/kg), which caused significant reduction in both vertex and temporal recordings of 40 Hz ASSR. Fig. 3.6-A shows the group summaries of ITC for vertex and temporal 40 Hz ASSR as heat maps for 60 minutes time point. Vertex recordings of 40 Hz ASSR showed no significant time effect (p=0.4143; F (2.604, 26.04) = 0.9644; epsilon = 0.8679). In contrast, there was a highly significant treatment effect (p<0.001; F (1.000, 10.00) = 32.65; epsilon = 1.000), and a significant time × treatment interaction (p<0.01; F (2.360, 23.60) = 3.882; epsilon = 0.7868).

Bonferroni post hoc comparisons showed a significant reduction in ITC by 0.3 mg/kg MK-801 at all the timepoints (p<0.01-p<0.001), as compared to vehicle (fig. 3.6-B).
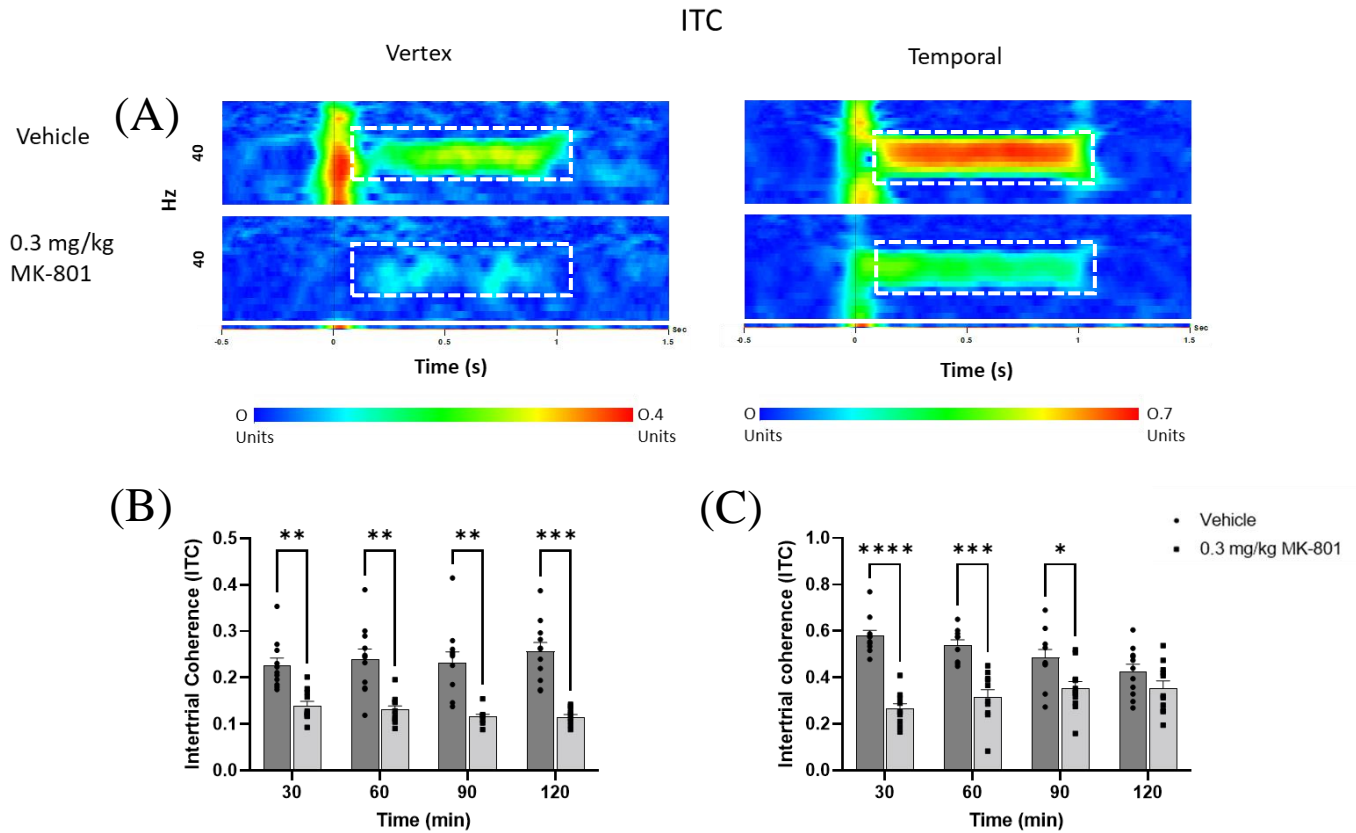
Figure 3.6. Effect of 0.3 mg/kg MK-801 on ITC of vertex and temporal 40 Hz ASSR. Heat map summaries of ITC at 60 minutes (A). Group summaries of the ITC at 30, 60, 90 and 120 minutes after vehicle or 0.3 mg/kg MK-801 treatment for vertex (B), and temporal (C) recordings of 40 Hz ASSR. Data are from a group of 11 rats. (*p<0.05, **p<0.01, ***p<0.001, ****p<0.0001); Bonferroni post hoc).

For 40 Hz ASSR temporal recording, repeated measures ANOVA for ITC showed a highly significant treatment effect (p<0.0001; F (1.000, 10.00) = 54.04; epsilon = 1.000), and a significant time × treatment interaction (p<0.001; F (2.208, 22.08) = 12.31; epsilon = 0.7361). However, there was no time effect (p=0.0899; F (2.199, 21.99) = 2.635; epsilon = 0.7330). Post

hoc comparisons showed a significant reduction by 0.3 mg/kg MK-801 at 30, 60, and 90 minutes timepoints ($p<0.05$-$p<0.0001$), as compared to vehicle (fig. 3.6-C).

Evoked power was also significantly affected by 0.3 mg/kg in both vertex and temporal recordings of 40 Hz ASSR (fig. 3.7-A). Vertex 40 Hz ASSR showed a significant treatment effect ($p<0.0001$; $F(1.000, 10.00) = 44.83$; epsilon = 1.000), and time × treatment interaction ($p<0.01$; $F(2.685, 26.85) = 5.300$; epsilon = 0.8951) with repeated measures ANOVA. However, there was no significant time effect ($p=0.6747$; $F(2.210, 22.10) = 0.4310$; epsilon = 0.7367). Post hoc comparisons showed a significant reduction in vertex evoked power at all the time points ($p<0.05$-$p<0.001$) by 0.3 mg/kg MK-801, relative to vehicle treatment (fig. 3.7-B).

Similarly, temporal recordings of 40 Hz ASSR showed a significant treatment effect ($p<0.05$; $F(1.000, 10.00) = 9.226$; epsilon = 1.000), and a significant time × treatment interaction ($p<0.01$; $F(2.414, 24.14) = 5.936$; epsilon = 0.8048). However, there was no significant time effect ($p=0.4583$; $F(1.769, 17.69) = 0.7815$; epsilon = 0.5896). Post hoc comparisons showed that 0.3 mg/kg MK801 significantly reduced 40 Hz ASSR only at 30 minutes timepoint ($p<0.05$-$p<0.001$), relative to vehicle treatment (fig. 3.7-C).

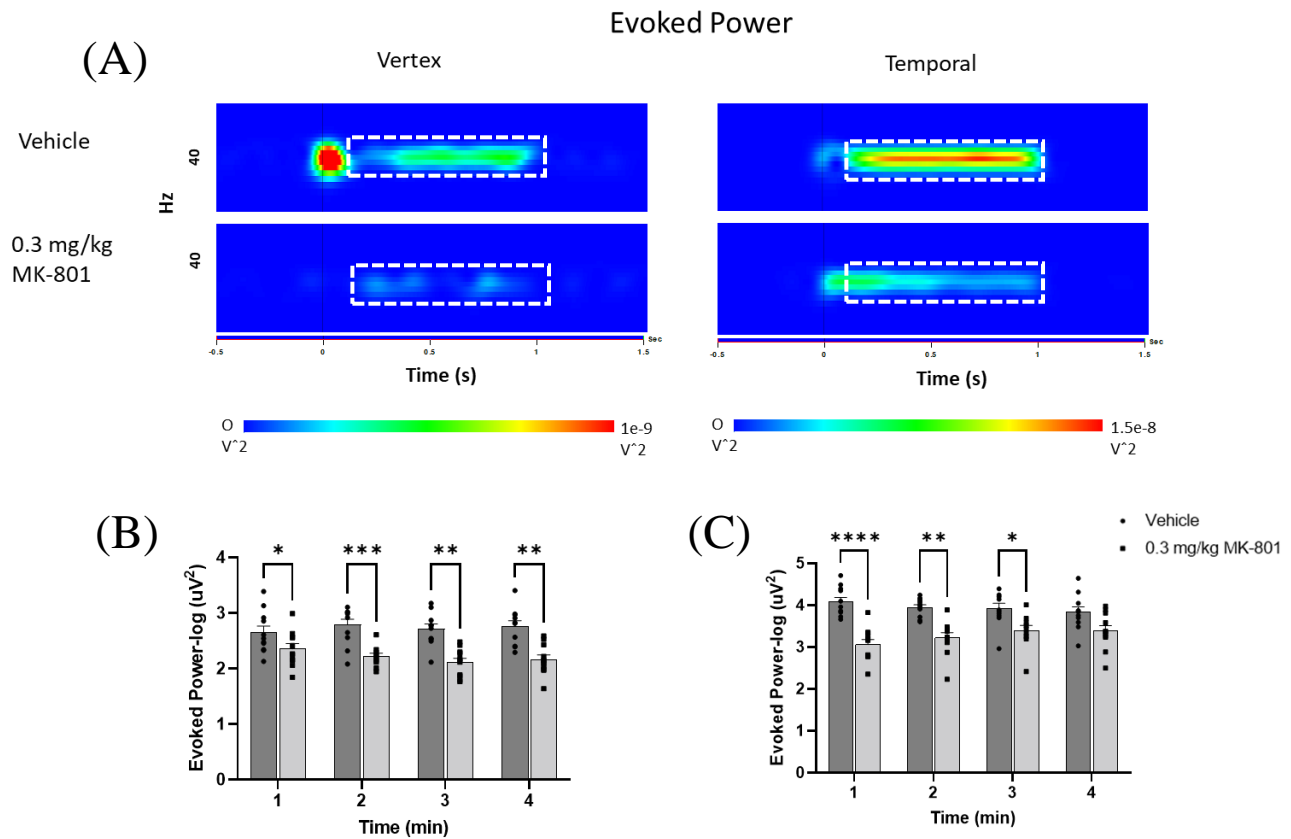***Figure 3.7.*** Effect of 0.3 mg/kg MK-801 on evoked power of vertex and temporal 40 Hz ASSR. Heat map summaries at 60 minutes time point (A). Group summaries of the evoked power at 30, 60, 90 and 120 minutes after vehicle or 0.3 mg/kg MK-801 treatment for vertex (B), and temporal (C) recordings of 40 Hz ASSR. Data are from a group of 11 rats. (*p<0.05, **p<0.01, ***p<0.001, ****p<0.0001); Bonferroni post hoc).

The 40 Hz ASSR is a promising tool to probe the neural synchrony of cortical populations, evoked to oscillate at the gamma frequency (Uhlhaas and Singer, 2010). Gamma oscillations play an essential role in sensory processing and integrating neural activity across brain areas (Tallon-Baudry and Bertrand, 1999; Cardin, 2016).   The utility of 40 Hz ASSR as a translational biomarker for gamma oscillations depends on its thorough characterization including the best coordinates for a robust and reliable signal. With this in mind, the first part of this study tried to ascertain how recording sites may affect the 40 Hz ASSR.

Different techniques like low-resolution electroencephalographic tomography (LORETA), minimum norm (MinNorm), and independent component analysis to map the source of ASSR through current density reconstruction have revealed several cortical and subcortical areas as generators of ASSR (Reyes et al., 2005; Farahani et al., 2017). These areas may process auditory signals in a hierarchical or parallel fashion (Reyes et al., 2005).

There have been contrasting results regarding the source of 40 Hz ASSR. Some studies have reported primary auditory cortex as a core structure for auditory processing with the highest 40 Hz ASSR sensitivity and amplitude (Herdman et al., 2003; Draganova et al., 2008; Wilson et al., 2008; Brugge et al., 2009; Wang et al., 2018). In contrast, other studies have reported widely distributed neural circuits in the parietal, frontal and temporal cortices as putative sources of the 40 Hz ASSR (Tada et al., 2019; Krom et al., 2020). Medial geniculate body (MGB) in the auditory thalamus is traditionally considered as the primary relay center for auditory stimuli that get routed through the so-called lemniscal pathway, which feeds forward the information to higher cortical areas, especially the primary auditory cortex (Bartlett, 2013). However, studies

have shown that there are other non-canonical thalamic nuclei involved in non-lemniscal auditory processing that innervate a wide range of brain areas through feedforward and feedback connections (Lee, 2015).

Notwithstanding the multiple pathways for auditory processing referred above, because electrical activity responsible for ASSR may travel through volume conduction, it is conceivable that the same ASSR signal is recorded at different intensities from different sites through EEG/MEG. This is a fundamental question that needs an answer. In the current study, we recorded ASSR from two distinct areas (Vertex and temporal), simultaneously. As the principle of volume conduction suggests, a traveling wave in the form of neural oscillation will lose its intensity (amplitude) as it travels farther from the source. Moreover, it will show higher latencies at farther distances from the primary source. We wanted to test whether recordings from vertex and temporal areas indicate a common source or two different sources for 40 Hz ASSR. Our results showed a several folds higher temporal 40 Hz ASSR (evoked power and ITC) as compared to vertex, which can be explained through volume conduction if temporal cortex is considered as the primary source for 40 Hz ASSR. Under such conditions, vertex recordings of the 40 Hz ASSR, which are being relayed from the temporal cortex, will show a weaker 40 Hz ASSR, as seen in the current study. However, we did not see any difference in latencies, as suggested by the volume conduction principle (fig. 2 supp). Previously, other studies have also reported stronger ITC and evoked power of 40 Hz ASSR from the temporal region as compared to vertex (Kozono et al., 2019). This observation is confirmed in our study. These findings can alternatively be explained simply as vertex and temporal regions as two separate sources, generating 40 Hz ASSR with different intensities. Our follow up pharmacological study (see below) substantiates this position. Moreover, as discussed previously, there was a significant

97

difference in the variance of the signal between vertex and the auditory cortex. We also performed correlation analysis for the evoked power across sessions from vertex and temporal recordings of 40 Hz ASSR. There was a moderate correlation between sessions for vertex recorded ASSR; , temporal recordings showed a poor correlation between session 1 and the rest of the sessions (table 3.2). This further suggests that 40 Hz recordings from these two areas represent two distinct sources of 40 Hz ASSR. Of course, It is possible that they are not completely independent and may interact with each other in some way that is not obvious at this time.

As far as we know, there are no previous reports of studies comparing two recording sites in terms of their reliability over an extended period of time. Thus, we measured the test-retest reliability of 40 HZ ASSR recordings from vertex and temporal areas obtained over a period of two weeks by calculating their ICC. Vertex 40 Hz ASSR showed a good test-retest reliability, while temporal 40 Hz ASSR had poor test-retest reliability. Analysis of % coefficient of variation further revealed a higher data dispersion for temporal 40 Hz ASSR, as compared to vertex. To our knowledge, this is the first study to compare the test-retest reliability of 40 Hz ASSR simultaneously recorded from two different areas in rodents. The reliability of 40 Hz ASSR as a biomarker is important for translational application in psychiatric research. Previous studies have reported 40 Hz ASSR from vertex region (i.e., Cz electrode) to show good test-retest reliability in humans (McFadden et al., 2014; Hirano et al., 2020) and rodents (Raza and Sivarao, 2021). Consistent results from human and animal studies provide compelling evidence for the potential of 40 Hz ASSR as a reliable biomarker, recorded specifically from the vertex region.

In the next part of this study, we tested the responsivity of 40 Hz ASSR from vertex and temporal regions. MK801 doses (0.025, 0.05, and 0.1 mg/kg) were selected to span a range of occupancies (20-60%; Fernandes et al., 2015). At these doses, vertex 40 Hz ASSR showed reduction by MK-801 in a dose-dependent manner, while temporal 40 Hz ASSR was largely unaffected, although 0.025 mg/kg dose only caused a significant increase in evoked power and ITC at certain time points. However, there is a precedent from studies showing augmented 40 Hz ASSR by NMDA antagonists with low to moderate affinity and rapid kinetics like ketamine (Plourde et al., 1997) and memantine (Light et al, 2017; Raza and Sivarao, unpublished data). This may suggest that low-dose NMDA antagonists may be useful to improve 40 Hz circuit function. However, a feature that would most certainly limit the utility of low-dose NMDA antagonists like ketamine to improve ASSR response would be the concomitant increase in the background or non-stimulus-related gamma power, regarded as a neurophysiological signature for noise (Pinault, 2008, 2014). The qualitatively different responses noted for vertex ASSR vs. temporal ASSR suggests that these sources may be substantially different from each other. In a follow-up study, we tested a higher MK-801 dose (0.3 mg /kg) that shows an NMDAR occupancy close to saturation (Fernandes et al. 2015). At this high dose of MK-801, both vertex and temporal 40 Hz ASSR were significantly attenuated (fig. 3.6).

Previously, there have been contradictory results regarding the effect of NMDAR inhibition through pharmacological or genetic manipulations on 40 Hz ASSR. Studies have reported, no change (Sullivan et al., 2015), a decrease followed by an increase (Plourde et al., 1997); Vohs et al., 2012; O'Donnell et al., 2013; Leishman et al., 2015; Sullivan et al., 2015) or decrease (Sivarao et al., 2013; Raza and Sivarao, 2021; Schuelert et al. 2018) in 40 Hz ASSR in response to disruption of NMDAR transmission in rodents and humans. Based on these findings,

it appears that the choice of the NMDA antagonist may have a bearing on the kind of response one sees. For example, ketamine is a low affinity (Ki ~ 330 nM) antagonist that shows rapid on-off kinetics at the NMDA receptor (Wallach et al., 2016). Thus, sustained and substantive blockade at the receptor site is hard to achieve. On the other hand, MK801 (Ki, 2.5 nM) can result in a relatively irreversible and long-lasting blockade of the NMDA channel (Hakami et al., 2009; Davies et al., 1988). Indeed, genetic ablation of NMDAR, specifically on PV+ neurons, consistently results in reduction of 40 Hz ASSR in rodents (Carlén et al., 2012; Nakao and Nakazawa, 2014).

In summary, 40 Hz ASSR recorded from vertex consistently showed high test-retest reliability and was highly sensitive to NMDAR inhibition, as reported previously (Raza and Sivarao, 2021). Whereas temporal 40 Hz ASSR showed poor test-retest reliability and lower sensitivity to MK-801 treatment. Previous studies have consistently reported 40 Hz ASSR deficits in schizophrenia patients (Kwon et al., 1999; Brenner et al., 2003; Light et al., 2006; Krishnan et al., 2009; Spencer et al., 2009). Thus, results from the current study further support that vertex area represents an attractive region for recording 40 Hz ASSR in rodent models, given its test-retest reliability and high sensitivity to NMDA antagonism. Furthermore, 40 Hz ASSR recorded from vertex and temporal sites seems to originate from two distinct circuits, with different degrees of reliability and sensitivity toward NMDA antagonists. Our study fills an important gap in the context of optimizing 40 Hz ASSR recording paradigms in rodent models. Standardization of 40 Hz ASSR recording procedures will enable a way to compare data across laboratories and studies.

References

Bartlett, E. L. (2013). The organization and physiology of the auditory thalamus and its role in processing acoustic features important for speech perception. Brain and Language, 126(1), 29. https://doi.org/10.1016/J.BANDL.2013.03.003

Borck, G., Rehman, A. U., Lee, K., Pogoda, H., Kakar, N., Ameln, S. Von, … Kubisch, C. (2011). Loss-of-Function Mutations of ILDR1 Cause Autosomal-Recessive Hearing Impairment DFNB42, 127–137. https://doi.org/10.1016/j.ajhg.2010.12.011

Brenner, C. A., Sporns, O., Lysaker, P. H., & O'Donnell, B. F. (2003). EEG synchronization to modulated auditory tones in schizophrenia, schizoaffective disorder, and schizotypal personality disorder. The American Journal of Psychiatry, 160(12), 2238–2240. https://doi.org/10.1176/APPI.AJP.160.12.2238

Brenner, CA, Krishnan, GP, Vohs, JL, Ahn, WY, Hetrick, WP, Morzorati, SL, O'Donnell, BF (2009). Steady state responses: electrophysiological assessment of sensory function in schizophrenia. In Schizophrenia Bulletin (Vol. 35, Issue 6, pp. 1065–1077). Oxford Academic. https://doi.org/10.1093/schbul/sbp091

Brugge, J. F., Nourski, K. V., Oya, H., Reale, R. A., Kawasaki, H., Steinschneider, M., and Howard, M. A. (2009). Coding of repetitive transients by auditory cortex on Heschl's gyrus. Journal of Neurophysiology, 102(4), 2358–2374. https://doi.org/10.1152/JN.91346.2008

Cardin, J. A. (2016). Snapshots of the Brain in Action: Local Circuit Operations through the Lens of γ Oscillations. Journal of Neuroscience, 36(41), 10496–10504. https://doi.org/10.1523/JNEUROSCI.1021-16.2016

Carlén, M., Meletis, K., Siegle, J. H., Cardin, J. A., Futai, K., Vierling-Claassen, D., … Tsai, L.-H. (2012). A critical role for NMDA receptors in parvalbumin interneurons for gamma rhythm induction and behavior. Molecular Psychiatry, 17(5), 537–548. https://doi.org/10.1038/mp.2011.31

Conti, G., Santarelli, R., Grassi, C., Ottaviani, F., and Azzena, G. B. (1999). Auditory steady-state responses to click trains from the rat temporal cortex. Clinical Neurophysiology, 110(1), 62–70. https://doi.org/10.1016/S0168-5597(98)00045-8

Davies, S. N., Martin, D., Millar, J. D., Aram, J. A., Church, J., & Lodge, D. (1988). Differences in results from in vivo and in vitro studies on the use-dependency of N-methylaspartate antagonism by MK-801 and other phencyclidine receptor ligands. European Journal of Pharmacology, 145(2), 141–151. https://doi.org/10.1016/0014-2999(88)90225-7

Draganova, R., Ross, B., Wollbrink, A., and Pantev, C. (2008). Cortical Steady-State Responses to Central and Peripheral Auditory Beats. Cerebral Cortex, 18(5), 1193–1200. https://doi.org/10.1093/CERCOR/BHM153

Farahani, E. D., Goossens, T., Wouters, J., and van Wieringen, A. (2017). Spatiotemporal reconstruction of auditory steady-state responses to acoustic amplitude modulations: Potential sources beyond the auditory pathway. NeuroImage, 148, 240–253. https://doi.org/10.1016/J.NEUROIMAGE.2017.01.032

Farahani, E. D., Wouters, J., & van Wieringen, A. (2019). Contributions of non-primary cortical sources to auditory temporal processing. NeuroImage, 191, 303–314. https://doi.org/10.1016/J.NEUROIMAGE.2019.02.037

Farahani, E. D., Wouters, J., & van Wieringen, A. (2021). Brain mapping of auditory steady-state responses: A broad view of cortical and subcortical sources. Human Brain Mapping, 42(3), 780–796. https://doi.org/10.1002/HBM.25262

Fernandes, A., Wojcik, T., Baireddy, P., Pieschl, R., Newton, A., Tian, Y., Hong, Y., Bristow, L., & Li, Y. W. (2015). Inhibition of in vivo [3H]MK-801 binding by NMDA receptor open channel blockers and GluN2B antagonists in rats and mice. European Journal of Pharmacology, 766, 1–8. https://doi.org/10.1016/j.ejphar.2015.08.044

Haghighi, S. J., Komeili, M., Hatzinakos, D., and Beheiry, H. El. (2018). 40-Hz ASSR for Measuring Depth of Anaesthesia During Induction Phase. IEEE Journal of Biomedical and Health Informatics, 22(6), 1871–1882. https://doi.org/10.1109/JBHI.2017.2778140

Herdman, A. T., Wollbrink, A., Chau, W., Ishii, R., Ross, B., and Pantev, C. (2003). Determination of activation areas in the human auditory cortex by means of synthetic aperture magnetometry. NeuroImage, 20(2), 995–1005. https://doi.org/10.1016/S1053-8119(03)00403-8

Hirano, Y., Nakamura, I., Tamura, S., and Onitsuka, T. (2020). Long-Term Test-Retest Reliability of Auditory Gamma Oscillations Between Different Clinical EEG Systems. Frontiers in Psychiatry, 11, 876. https://doi.org/10.3389/FPSYT.2020.00876/BIBTEX

Ip, C. T., Ganz, M., Ozenne, B., Sluth, L. B., Gram, M., Viardot, G., … Christensen, S. R. (2018). Pre-intervention test-retest reliability of EEG and ERP over four recording intervals. International Journal of Psychophysiology, 134, 30–43. https://doi.org/10.1016/j.ijpsycho.2018.09.007

Koo, T. K., and Li, M. Y. (2016). A Guideline of Selecting and Reporting Intraclass Correlation Coefficients for Reliability Research. Journal of Chiropractic Medicine, 15(2), 155. https://doi.org/10.1016/J.JCM.2016.02.012

Kozono, N., Honda, S., Tada, M., Kirihara, K., Zhao, Z., Jinde, S., … Mihara, T. (2019). Auditory Steady State Response; nature and utility as a translational science tool. Scientific Reports, 9(1), 8454. https://doi.org/10.1038/s41598-019-44936-3

Krishnan, G. P. P., Hetrick, W. P. P., Brenner, C. A. A., Shekhar, A., Steffen, A. N. N., & O'Donnell, B. F. F. (2009). Steady state and induced auditory gamma deficits in schizophrenia. NeuroImage, 47(4), 1711–1719. https://doi.org/10.1016/j.neuroimage.2009.03.085

Krom, A. J., Marmelshtein, A., Gelbard-Sagiv, H., Tankus, A., Hayat, H., Hayat, D., … Nir, Y. (2020). Anesthesia-induced loss of consciousness disrupts auditory responses beyond primary cortex. Proceedings of the National Academy of Sciences of the United States of America, 117(21). https://doi.org/10.1073/PNAS.1917251117

Kwon, J. S., O'Donnell, B. F., Wallenstein, G. V., Greene, R. W., Hirayasu, Y., Nestor, P. G., Hasselmo, M. E., Potts, G. F., Shenton, M. E., & McCarley, R. W. (1999). Gamma

Frequency–Range Abnormalities to Auditory Stimulation in Schizophrenia. Archives of General Psychiatry, 56(11), 1001. https://doi.org/10.1001/archpsyc.56.11.1001

Lee, C. C. (2015). Exploring functions for the non-lemniscal auditory thalamus. Frontiers in Neural Circuits, 9(November), 1–8. https://doi.org/10.3389/FNCIR.2015.00069/BIBTEX

Leishman, E., O'donnell, B. F., Millward, J. B., Vohs, J. L., Rass, O., Krishnan, G. P., … Morzorati, S. L. (2015). Phencyclidine Disrupts the Auditory Steady State Response in Rats. https://doi.org/10.1371/journal.pone.0134979

Light, G. A., Hsu, J. L., Hsieh, M. H., Meyer-Gomes, K., Sprock, J., Swerdlow, N. R., & Braff, D. L. (2006). Gamma Band Oscillations Reveal Neural Network Cortical Coherence Dysfunction in Schizophrenia Patients. 60(11), 1231–1240. https://doi.org/10.1016/j.biopsych.2006.03.055

Light, G. A., Zhang, W., Joshi, Y. B., Bhakta, S., Talledo, J. A., & Swerdlow, N. R. (2017). Single-Dose Memantine Improves Cortical Oscillatory Response Dynamics in Patients with Schizophrenia. Neuropsychopharmacology, 42(13), 2633–2639. https://doi.org/10.1038/npp.2017.81

McFadden, K. L., Steinmetz, S. E., Carroll, A. M., Simon, S. T., Wallace, A., and Rojas, D. C. (2014). Test-Retest Reliability of the 40 Hz EEG Auditory Steady-State Response. PLOS ONE, 9(1), e85748. https://doi.org/10.1371/JOURNAL.PONE.0085748

Nakao, K., and Nakazawa, K. (2014). Brain state-dependent abnormal LFP activity in the auditory cortex of a schizophrenia mouse model. Frontiers in Neuroscience, 8(8 JUL). https://doi.org/10.3389/FNINS.2014.00168

O'Donnell, B. F., Vohs, J. L., Krishnan, G. P., Rass, O., Hetrick, W. P., and Morzorati, S. L. (2013). The auditory steady-state response (ASSR). In Supplements to Clinical neurophysiology (Vol. 62, pp. 101–112). https://doi.org/10.1016/B978-0-7020-5307-8.00006-5

Pinault, D. (2008). N-methyl d-aspartate receptor antagonists ketamine and MK-801 induce wake-related aberrant gamma oscillations in the rat neocortex. Biological Psychiatry, 63(8), 730–735. https://doi.org/10.1016/j.biopsych.2007.10.006

Pinault, D. (2014). N-Methyl D-Aspartate Receptor Antagonists Amplify Network Baseline Gamma Frequency (30–80 Hz) Oscillations: Noise and Signal. AIMS Neuroscience 2014 2:169, 1(2), 169–182. https://doi.org/10.3934/NEUROSCIENCE.2014.2.169

Plourde, G., Baribeau, J., and Bonhomme, V. (1997). Ketamine increases the amplitude of the 40-Hz auditory steady-state response in humans. British Journal of Anaesthesia, 78(5), 524–529. https://doi.org/10.1093/bja/78.5.524

Rass, O., Krishnan, G., Brenner, C. A., Hetrick, W. P., Merrill, C. C., Shekhar, A., & O'Donnell, B. F. (2010). Auditory steady state response in bipolar disorder: Relation to clinical state, cognitive performance, medication status, and substance disorders. Bipolar Disorders, 12(8), 793–803. https://doi.org/10.1111/j.1399-5618.2010.00871.x

Raza, M. U., and Sivarao, D. V. (2021). Test-retest reliability of tone- and 40 Hz train-evoked gamma oscillations in female rats and their sensitivity to low-dose NMDA channel

blockade. Psychopharmacology 2021 238:8, 238(8), 2325–2334.
https://doi.org/10.1007/S00213-021-05856-1

Reyes, S. A., Lockwood, A. H., Salvi, R. J., Coad, M. Lou, Wack, D. S., and Burkard, R. F.
(2005). Mapping the 40-Hz auditory steady-state response using current density
reconstructions. Hearing Research, 204(1–2), 1–15.
https://doi.org/10.1016/J.HEARES.2004.11.016

Seymour, R. A., Rippon, G., Gooding-Williams, G., Sowman, P. F., & Kessler, K. (2020).
Reduced auditory steady state responses in autism spectrum disorder. Molecular Autism,
11(1), 56. https://doi.org/10.1186/s13229-020-00357-y

Sivarao, D. V. (2015). The 40-Hz auditory steady-state response: A selective biomarker for
cortical NMDA function. Annals of the New York Academy of Sciences, 1344(1), 27–36.
https://doi.org/10.1111/nyas.12739

Sivarao, D. V., Chen, P., Senapati, A., Yang, Y., Fernandes, A., Benitex, Y., … Ahlijanian, M.
K. (2016). 40 Hz Auditory Steady-State Response Is a Pharmacodynamic Biomarker for
Cortical NMDA Receptors. Neuropsychopharmacology, 41(9), 2232.
https://doi.org/10.1038/NPP.2016.17

Sivarao, D. V., Frenkel, M., Chen, P., Healy, F. L., Lodge, N. J., and Zaczek, R. (2013). MK-801
disrupts and nicotine augments 40 Hz auditory steady state responses in the auditory cortex
of the urethane-anesthetized rat. Neuropharmacology, 73, 1–9.
https://doi.org/10.1016/j.neuropharm.2013.05.006

Spencer, K. M., Nestor, P. G., Niznikiewicz, M. A., Salisbury, D. F., Shenton, M. E., and
McCarley, R. W. (2003). Abnormal Neural Synchrony in Schizophrenia. Journal of
Neuroscience, 23(19), 7407–7411. https://doi.org/10.1523/JNEUROSCI.23-19-07407.2003

Stacho, M., & Manahan-Vaughan, D. (2022). Mechanistic flexibility of the retrosplenial cortex
enables its contribution to spatial cognition. Trends in Neurosciences, 45(4), 284–296.
https://doi.org/10.1016/J.TINS.2022.01.007

Sullivan, E. M., Timi, P., Elliot Hong, L., O'Donnell, P., Hong, L. E., and O'Donnell, P. (2015).
Effects of NMDA and GABA-A receptor antagonism on auditory steady-state
synchronization in awake behaving rats. International Journal of
Neuropsychopharmacology, 18(7), 1–7. https://doi.org/10.1093/ijnp/pyu118

Tada, M., Kirihara, K., Ishishita, Y., Takasago, M., Kunii, N., Uka, T., … Kasai, K. (2019).
Global and Parallel Cortical Processing of Auditory Gamma Oscillatory Responses in
Humans. SSRN Electronic Journal. https://doi.org/10.2139/ssrn.3417938

Tallon-Baudry, C., and Bertrand, O. (1999). Oscillatory gamma activity in humans and its role in
object representation. Trends in Cognitive Sciences, 3(4), 151–162.
https://doi.org/10.1016/S1364-6613(99)01299-1

Thuné, H., Recasens, M., and Uhlhaas, P. J. (2016). The 40-Hz auditory steady-state response in
patients with schizophrenia a meta-Analysis. JAMA Psychiatry, 73(11), 1145–1153.
https://doi.org/10.1001/jamapsychiatry.2016.2619

Uhlhaas, P. J., and Singer, W. Abnormal neural oscillations and synchrony in schizophrenia, 11

§ (2010). Nature Publishing Group. https://doi.org/10.1038/nrn2774

Vann, S. D., Aggleton, J. P., & Maguire, E. A. (2009). What does the retrosplenial cortex do? Nature Reviews Neuroscience 2009 10:11, 10(11), 792–802. https://doi.org/10.1038/nrn2733

Vohs, J. L., Chambers, R. A., O'Donnell, B. F., Krishnan, G. P., and Morzorati, S. L. (2012). Auditory steady state responses in a schizophrenia rat model probed by excitatory/inhibitory receptor manipulation. International Journal of Psychophysiology, 86(2), 136–142. https://doi.org/10.1016/j.ijpsycho.2012.04.002

Wallach, J., Kang, H., Colestock, T., Morris, H., Bortolotto, Z. A., Collingridge, G. L., Lodge, D., Halberstadt, A. L., Brandt, S. D., & Adejare, A. (2016). Pharmacological Investigations of the Dissociative 'Legal Highs' Diphenidine, Methoxphenidine and Analogues. PLoS ONE, 11(6). https://doi.org/10.1371/JOURNAL.PONE.0157021

Wang, X., Li, Y., Chen, J., Li, Z., Li, J., and Qin, L. (2020). Aberrant Auditory Steady-State Response of Awake Mice After Single Application of the NMDA Receptor Antagonist MK-801 Into the Medial Geniculate Body. International Journal of Neuropsychopharmacology, 23(7), 459–468. https://doi.org/10.1093/ijnp/pyaa022

Wang, Y., Ma, L., Wang, X., and Qin, L. (2018). Differential modulation of the auditory steady state response and inhibitory gating by chloral hydrate anesthesia. Scientific Reports, 8(1). https://doi.org/10.1038/S41598-018-21920-X

Weickert, C. S., Weickert, T. W., Pillai, A., and Buckley, P. F. (2013). Biomarkers in Schizophrenia: A Brief Conceptual Consideration. Disease Markers, 35(1), 3. https://doi.org/10.1155/2013/510402

Wilson, T. W., Hernandez, O. O., Asherin, R. M., Teale, P. D., Reite, M. L., and Rojas, D. C. (2008). Cortical gamma generators suggest abnormal auditory circuitry in early-onset psychosis. Cerebral Cortex, 18(2), 371–378. https://doi.org/10.1093/CERCOR/BHM062

CHAPTER 4. A UNIQUE PROFILE OF CLOZAPINE IN IMPROVING 40 HZ ASSR AND ITS PROTECTION AGAINST MK-801-INDUCED DISRUPTION

Abstract

Rationale. Previously, we have shown that MK-801 treatment causes a dose-dependent reduction in 40 Hz ASSR from vertex recordings. For 40 Hz ASSR to be useful pharmacodynamic biomarker, it needs to be bidirectionally modulated by drug treatment. Therefore, in the current study, we tested the hypothesis if 40 Hz ASSR can be augmented by D-serine (an NMDAR co-agonist), or with antipsychotic treatment.

Objective. We investigated whether treatment with D-serine, or an antipsychotic can enhance 40 Hz ASSR. Furthermore, we investigated the protective effect of these drugs on MK-801-induced disruption in 40 Hz ASSR

Methods. We carried out six separate studies testing the effect of D-serine, haloperidol (a typical antipsychotic), or clozapine (an atypical antipsychotic) treatment only or before MK-801 treatment, in a crossover study design. D-serine doses selected for this study (30-500 mg/kg, SC) have shown to cause a robust increase in extracellular D-serine levels in the brain. Moreover, doses for clozapine and haloperidol were chosen to reflect clinically relevant D2 occupancy. Auditory stimuli were presented (1KHz tone, 50 msec duration, and 40 clicks for 1 second (40 Hz), 65 dB, 3-sec ITI, 5- sec sweeps, 75 trials) at 30, 60, 90- and 120-minutes post-treatment. Recordings were made from the vertex electrode using a cerebellar reference. In the D-serine, or antipsychotics pre-treatment studies, drugs were administered 20 minutes before MK-801 (0.1 mg/kg, SC) administration. ASSR was recorded at 30, 60, 90- and 120-minutes post-MK-801 injection.

Results. Treatment with D-serine (30, 60, or 120 mg/kg, SC) did not have any effect on 40 Hz ASSR. Similarly, pretreatment of D-serine with relatively higher doses (250, or 500 mg/kg, SC) did not provide any protection against MK-801 induced disruption in 40 Hz ASSR. As compared to haloperidol (0.02, 0.04, or 0.08 mg/kg, SC), which showed no improvement in 40 Hz ASSR, treatment with clozapine (2.5, 5, and 10 mg/kg, SC) caused a significant improvement in the 40 Hz ASSR (evoked power, and ITC) in a dose and time-dependent manner. Furthermore, only clozapine (10 mg/kg, SC) showed a partial protection against MK-801-induced 40 Hz ASSR deficits (ITC, and evoked power), whereas haloperidol (0.04, or 0.08 mg/kg, SC) had no ameliorative effect against MK-801. Moreover, as shown previously (Raza and Sivarao, 2021), MK801 produced robust deficits in 40 Hz ASSR in all MK-801 related studies.

Conclusion. These studies highlight the following: 1. Only clozapine improves sensory transmission by itself; 2. Pretreatment with only clozapine is partially protective against NMDA disruption; 3. Our work illustrates the utility of the 40 Hz ASSR as a circuit-based pharmacodynamic biomarker, which can be bidirectionally modulated by pharmacological treatment.

Schizophrenia is a serious mental disorder exhibiting psychotic, emotional, and cognitive symptoms. Currently available antipsychotics target dopamine D2 receptors and are effective in managing psychosis but remain ineffective against negative and cognitive symptoms (Leucht et al., 2009). Unlike psychotic symptoms, which often wax and wane, negative and cognitive symptoms are persistent throughout the duration of the disease. Considerable evidence now supports negative and cognitive symptoms as the core feature of schizophrenia, impacting patient outcomes over the long-term (Gold, 2004; Hyman and Fenton, 2003; Üçok et al., 2013). Cognitive and negative symptoms also precede psychosis onset and may determine real world functioning ability of the affected patients (Green and Nuechterlein, 1999; Green, 2006).

Over the years, the N-methyl D-aspartic acid receptor (NMDAR) hypofunction hypothesis has gained traction as a way to explain the symptomatology of schizophrenia. It started from the observation that non-competitive NMDAR antagonists like phencyclidine (PCP) and ketamine induce schizophrenia-like symptoms, including behavioral and cognitive symptoms, in healthy humans (Allen and Young, 1978; Luby et al., 1962). Furthermore, NMDAR antagonists were shown to exacerbate schizophrenia symptoms in recovering patients (Javitt and Zukin, 1991). Interestingly, dosing preclinical species with NMDA antagonists has resulted in cognitive (e.g., attention, working memory) (Egerton et al., 2005), behavioral (e.g., social interaction, stereotyped behavior) (Murray and Horita, 1979; Sams-Dodd, 1995), and sensory motor deficits (e.g., MMN, sensory gating, PPI) (Mansbach and Geyer, 1989; Bristow et al., 2016) mimicking schizophrenia like symptoms. This has led to the evaluation of NMDAR targeted therapies, which have shown modest effects in small clinical trials (for a review, see Singh and Singh, 2011), mainly based on symptom improvement (Ermilov et al., 2013). It is to

be noted that these trials did not use any objective biomarkers for demonstrating D-serine induced changes, short of the symptomatic improvement. In the absence of objective biomarkers, despite encouraging symptomatic data, there is a reluctance in the pharmaceutical industry to invest in large scale clinical trials to evaluate new and emerging targets (Venkatasubramanian & Keshavan, 2016).

In previous chapters, I have discussed how vertex-recorded 40 Hz ASSR is exquisitely sensitive to NMDA mechanism. This is also a response that we have replicated multiple times in our experiments, which indicates a high degree of reliability. For an index like 40 Hz ASSR to be useful as a pharmacodynamic biomarker, it needs to be bidirectionally modulated by drug treatment. Since acute treatment with NMDA channel blocker attenuated the 40 Hz ASSR response, we hypothesized that any pharmacological intervention designed to increase NMDAR activation may do the opposite. We evaluated this in several stages. One, we tested the effect of a wide range of doses of D-serine, a co-agonist at the glycine-modulatory site on the NMDA receptor (Balu and Coyle, 2015). In a follow up study, we gave MK801 minutes following D-serine administration to see if D-serine would blunt the effect of MK801 on the 40 Hz ASSR measure. We saw no evidence for D-serine augmenting the 40 Hz ASSR by itself or blunting the effect of MK801 on the 40 Hz ASSR.

In the next part of the study, we evaluated the effect of an atypical antipsychotic clozapine at doses that mimic clinically relevant D2 receptor occupancy, on the 40 Hz ASSR. Clozapine robustly and dose-dependently improved 40 Hz ASSR. However, haloperidol, a typical antipsychotic, at doses shown to yield comparable D2 occupancy, showed no effect on the 40 Hz ASSR. Lastly, pretreatment with clozapine but not haloperidol blunted the effect of a subsequent dose of MK801-mediated disruption of the 40 Hz ASSR.

109

General

6–8-week-old female Sprague Dawley rats (150–200 g) were purchased from Envigo (Indianapolis, IN) and were placed in group housed environment with free access to food and water. After surgery animal were housed individually to prevent damage to the head-mounted EEG hardware. All the experimental procedures on animals were approved by the Institutional Animal Care and Use Committee of the East Tennessee State University (#180901).

Surgery

All surgeries were performed as described previously (Raza and Sivarao, 2021). In Brief, animals were anaesthetized with 5% isoflurane (induction 5%; maintenance, 1-2% with 1 L/min oxygen. The head area was shaved and then was secured in a stereotaxic frame. Alcohol and povidone-iodine swabs were used to clean the surgery area. Bupivacaine (0.25 %, 8mg/kg, sc) was infiltrated through the subcutaneous field as a local anesthesia and ketoprofen (5 mg/kg, sc) was used for perioperative analgesia. A midline incision was made, and membranes were scraped through blunt dissection to expose the skull. A solution of 3% hydrogen peroxide was introduced drop by drop to disinfect the area and was mopped up and dried. Four burr holes were made into the skull using an aseptic drill bit at the following coordinates: 1mm anterior and 1mm lateral (right) to bregma (targeting the prefrontal cortex), 4.5 mm posterior and 1mm lateral (left) to bregma (targeting the vertex region), 2 mm posterior and 2mm lateral (left) to lambda (reference), and 2 mm posterior and 2 mm lateral (right) to lambda (ground). Electrodes with attached wires were gently screwed into the burr holes while keeping the underlying dura intact.

Electrodes were completely covered with dental cement. A recording head mount (Pinnacle Technology, Lawrence, KS) was placed on the dental cement after it had cured, and electrode wires were attached to the head mount wires with a solder. All the exposed wires were covered with a second layer of dental cement. The surgery area was closed with sutures and rats were given at least 10 days to recover. After recovery, rats were handled and acclimated to the recording set up several times on separate days before any experiments were started.

EEG Recording Protocol

Rats were placed in the recording chamber for at least 10 minutes before starting each experiment. EEG recordings were carried out as described previously (Raza and Sivarao, 2021). Rats were connected to the recording setup through a shielded cable fitted with a head stage preamplifier (10X) (Pinnacle Technology, Lawrence, KS). The EEG signals were routed through an analog adapter, to a differential amplifier (100X; DP-304A, Warner Instruments Inc). Thus, the EEG signal was amplified a thousand-fold. The amplified signal was acquired by an analog to digital conversion board (CED Micro 1401-3). The auditory stimuli were presented through 3" 4-Ohm house speakers (DROK, B00LSEVA8I), fixed at the center of the ceiling of each recording chamber. Auditory stimuli including a tone and a 40 Hz click train were produced in Signal v7.01 software and delivered through the acquisition system (CED Micro 1401-3; Cambridge Electronics Design (CED), Cambridge, UK), which also concurrently recorded the EEG as consecutive sweeps. A 1 KHz tone as a sinusoidal wave with 50 msec duration and 65 dB intensity was presented a second after a 5 s sweep stimulus was initiated. The tone stimulus was followed by a train of 40 clicks for a duration of 1 sec (40 Hz), 3 seconds after the sweep initiation. In the D-serine study only, the duration of click-trains lasted for 2 sec, delivering a

total of 80 clicks. In all experiments, the 40 Hz click train had an intensity of 65 dB, as measured by a sound pressure meter and each click resulted from a 1 ms 3 or 5 V square wave that was fed to the house amplifier. Inter-stimulus interval (ISI) between tone stimulus and 40 Hz click train was 2 sec in each trial, while the inter-trial interval (ITI) between the end of 40 Hz click train and the next tone stimulus was 3 sec. The auditory stimuli were repeatedly presented in 75 trials. In this study, we report the EEG data recorded only from vertex electrode. EEG data was recorded at 30, 60, 90 and 120 minutes in four sessions, as typically there were four total treatments in this cross-over design. A washout period of at least 3 days was allowed between recording sessions.

EEG Data Analysis

The use of head stage amplification (10X; Pinnacle Technologies) greatly reduced movement artifacts, however chewing-associated artifacts were present intermittently. The trial exclusion criteria followed the removal of a trial if an artifact coincided with the auditory stimulus duration, thus typically <5% the 75 trials were excluded. The preliminary data analysis was performed using the Signal v7.01 software. Artifact free trials were averaged for each rat. Averaged trials clearly showed tone-evoked event related potential (ERP) and 40 Hz click train-evoked ASSR (fig. 3 supp). Although, both tone and 40 Hz click-train stimuli were presented, we focused only on analyzing 40 Hz ASSR. Evoked response for the tone stimulus was used only as a reference. Averaged trials were then digitally band-pass filtered to 35-45 Hz through 2nd order Butterworth, zero-phase shift, infinite impulse response (IIR) filter. The group averages were obtained from the averaged trials to represent summary results.

Time-frequency analysis (TFA) was performed in the EMSE data editor software v5.6.1 (Cortech solutions, Wilmington, NC). Raw data files from signal software v7.1 were first

112

exported as text files and imported into EMSE v5.X software (Cortech Solutions Inc., Wilmington, NC). TFA was performed through Morlet transformation to measure evoked power and inter-trial phase coherence (ITC). ITC (also known as phase synchrony or phase locking factor (PLF) is a measure of trial-to-trial phase consistency in the 40 Hz ASSR, while evoked power is the measure of averaged 40 Hz ASSR power. Both ITC and evoked power measure 40 Hz ASSR signal, which is time-locked to stimulus onset (Brian J. Roach and Mathalon, 2008). Peak and area measurements of 40 Hz ASSR for ITC and evoked power were obtained to perform statistical analysis. The initial 0.2 milliseconds of evoked response from the ASSR were excluded for measurements (fig. 3 supp). The initial response (i.e., ~200 milliseconds) is considered transient response, or transient gamma band response (tGBR), and is a broadband frequency response (Pantev et al., 1993). Whereas the response period after ~ 200 milliseconds represent cortical entrainment to the modulating frequency as ASSR (i.e., 40 Hz ASSR in the current study) (Hari et al., 1989). TFA was also performed on the concatenated data from each group to obtain summary results for representation.

Pharmacology

D-serine study. D-serine (Sigma-Aldrich) was dissolved in 0.9% sterile saline to make 1g/ml stock solution, which was kept in aliquots at -20 oC. Fresh dilutions were made from the stock solution before the start of each experiment. In the D-serine only study, rats were injected with either vehicle or D-serine (30, 60, and 120 mg/kg, SC). Whereas in the D-serine pre-treatment study, rats were first injected with either vehicle or D-serine (250, and 500 mg/kg, SC). Then after at least 20 minutes rats were injected again either with vehicle or 0.1 mg/kg MK-801. MK-801 maleate (Sigma-Aldrich) was dissolved in 0.9% sterile saline to obtain 0.1 mg/ml MK-

113

801 free base solution and was stored at 4ºC in aliquots. ASSR recording were made at 30-, 60-, 90- and 120-minutes time points. Animals were given at least 3 days for the washout period and the same procedure was repeated. A cross-over design was followed which spanned across 4 session for 2 weeks.

Clozapine study. Clozapine (Sigma-Aldrich) was dissolved in glacial acetic acid (50 ml). Then 0.9% sterile saline was added to make stock solution of 10mg/ml with the final acetic acid concentration of 10%. The final pH was adjusted to 6.0 by adding sodium bicarbonate. Dilutions at 2.5 and 5 mg/ml clozapine were made from the 10 mg/ml stock solution. Fresh clozapine solutions were prepared before each recording session. The vehicle solution (i.e., 0.9 % saline) also had pH of 6.0. In the clozapine only study, rats were injected with either vehicle or clozapine (2.5, 5, and 10 mg/kg, SC) While in clozapine pretreatment study, rats were pre-treated with either vehicle or clozapine (5, and 10 mg/kg, SC). Then after at least 20 minutes, rats were injected again either with vehicle or 0.1 mg/kg MK-801. ASSR recordings were carried out as described above.

Haloperidol study. Haloperidol (Sigma-Aldrich) stock solution at 0.8 mg/ml was made following the same protocol as for clozapine solution. Dilutions were made at 0.02 and 0.04 mg/ml from the stock solution. The final pH of vehicle for haloperidol study was also adjusted to 6.0. In the haloperidol only study, rats were injected with either vehicle or haloperidol (0.02, 0.04, and 0.08 mg/kg, SC). In the haloperidol pre-treatment study, rats were first injected with either vehicle or haloperidol (0.04, and 0.08 mg/kg, SC). Then after at least 20 minutes rats were injected again either with vehicle or 0.1 mg/kg MK-801. ASSR recording were made at 4 time points across 4 sessions, as described in the D-serine section above.

In the literature, wide range of D-serine doses have been used from as low as 30 mg/kg to as high as 2g/kg. We followed previous studies (Fone et al., 2020; Hasegawa et al., 2019) to choose D-serine dose ranges (30-500 mg/kg). These doses show a significant increase in brain D-serine levels as compared to baseline without significantly increasing creatine levels. Doses selected for clozapine (2.5-10 mg/kg) and haloperidol (0.02-0.08 mg/kg) have been reported to yield clinically relevant D2 receptor occupancy, after acute dosing (Kapur et al., 2003; Seeman and Kapur, 2000). A schematic of the study designs is shown in fig. 4.1 (A and B).

Statistical Analysis

The first key objective of the study was to measure the improvement in 40 Hz ASSR caused by D-serine or antipsychotics by themselves. While the second objective was to measure the protective effect of D-serine or antipsychotics pretreatment on MK-801-induced disruption. A two-way analysis of variance (ANOVA) repeated measures design (mixed-effect model; GraphPad Prism, v9.1) was implemented to determine treatment effect. Time of recording and treatment groups were selected as row and column factors, respectively. Quantile-quantile (q-q) plot was used to ensure data normality. In case the data are non-linear, which happened infrequently, we log transformed the data first to confirm linearity and then, parametric statistics were applied. Greenhouse-Geisser correction was implemented without assuming sphericity. Dunnett's post hoc analyses were used to measure treatment significance and vehicle group or vehicle + MK-801 group were selected as comparators.
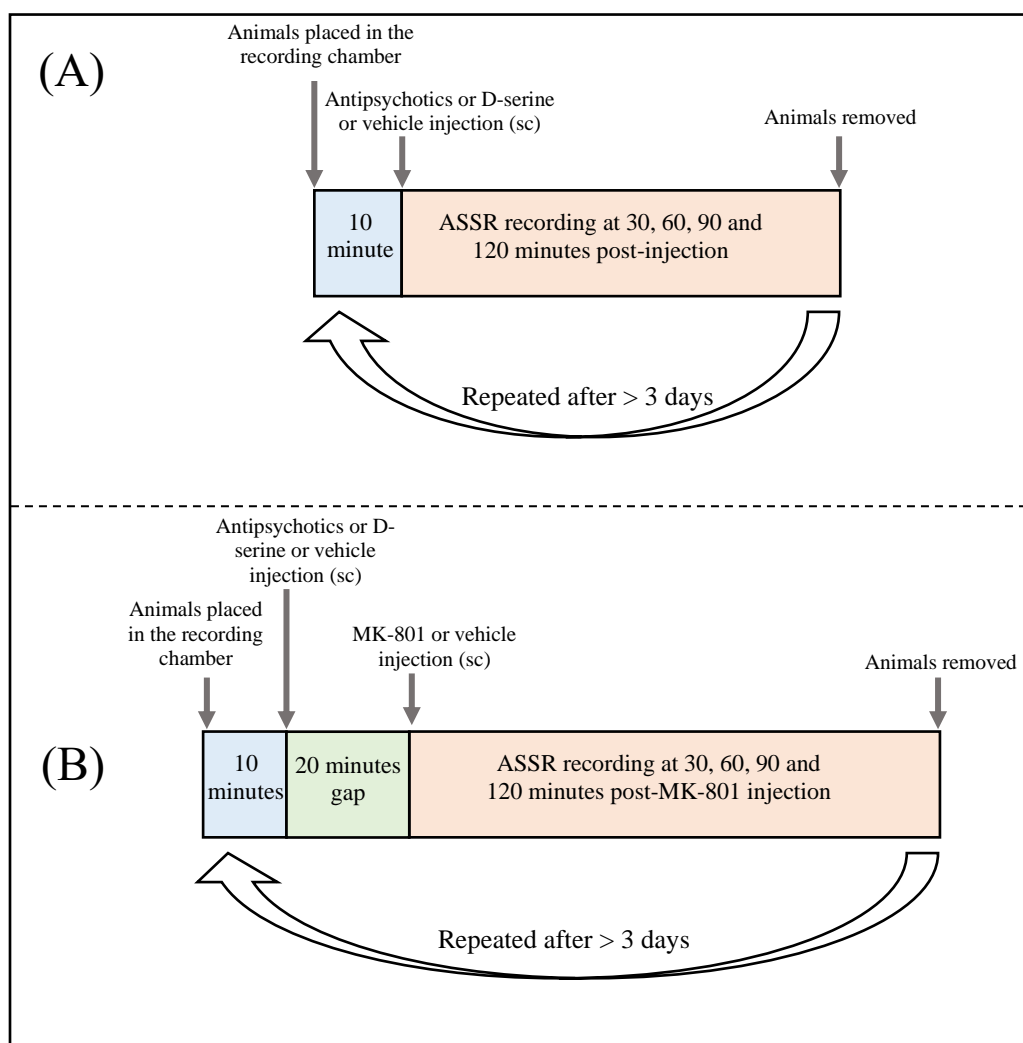
Figure 4.1. Schematic representations of the study design. Vehicle, antipsychotics, or D-serine only (A), and vehicle, antipsychotics, or D-serine pretreatment before MK-801 pharmacology study (b). (sc) subcutaneous.

D-Serine Showed No Effect On 40 Hz ASSR And Did Not Prevent MK-801-Induced Deficits

In the first study, we treated rats with vehicle or D-serine (30-120 mg/kg) alone. There was no effect of D-serine on 40 Hz ASSR. Mixed-effects ANOVA showed no significant treatment effect of D-serine on ITC (p=0.15; $F_{(2.2, 19.4)}$ = 2.03; epsilon = 0.72). There was no significant time effect (p=0.34; $F_{(2.418, 21.76)}$ = 1.132; epsilon = 0.80), or time x treatment interaction (p=0.34; $F_{(4.202, 37.81)}$ = 0.6522; epsilon = 0.47). Similarly, evoked power also showed no significant treatment effect (p=0.15; $F_{(2.291, 20.62)}$ = 1.993; epsilon = 0.76), time effect, (p=0.29; $F_{(2.109, 18.98)}$ = 1.311; epsilon = 0.70), or time x treatment interaction (p=0.63; $F_{(3.618, 32.56)}$ = 0.6199; epsilon = 0.40). Fig. 4.2 shows the group summaries of ITC (A) and evoked power (B) at 30, 60, 90 and 120 minutes after vehicle or 30-120 mg/kg D-serine treatment.
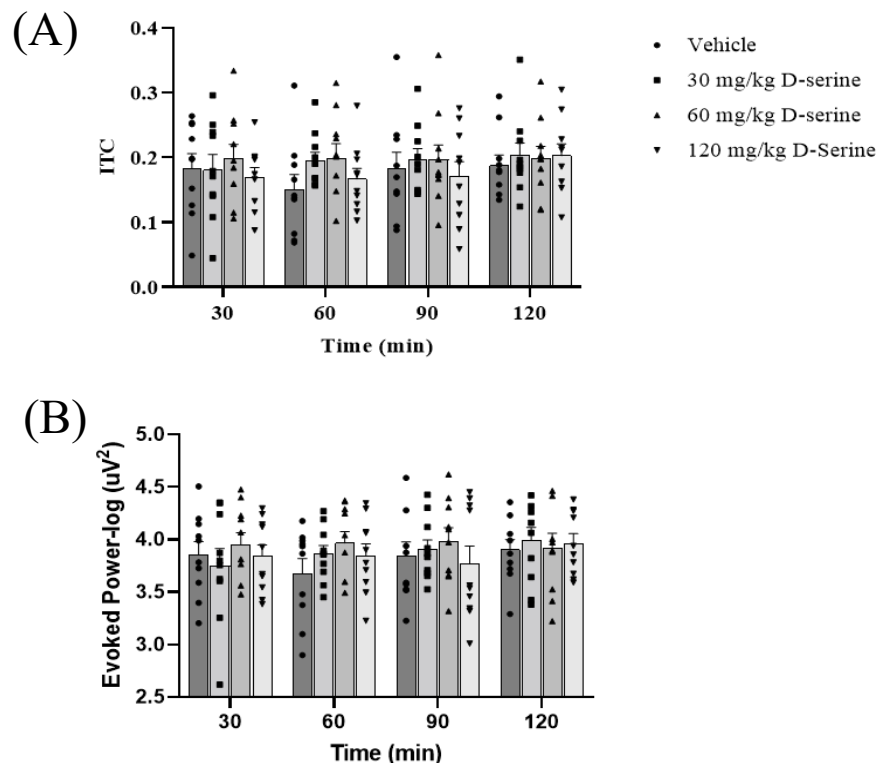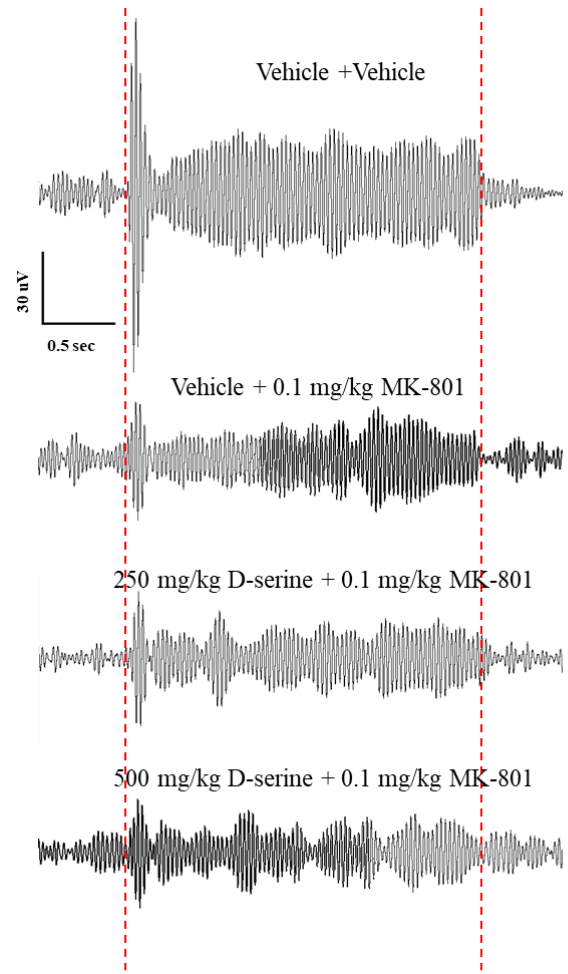
Figure 4.2. Effect of D-serine on 40 Hz ASSR. Group summaries of ITC (A) and evoked power (B) of 40 Hz ASSR at 30, 60, 90 and 120 minutes after vehicle or D-serine treatment. Data are from a group of 10 rats. (Dunnett's post hoc, vehicle comparator). (ITC) inter-trial coherence.

Next, we tested the protective effect of relatively higher doses of D-serine (250-500 mg/kg) pretreatment on MK-801-induced disruption in 40 Hz ASSR (fig. 4.3-A).

Mixed-effects ANOVA showed a significant treatment effect ($p < 0.001$; $F_{(1.436, 14.36)} = 14.83$; epsilon = 0.48), while no significant time effect ($P = 0.70$; $F_{(2.154, 21.54)} = 0.3808$; epsilon = 0.72) or time x treatment interaction ($P = 0.09$; $F_{(4.097, 40.97)} = 2.15$; epsilon = 0.72). Dunnett's post hoc analysis showed a significant reduction in evoked power by 0.1 mg/kg MK-801 at all-time points ($p < 0.05$-$p < 0.01$), as compared to vehicle groups. However, pretreatment with D-serine showed no significant protection against MK-801 induced disruption. Fig. 4.3-B shows the group summaries of evoked power.

(A)

Vehicle +Vehicle

30 uV

0.5 sec

Vehicle + 0.1 mg/kg MK-801

250 mg/kg D-serine + 0.1 mg/kg MK-801

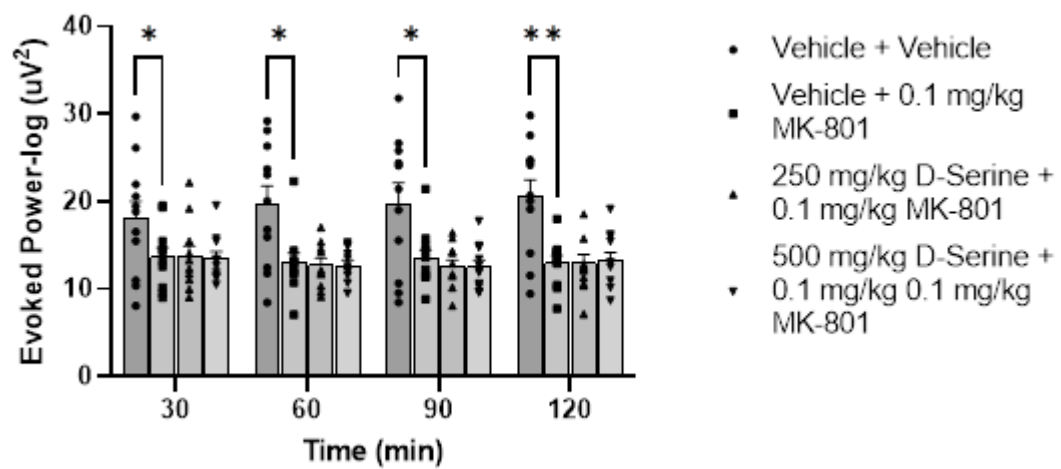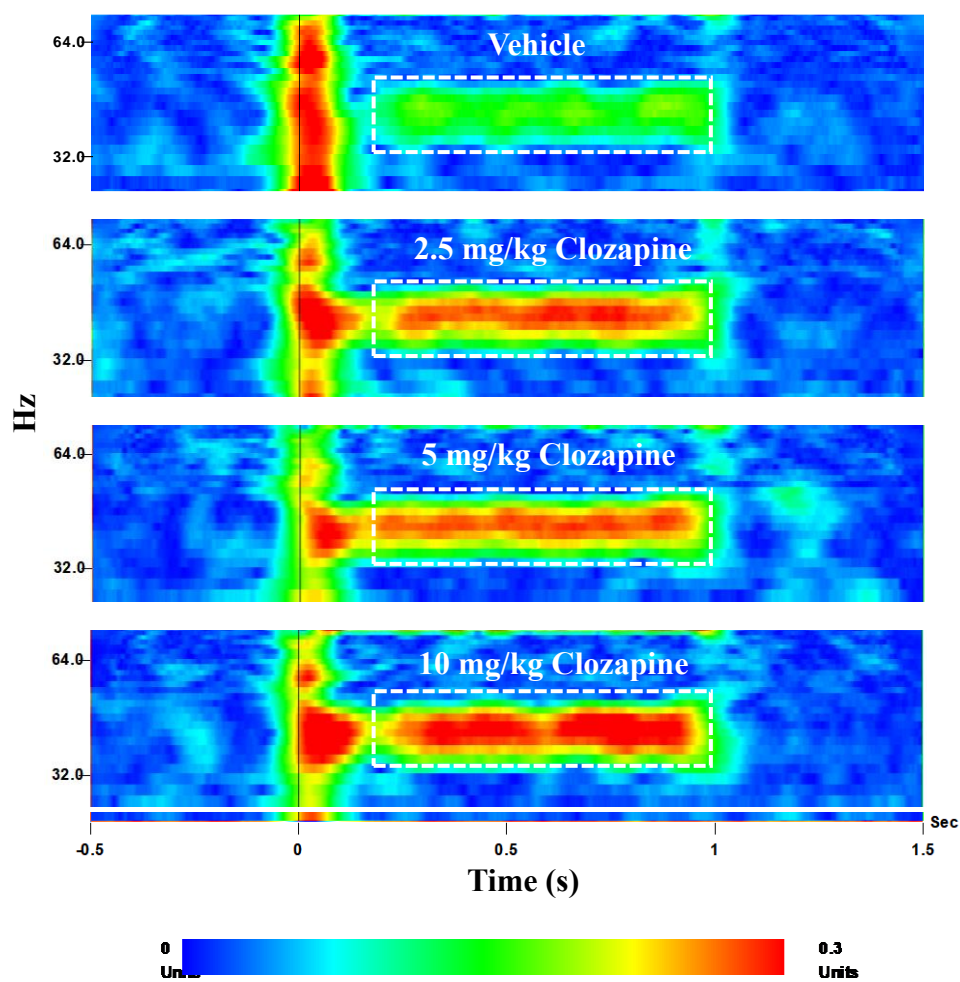500 mg/kg D-serine + 0.1 mg/kg MK-801

(B)

Figure 4.3. Effect of D-serine pretreatment on MK-801-induced deficits in 40 Hz ASSR. A compilation of grand averages of 35-45 Hz filtered 40 Hz ASSR 60 minutes after MK-801 treatment (A). Group summaries of evoked power of 40 Hz ASSR at 30,60,90 and 120 minutes after MK-801 treatment (B). Data are from a group of 10 rats. Asterisks indicate significant differences between vehicle + vehicle and vehicle + MK-801 groups (*p<0.05, **p<0.01; Dunnett's post hoc, vehicle + MK-801 comparator). (ITC) inter-trial coherence.

Clozapine By Itself Improved 40 Hz ASSR In A Dose Related Manner

Our results showed a significant augmentation in 40 Hz ASSR after treatment with clozapine in a dose related manner. Mixed-effect ANOVA showed a significant treatment effect on ITC across all time points from 30-120 minutes post-vehicle or clozapine injection ($p<0.0001$; $F_{(2.6, 28.4)} = 33.10$; epsilon = 0.86). However, no significant time effect ($P=0.38$; $F_{(2.4, 26.6)} = 1.04$; epsilon = 0.80) or time x treatment interaction ($P=0.57$; $F_{(5.9, 65.3)} = 0.79$; epsilon = 0.66) was seen. Evoked power also showed a significant treatment effect ($p<0.001$; $F_{(2.433, 26.76)} = 10.69$; epsilon = 0.81), while no significant time effect ($P=0.75$; $F_{(2.610, 28.71)} = 0.36$; epsilon = 0.87) or interaction of time x treatment ($P=0.27$; $F_{(5.290, 58.19)} = 1.289$; epsilon = 0.59) was observed. Fig. 4.4 shows the group summary of ITC (A) and evoked power (B) at the 30 minutes-post vehicle or clozapine injection, represented as heat maps. Dunnett's post hoc analysis showed a significant increase in ITC by 5 ($p<0.01$-$p<0.001$) and 10 mg/kg ($p<0.05$-$p<0.0001$) clozapine doses across all time points, as compared to vehicle. While increase in ITC by 2.5 mg/kg clozapine was significant up to 90 minutes post-injection ($p<0.05$-$p<0.001$). Moreover, 10 mg/kg clozapine significantly increased evoked power up to 90 minutes time point ($p<0.05$-$p<0.001$), whereas 2.5 and 5 mg/kg clozapine showed significant improvement at only 30 minutes post-injection ($p<0.05$ and $P<0.01$, respectively). Fig. 4.4-C and D summarizes the dose and time course effects of vehicle or clozapine (2.5, 5 or 10 mg/kg) on ITC and evoked power
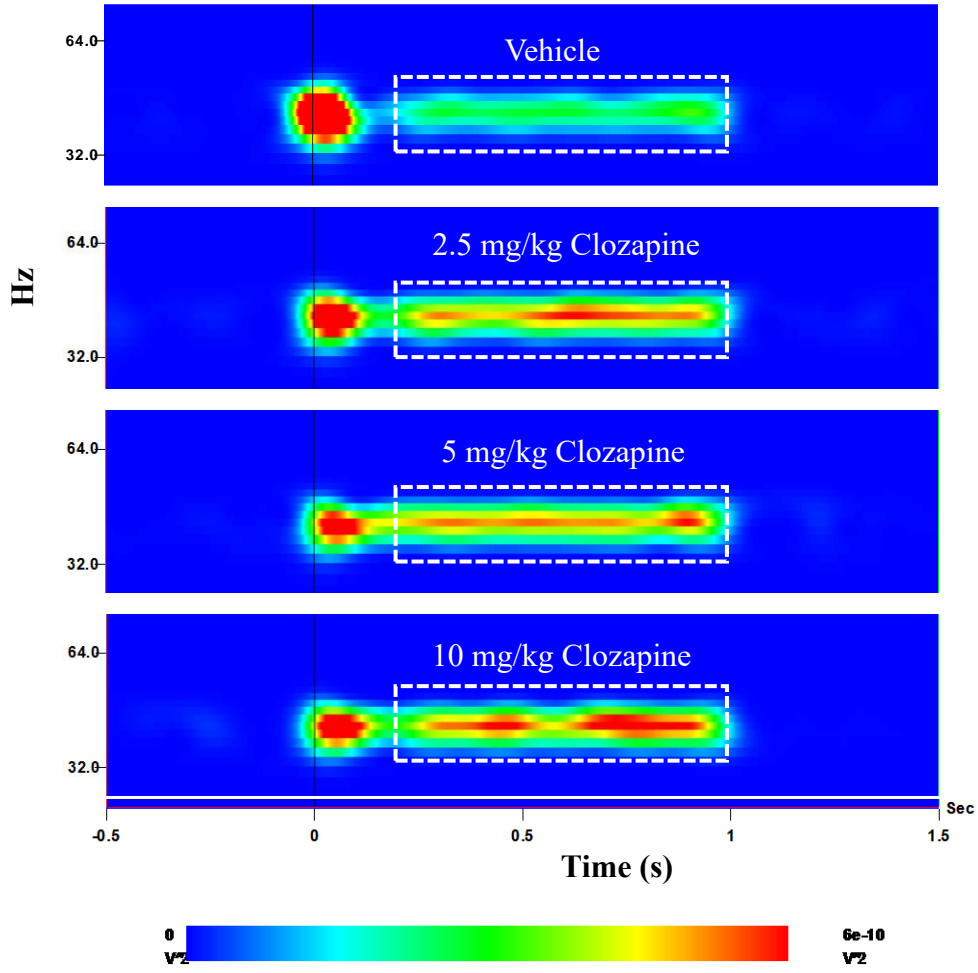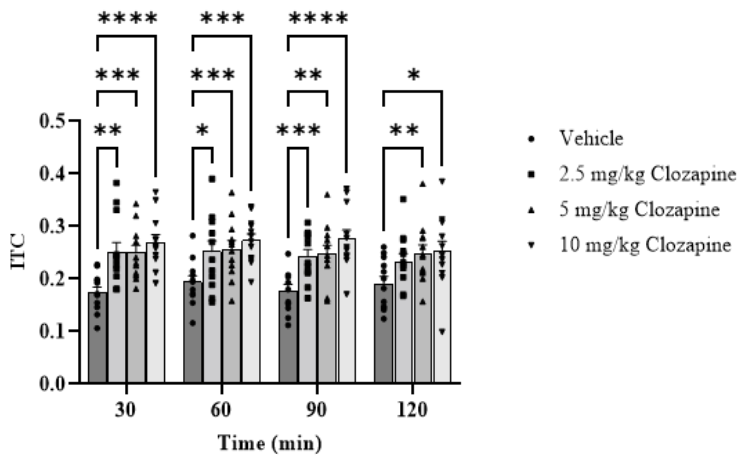
(A)

ITC

(B)

Evoked Power

Vehicle

2.5 mg/kg Clozapine

5 mg/kg Clozapine

10 mg/kg Clozapine

Hz

Time (s)

(C)

(D)

- Vehicle
- 2.5 mg/kg Clozapine
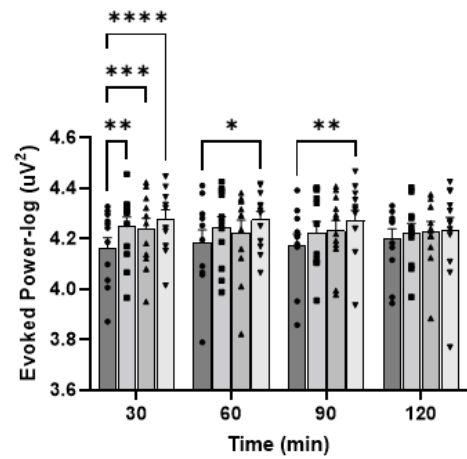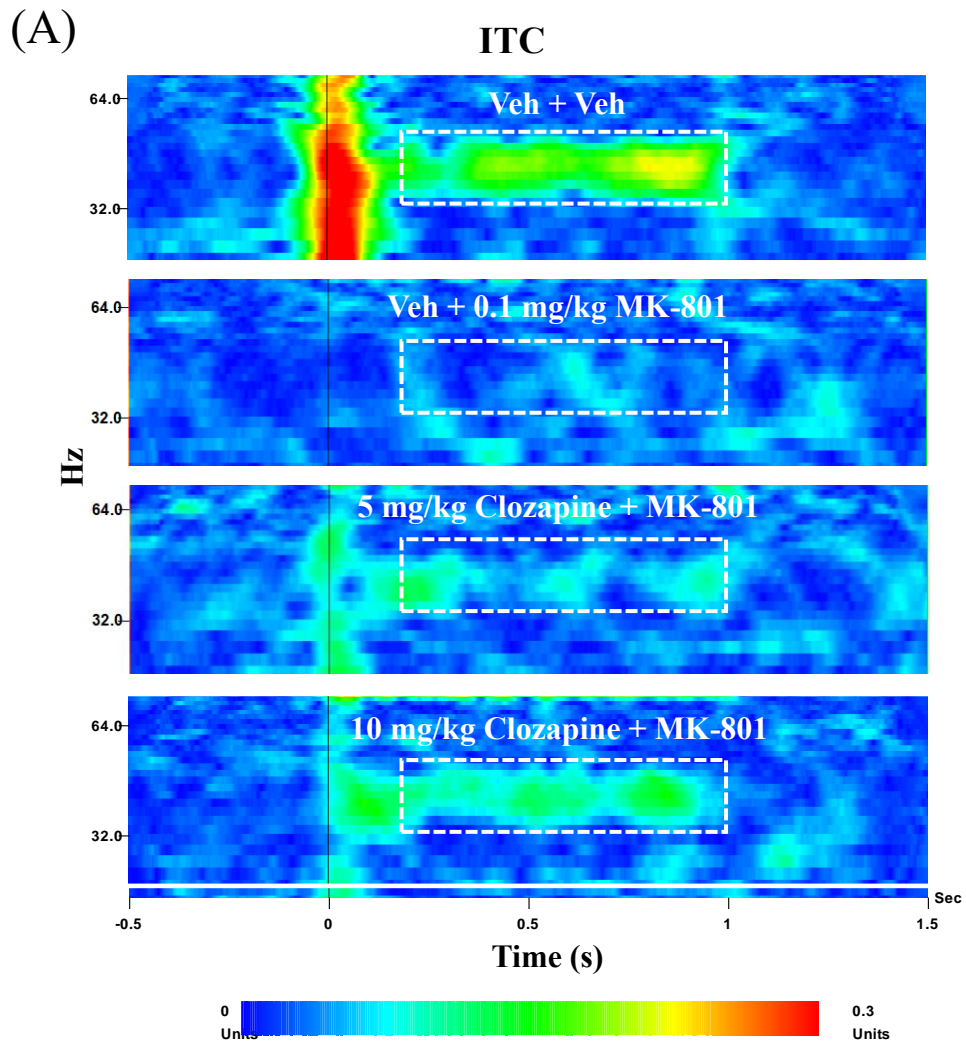- 5 mg/kg Clozapine
- 10 mg/kg Clozapine

Figure 4.4. Effect of clozapine on 40 Hz ASSR. Heat-map summaries of ITC (A) and evoked power (B) of 40 Hz ASSR at 30 minutes after vehicle or clozapine (2.5, 5, or 10 mg/kg, sc) treatment. Group summaries of ITC (C) and evoked power (D) data at 30,60,90 and 120 minutes after vehicle or clozapine treatment. Data are from a group of 11 rats. (*p<0.05, **p<0.01, ***p<0.001, ****p<0.0001; Dunnett's post hoc; vehicle comparator). (ITC) inter-trial coherence.

Clozapine Pretreatment Partially Protected Against MK-801-Induced Deficits In 40 Hz ASSR

Next, we tested if clozapine could improve MK-801-induced deficits in 40 Hz ASSR measures. Rats were given either vehicle only, vehicle before 0.1 mg/kg MK-801 treatment, or 5 or 10 mg/kg clozapine before MK-801 treatment. Mixed-effects ANOVA showed a highly significant effect of treatment (P<0.0001; F (2.1, 19.0) = 19.37; epsilon = 0.70) and a significant time x treatment interaction (P<0.05; F (4.9, 44.0) = 3.19; epsilon = 0.54) but no time effect (P=0.69; F (2.7, 24.1) = 0.46; epsilon = 0.89) on ITC. Fig. 4.5 represents TFA heat maps of concatenated group data for ITC (A) and evoked power (B) at 60 minutes. Dunnett's post hoc analysis showed a highly significant MK-801-induced reduction in ITC (fig. 4.5-C) at 60, 90 and 120 minutes as compared to vehicle + vehicle group (p<0.01-p<0.0001). Pretreatment with 10 mg/kg clozapine significantly protected against MK-801-induced reduction in ITC at only 60- and 120-minutes time-points (P<0.05), while 5 mg/kg clozapine showed significant protection at only 120 minutes (p<0.05, vehicle + MK-801 comparator).

Evoked power also showed a significant treatment effect (P<0.0001; F (2.222, 20.00) = 20.20; epsilon = 0.74) and a significant time x treatment interaction (P<0.05; F (4.938, 44.44) = 2.74; epsilon = 0.54) but no time effect (P=0.97; F (2.911, 26.20) = 0.075; epsilon = 0.97). In post hoc analysis, 10 mg/kg clozapine group showed a highly significant protective effect on evoked power at 60, 90 and 120 minutes (p<0.01), while 5 mg/kg group was only significantly

protective at 60 minutes as compared to vehicle + MK-801 group. Moreover, the protective

effect of clozapine pretreatment on ITC and evoked power was partial against MK-801 induced

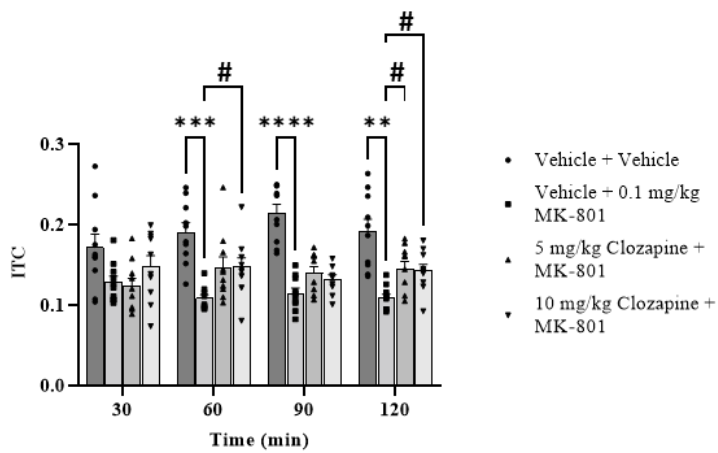disruption. Group summary results are presented in fig. 4.5 (C and D).

(A) ITC

(B) Evoked Power

(C)

(D)
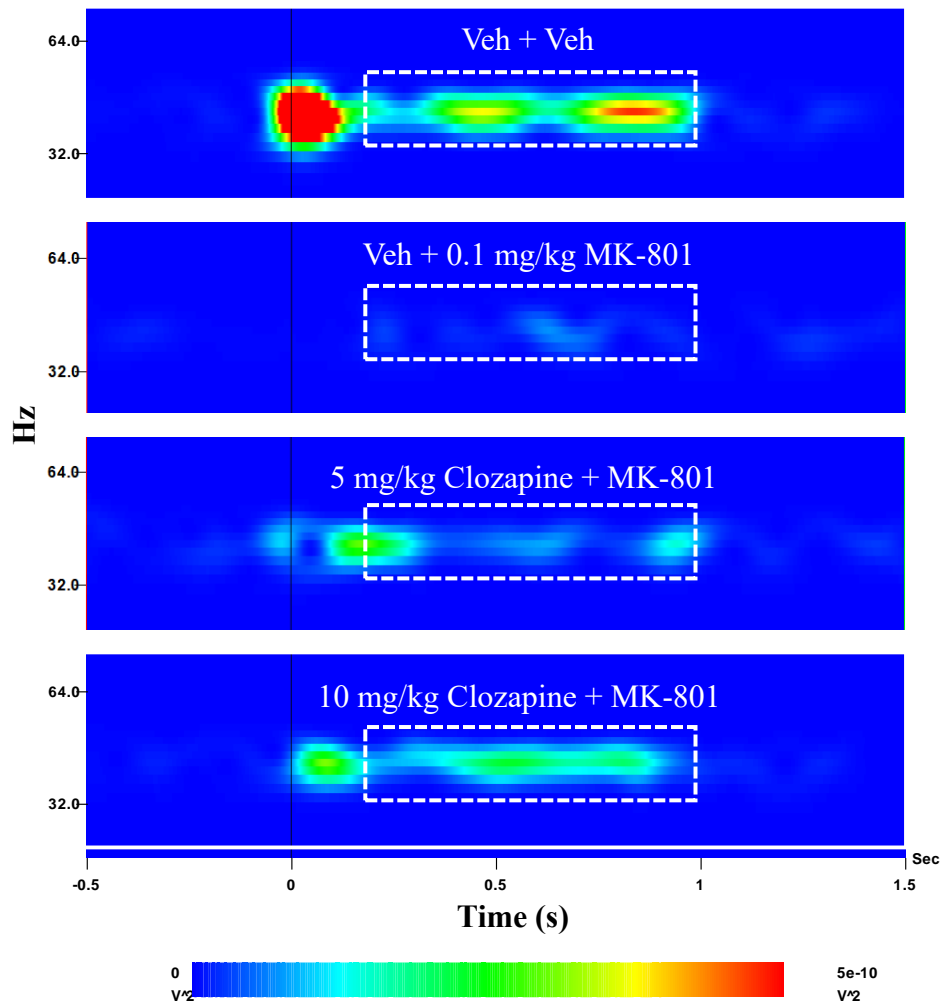
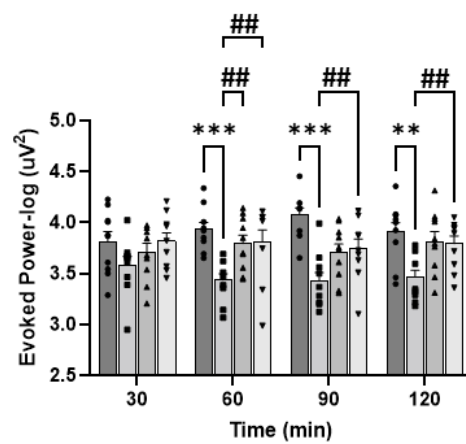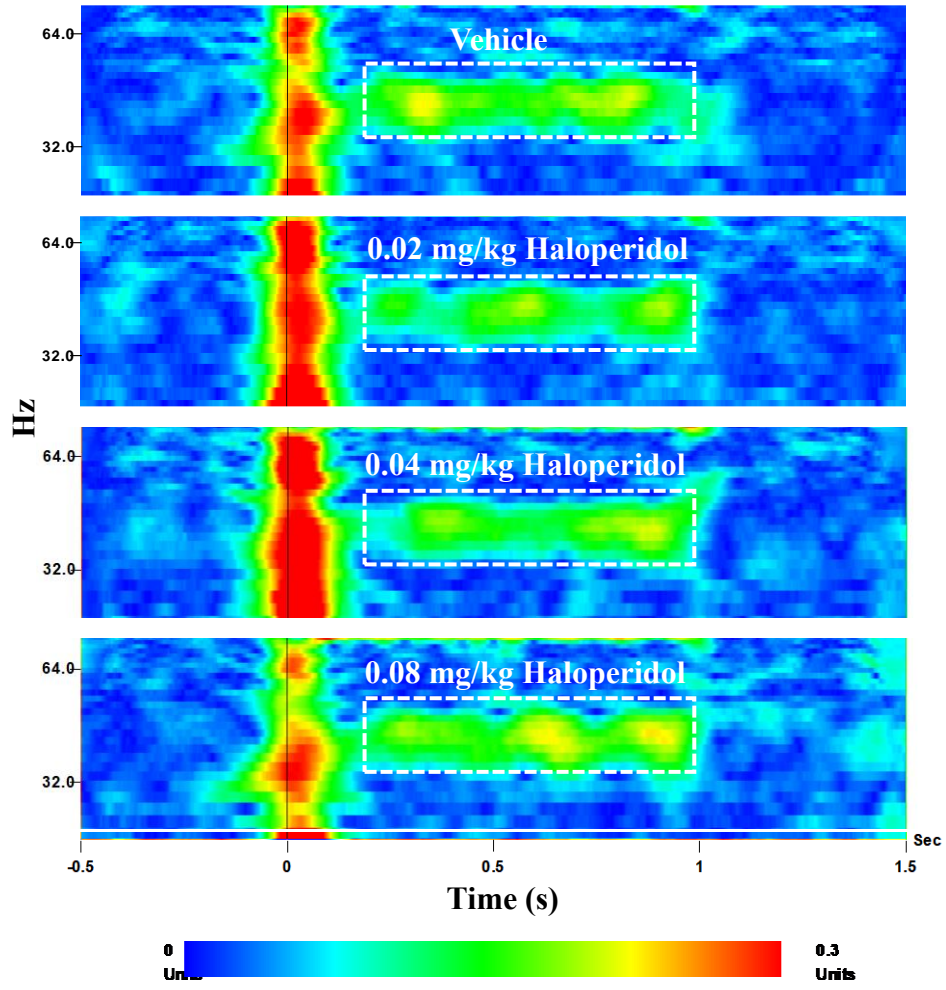**(B)** Evoked Power

(C)

(D)

Figure 4.5. Effect of clozapine pretreatment on MK-801-induced disruption in 40 Hz ASSR. Heat-map summaries of ITC (A) and evoked power (B) of 40 Hz ASSR at 30 minutes after vehicle or MK-801 treatment. Group summaries of ITC (C) and evoked power (D) data at 30, 60, 90 and 120 minutes after vehicle or MK-801 treatment. Data are from a group of 10 rats. Asterisks indicate significant differences between vehicle + vehicle and vehicle + MK-801 groups (**$p<0.01$, ***$p<0.001$, ****$p<0.0001$), while number sign represent significant differences between vehicle + MK-801 and clozapine + MK-801 groups (#$p<0.05$, ##$p<0.01$; Dunnett's post hoc, vehicle + MK-801 comparator). (ITC) inter-trial coherence.

Treatment With Haloperidol Did Not Improve 40 Hz ASSR

There was no improvement observed in 40 Hz ASSR after haloperidol treatment. Mixed-effects ANOVA showed no significant effect of haloperidol treatment on ITC ($p=0.86$; $F_{(1.8, 14.2)} = 0.12$; epsilon = 0.59), also there was no significant time effect ($p=0.15$; $F_{(1.849, 14.79)} = 2.164$; epsilon = 0.61), or time treatment interaction ($p=0.31$; $F_{(3.422, 27.37)} = 1.246$; epsilon = 0.38). Evoked power also did not show any significant treatment effect ($p=0.45$; $F_{(1.869, 14.95)} = 0.82$; epsilon = 0.62), no significant time effect ($p=0.09$; $F_{(2.294, 18.35)} = 2.58$; epsilon = 0.76), or time x treatment interaction ($p=0.12$; $F_{(4.001, 32.01)} = 1.955$; epsilon = 0.44). Fig. 4.6 shows heat maps of ITC (A) and evoked power (B) at 30 minutes after vehicle or 0.02-0.08 mg/kg haloperidol treatment. Results are presented as group summaries in fig. 4.6 (C and D).
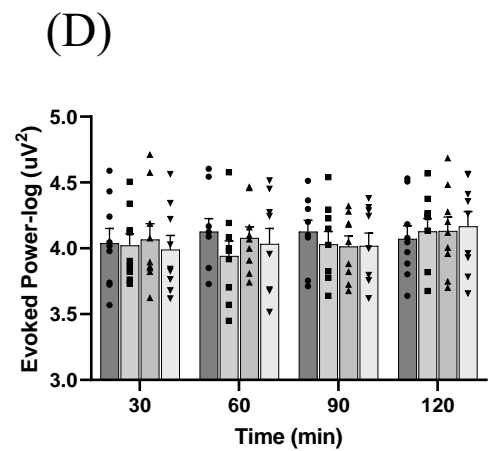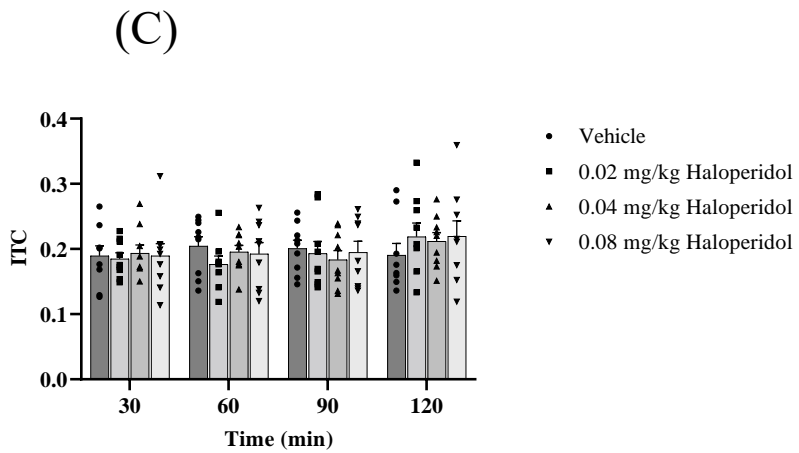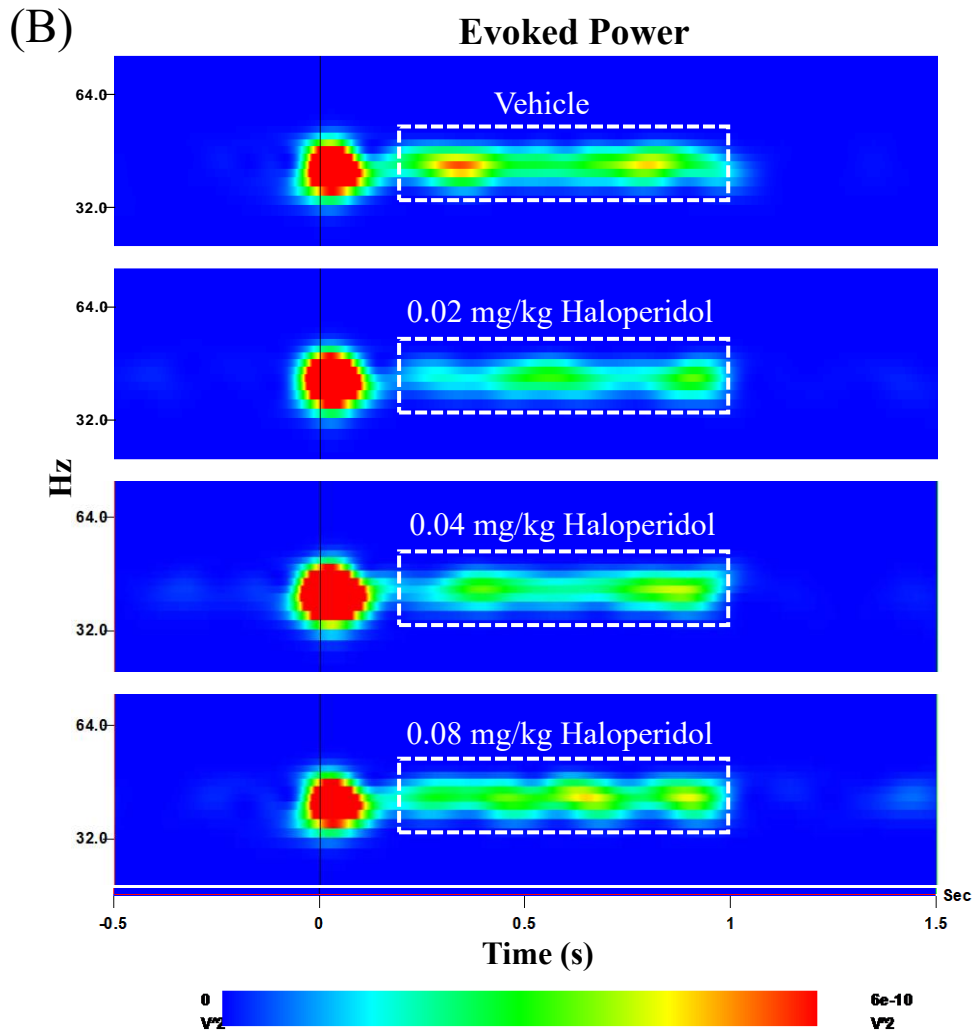
(A)

ITC

Vehicle

0.02 mg/kg Haloperidol

0.04 mg/kg Haloperidol

0.08 mg/kg Haloperidol

Time (s)

Hz

(B)

Evoked Power

(C)

(D)

Figure 4.6. Effect of haloperidol on 40 Hz ASSR. Heat-map summaries of ITC (A) and evoked power (B) of 40 Hz ASSR at 30 minutes after vehicle or haloperidol (0.02, 0.04, or 0.08 mg/kg, sc) treatment. Group summaries of ITC (A) and evoked power (D) data at 30, 60, 90 and 120 minutes after vehicle or haloperidol treatment. Data are from a group of 9 rats. (ITC) inter-trial coherence. Dunnett's post hoc, and vehicle comparator.

Haloperidol Pre-Treatment Had No Ameliorative Effect Against MK-801-Induced Disruption

Pretreatment with haloperidol also had no protective effect against MK-801-induced disruption of 40 Hz ASSR. Mixed-effects ANOVA revealed a highly significant treatment effect for ITC ($p < 0.0001$; $F_{(1.8, 12.6)} = 24.51$; epsilon = 0.6). There was also a significant time effect ($p < 0.001$; $F_{(1.427, 9.989)} = 22.56$; epsilon = 0.47), and time x treatment interaction ($p < 0.01$; $F_{(2.958, 17.09)} = 5.364$; epsilon = 0.33). Dunnett's post hoc analysis showed a significant reduction by 0.1 mg/kg MK-801 ($p < 0.01$) at 60-, 90-, and 120-minutes time points, as compared to vehicle + vehicle group. Haloperidol pretreatment showed no significant protective effect against MK-801 induced reduction in ITC.

Furthermore, evoked power also showed a significant treatment effect ($p < 0.01$; $F_{(1.750, 12.25)} = 13.46$; epsilon = 0.58), and a significant time x treatment interaction ($p < 0.05$; $F_{(3.481, 20.11)} = 2.98$; epsilon = 0.39). However, there was no significant time effect ($p = 0.09$; $F_{(0.3250, 2.275)} = 6.11$; epsilon = 0.11). Post hoc analysis showed a significant reduction by 0.1 mg/kg MK-801 ($p < 0.01$) at 60-, 90-, and 120-minutes time points, as compared to vehicle + vehicle group. However, haloperidol failed to show any protection against MK-801-induced reduction in evoked power Fig 4.7 (A-D) shows heat maps and group summaries of ITC and evoked power.
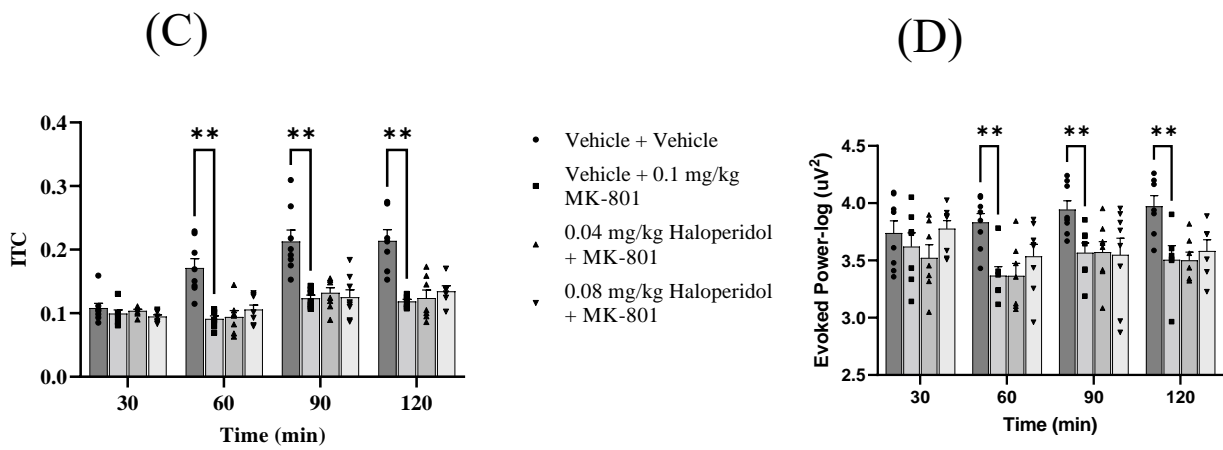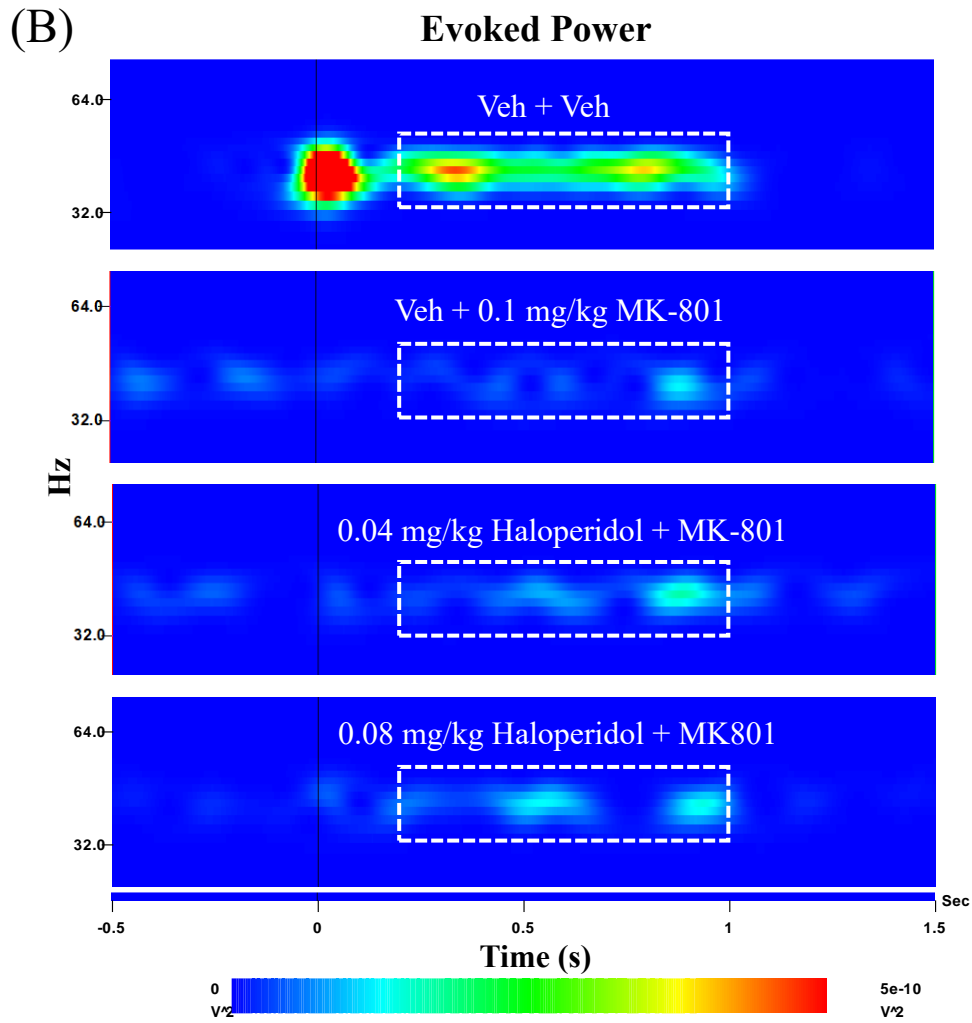
(A)

ITC

(B) **Evoked Power**

(C)

(D)
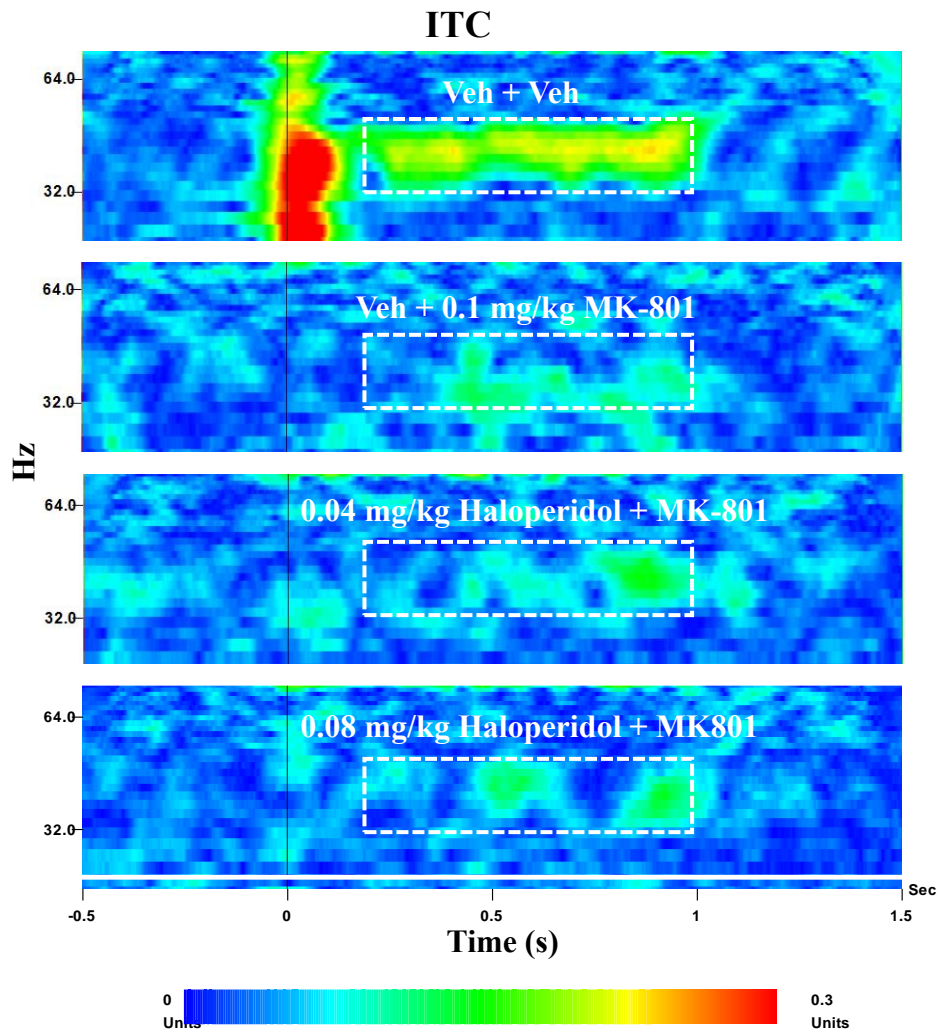
Figure 4.7. Effect of haloperidol pretreatment on MK-801-induced deficits in 40 Hz ASSR. Heat-map summaries of ITC (A) and evoked power (B) of 40 Hz ASSR at 30 minutes after MK-801 treatment. Group summaries of ITC (C) and evoked power (D) data at 30, 60, 90 and 120 minutes after MK-801 treatment. Data are from a group of 8 rats. Asterisks indicate significant differences between vehicle + vehicle and vehicle + MK-801 groups (**p<0.01; Dunnett's post hoc, vehicle + MK-801 comparator). (ITC) inter-trial coherence.

Discussion

40 Hz ASSR is a candidate biomarker to test NMDAR- dependent neural synchrony in the cortical circuits (Sivarao et al., 2016). Neural synchrony, which is an important prerequisite for sensory-evoked gamma, plays an important role in attention, memory, and cognitive processes (Fries et al., 2001; Gray et al., 1990; Landau and Fries, 2012). Thus, it is reasonable to assume that disruption in the cortical synchrony in the form of ASSR may contribute to sensory and cognitive deficits. Indeed, deficits in 40 Hz ASSR predict clinical outcomes in individuals at high risk for schizophrenia as well as in patients (Grent-'t-Jong et al., 2021; Molina et al., 2020).

In addition to being a biomarker correlated with symptoms and functional outcomes, the 40 Hz ASSR may be also leveraged as an easily accessed neural synchrony marker that is also robustly translational. The current body of literature indicates that 40 Hz ASSR may involve the activity of cortical pyramidal-interneuron or the so-called PING networks that are also involved in evoked gamma oscillations. For example, optogenetic driving of the layer 2/3 PV+ basket cells result in a robust entrainment of these cells when the driving frequency is around 40 Hz. Additionally, this also results in a robust increase in evoked field gamma oscillations (Cardin et al., 2009). Moreover, genetic ablation in mice of the NR1 subunit, the obligatory component of the heteromeric NMDAR, results in a specific deficit of gamma entrainment, centered ~ 40 Hz (Carlén et al., 2012). Even more pertinent to our work, ASSR protocol in these NR1 mutant mice

evoke a significantly attenuated ASSR response at 40 Hz. Lastly, we have shown that acute NMDA antagonism also results in a robust and consistent attenuation of the 40 Hz ASSR response (Raza and Sivarao, Sivarao et al.,2016, Sivarao et al., 2013). While it is clear that 40 Hz ASSR is highly susceptible to NMDA disruption, we have yet to see any data showing its positive modulation to NMDA-based activation. The current work was done to test positive modulation of the 40 Hz ASSR by several pharmacological approaches.

First, we tested D-serine, a co-agonist believed to be active endogenously at NMDA receptors (Balu and Coyle, 2015). Indeed, several small clinical trials have demonstrated modest positive effects on ameliorating schizophrenia symptoms in patients using this approach (Singh and Singh, 2011). Interestingly, there is one small study that positively correlated endogenous D-serine levels in schizophrenia patients with evoked power of 40 Hz ASSR (Koshiyama et al., 2019). No such correlation was seen in healthy controls. Overall, it is robust and convincing *in vivo* data that show target engagement with D-serine treatment are lacking. As an attempt towards filling this gap, we evaluated 40 Hz ASSR response both through dose-response studies with D-serine as well as an attempted reversal of MK801-mediated disruption. As discussed in the results section, we reported an unambiguous lack of response. It is unclear why this is the case. For one, the therapeutic effect of D-serine in the small clinical trials alluded to above was after several weeks of chronic treatment. It is possible that chronic treatment might have a better outcome than the current result. However, it has been reported that hippocampal glycine site on the NMDA receptors remains unsaturated and exogenous co-agonists can therefore augment NMDA receptor function (Bergeron et al., 1998). Unfortunately, our data does not seem to support this finding. At this time, it is unclear to us why this regimen was ineffective.

133

Previous studies, however, have shown that D-serine may improve cognitive deficits induced by NMDAR and acetylcholine receptor antagonists (Fone et al., 2020; Karasawa et al., 2008). Similarly, pharmacological stimulation of GMS through D-serine shows ameliorative effect on NMDAR-antagonist induced disruption in NMDAR function. (Gozzi et al., 2008) However, in other studies, D-serine was unable to improve NMDAR antagonist-caused deficits in sensory processing and stimulus-evoked gamma, which is consistent with our results (Hudson et al., 2016). It is important to note that these studies used significantly higher doses of D-serine (1-2 mg/kg) than the current study. Such high doses have been shown to also induce acute nephrotoxicity in rodents (Hasegawa et al., 2019).

We tested clozapine and haloperidol for their effects on the 40 Hz ASSR. Interestingly, both clozapine and haloperidol have been previously reported to acutely augment NMDA transmission *in vitro* (Arvanov et al., 1997). Interestingly, using a steady state visual paradigm that used photic stimulation at alpha (~10 Hz) frequency, it was reported schizophrenia patients responsive to clozapine showed a robust enhancement in the steady state response, relative to unresponsive patients who were also on clozapine (Jin et al., 1995). Based on these data, we hypothesize that clozapine would augment the ASSR. Of course, clozapine is a notoriously promiscuous drug that binds to a multitude of neurotransmitter receptors, including dopaminergic, serotonergic, muscarinic, adrenergic and histaminergic receptors of varying subtypes (Siafis et al., 2017). Thus, it would be a Herculean task to try todecipher what exactly was the mechanism that enabled a dose-dependent and robust activation of the 40 Hz ASSR. At this time, we are not able to pursue this line of research. Rather, we are reassured that 40 Hz ASSR is a neural synchrony measure that can be bidirectionally and robustly modulated by

pharmacological treatment. This is a very encouraging finding and lays the groundwork for using 40 Hz ASSR as a pharmacodynamic biomarker for drug development studies in future.

To the best of our knowledge, this is the first study to test and report such effects of clozapine on 40 Hz ASSR. Previous studies have reported that, as compared to any other antipsychotics, clozapine showed improvement in neurophysiological (e.g., evoked gamma, auditory evoked response (AER)) (Hudson et al., 2016; Umbricht et al., 1998), sensory-motor gating (e.g., pre-pulse inhibition (PPI)) (Hudson et al., 2016) and cognitive performance (Karasawa et al., 2008) function against NMDA antagonist-induced disruption. Moreover, clozapine shows a distinct clinical profile that separates it from the rest of antipsychotics (Leucht et al., 2013). It is highly effective against treatment-resistant schizophrenia, it improves cognitive and negative symptoms, and schizophrenia patients voluntarily stay on clozapine treatment regimen for far longer period than any other antipsychotic (Oh et al., 2020; Wagner et al., 2021). Our results further add to the differentiated profile of clozapine in comparison with a typical antipsychotic like haloperidol. It remains to be seen if this holds true with reference to atypical antipsychotics as well, that share a similar spectrum of affinities to the list of neurotransmitter receptors outlined above.

Although we focused only on EEG data from vertex for analyzing 40 Hz ASSR in the above sections, preliminary analysis of frontal EEG data from the same rats showed some very interesting effects of clozapine. For example, unlike the vertex response, the frontal ASSR tended to evolve more slowly, taking about 200-250 ms to establish robust 40 Hz entrainment. Clozapine, at all doses tested, showed a rapid entrainment relative to vehicle treatment. Indeed, this happened 100-150 ms faster than it did with the vehicle group (supplementary Figure 4). Moreover, this was not often associated with an increase in evoked power, particularly at lower

doses. This observation in which synchrony improves without an accompanying increase in signal power is a signature of "phase resetting" (Voloh & Womelsdorf, 2016). This entails, endogenous on-going oscillations are resetting their on-going phase to embrace the new phase (40 Hz). This is a very interesting research direction that has not been reported previously to be associated with any pharmacological treatment. We look forward to following up on this in future studies.

Haloperidol did not have the same effects as clozapine on the 40 Hz ASSR, despite the *in vitro* observation that it improved NMDA transmission (Arvanov et al., 1997). In the above paper, although haloperidol improved NMDA transmission, it did it at concentrations that were 3-5-fold greater than that of clozapine (Arvanov et al., 1997). Thus, it is possible that a higher dose of haloperidol would have shown an effect on NMDA transmission. However, we were careful to use only doses that were not associated with motoric side effects of antipsychotic drugs and were anchored to dose levels associated with clinically relevant D2 occupancy (Kapur et al., 2000). Doses above 0.1 mg/kg of haloperidol are associated with catalepsy in rats (Wadenberg et al., 2001).

In summary, this study showed that only clozapine, at acute concentrations that are comparable to clinical steady state concentrations, showed a robust augmentation of the 40 Hz ASSR. Although clozapine appears to mediate at least part of its effects by accelerating the phase resetting of on-going neural oscillations, it is not possible to predict the exact molecular mechanism for this without extensive and further research. For now, it is exciting to note that 40 Hz ASSR can be dose-dependently and bidirectionally modified by pharmacological treatments. These are promising results in further establishing this measure of evoked gamma synchrony as a potential pharmacodynamic biomarker. Once validated, such tools are invaluable in guiding

preclinical candidate selection, dose selection in early clinical development, and may be even useful for patient stratification and proof of concept studies.

References

Allen, R. M., and Young, S. J. (1978). Phencyclidine-induced psychosis. The American Journal of Psychiatry, 135(9), 1081–1084. https://doi.org/10.1176/AJP.135.9.1081

Arvanov, V. L., Liang, X., Schwartz, J., Grossman, S., & Wang, R. Y. (1997). Clozapine and haloperidol modulate N-methyl-D-aspartate- and non-N-methyl-D-aspartate receptor-mediated neurotransmission in rat prefrontal cortical neurons in vitro. The Journal of pharmacology and experimental therapeutics, 283(1), 226–234.

Balu, D. T., and Coyle, J. T. (2015). The NMDA receptor 'glycine modulatory site' in schizophrenia: d-serine, glycine, and beyond. Current Opinion in Pharmacology, 20, 109. https://doi.org/10.1016/J.COPH.2014.12.004

Bergeron, R., Meyer, T. M., Coyle, J. T., and Greene, R. W. (1998). Modulation of N-methyl-d-aspartate receptor function by glycine transport. Proceedings of the National Academy of Sciences of the United States of America, 95(26), 15730. https://doi.org/10.1073/PNAS.95.26.15730

Bristow, L. J., Easton, A. E., Li, Y. W., Sivarao, D. V., Lidge, R., Jones, K. M., Post-Munson, D., Daly, C., Lodge, N. J., Gallagher, L., Molski, T., Pieschl, R., Chen, P., Hendricson, A., Westphal, R., Cook, J., Iwuagwu, C., Morgan, D., Benitex, Y., … Olson, R. (2016). The Novel, Nicotinic Alpha7 Receptor Partial Agonist, BMS-933043, Improves Cognition and Sensory Processing in Preclinical Models of Schizophrenia. PLOS ONE, 11(7), e0159996. https://doi.org/10.1371/JOURNAL.PONE.0159996

Cardin, J. A., Carlén, M., Meletis, K., Knoblich, U., Zhang, F., Deisseroth, K., … Moore, C. I. (2009). Driving fast-spiking cells induces gamma rhythm and controls sensory responses. Nature, 459(7247), 663–667. https://doi.org/10.1038/nature08002

Carlén, M., Meletis, K., Siegle, J. H., Cardin, J. A., Futai, K., Vierling-Claassen, D., … Tsai, L.-H. (2012). A critical role for NMDA receptors in parvalbumin interneurons for gamma rhythm induction and behavior. Molecular Psychiatry, 17(5), 537–548. https://doi.org/10.1038/mp.2011.31

Egerton, A., Reid, L., McKerchar, C. E., Morris, B. J., and Pratt, J. A. (2005). Impairment in perceptual attentional set-shifting following PCP administration: A rodent model of set-shifting deficits in schizophrenia. Psychopharmacology, 179(1), 77–84. https://doi.org/10.1007/S00213-004-2109-Y/FIGURES/3

Ermilov, M., Gelfin, E., Levin, R., Lichtenberg, P., Hashimoto, K., Javitt, D. C., & Heresco-Levy, U. (2013). A pilot double-blind comparison of d-serine and high-dose olanzapine in treatment-resistant patients with schizophrenia. Schizophrenia Research, 150(2–3), 604–605. https://doi.org/10.1016/J.SCHRES.2013.09.018

Fone, K. C. F., Watson, D. J. G., Billiras, R. I., Sicard, D. I., Dekeyne, A., Rivet, J.-M. M., … Millan, M. J. (2020). Comparative Pro-cognitive and Neurochemical Profiles of Glycine Modulatory Site Agonists and Glycine Reuptake Inhibitors in the Rat: Potential Relevance to Cognitive Dysfunction and Its Management, 57(5), 2144–2166. Retrieved from

http://link.springer.com/10.1007/s12035-020-01875-9

Fries, P., Reynolds, J. H., Rorie, A. E., Desimone, R., and Schroeder, C. E. (2001). Modulation of Oscillatory Neuronal Synchronization by Selective Visual Attention. Science, 291(5508), 1560–1563. Retrieved from http://www.ncbi.nlm.nih.gov/pubmed/11222864

Gold, J. M. (2004). Cognitive deficits as treatment targets in schizophrenia. Schizophrenia Research, 72(1), 21–28. https://doi.org/10.1016/J.SCHRES.2004.09.008

Gozzi, A., Herdon, H., Schwarz, A., Bertani, S., Crestan, V., Turrini, G., and Bifone, A. (2008). Pharmacological stimulation of NMDA receptors via co-agonist site suppresses fMRI response to phencyclidine in the rat. Psychopharmacology, 201(2), 273–284. https://doi.org/10.1007/S00213-008-1271-Z

Gray, C. M., Engel, A. K., König, P., and Singer, W. (1990). Stimulus-Dependent Neuronal Oscillations in Cat Visual Cortex: Receptive Field Properties and Feature Dependence. European Journal of Neuroscience, 2(7), 607–619. https://doi.org/10.1111/J.1460-9568.1990.TB00450.X

Green, M. F., and Nuechterlein, K. H. (1999). Should Schizophrenia Be Treated as a Neurocognitive Disorder? Schizophrenia Bulletin, 25(2), 309–319. https://doi.org/10.1093/oxfordjournals.schbul.a033380

Green, M. F. (2006). Cognitive Impairment and Functional Outcome in Schizophrenia and Bipolar Disorder. The Journal of Clinical Psychiatry, 67(suppl 9), 3183. Retrieved from https://www.psychiatrist.com/jcp/bipolar/cognitive-impairment-functional-outcome-schizophrenia-bipolar-endophenotype-matrics

Grent-'t-Jong, T., Gajwani, R., Gross, J., Gumley, A., Krishnadas, R., Lawrie, S., … Uhlhaas, P. (2021). 40-Hz Auditory Steady-State Responses Characterize Circuit Dysfunctions and Predict Clinical Outcomes in Clinical High-Risk for Psychosis Participants: A Magnetoencephalography Study. Biological Psychiatry, 90(6), 419–429. https://doi.org/10.1016/J.BIOPSYCH.2021.03.018

Hari, R., Hämäläinen, M., and Joutsiniemi, S. L. (1989). Neuromagnetic steady-state responses to auditory stimuli. The Journal of the Acoustical Society of America, 86(3), 1033–1039. https://doi.org/10.1121/1.398093

Hasegawa, H., Masuda, N., Natori, H., Shinohara, Y., and Ichida, K. (2019). Pharmacokinetics and toxicokinetics of d-serine in rats. Journal of Pharmaceutical and Biomedical Analysis, 162, 264–271. https://doi.org/10.1016/J.JPBA.2018.09.026

Hudson, M. R., Rind, G., O'brien, T. J., and Jones, N. C. (2016). Reversal of evoked gamma oscillation deficits is predictive of antipsychotic activity with a unique profile for clozapine. Translational Psychiatry, 6, 784. https://doi.org/10.1038/tp.2016.51

Hyman, S. E., and Fenton, W. S. (2003). What are the right targets for psychopharmacology? Science, 299(5605), 350–351. https://doi.org/10.1126/SCIENCE.1077141/ASSET/9D34889E-24C3-4D02-857E-77DA0110A0EB/ASSETS/SCIENCE.1077141.FP.PNG

Javitt, D. C., and Zukin, S. R. (1991). Recent advances in the phencyclidine model of

schizophrenia. The American Journal of Psychiatry, 148(10), 1301–1308. https://doi.org/10.1176/AJP.148.10.1301

Jin, Y., Potkin, S. G., & Sandman, C. (1995). Clozapine Increases EEG Photic Driving in Clinical Responders. Schizophrenia Bulletin, 21(2), 263–268. https://doi.org/10.1093/SCHBUL/21.2.263

Kapur, S., Wadenberg, M. L., and Remington, G. (2000). Are animal studies of antipsychotics appropriately dosed? Lessons from the bedside to the bench. Canadian Journal of Psychiatry. Revue Canadienne de Psychiatrie, 45(3), 241–246. https://doi.org/10.1177/070674370004500302

Kapur, S., Vanderspek, S. C., Brownlee, B. A., and Nobrega, J. N. (2003). Antipsychotic dosing in preclinical models is often unrepresentative of the clinical condition: a suggested solution based on in vivo occupancy. The Journal of Pharmacology and Experimental Therapeutics, 305(2), 625–631. https://doi.org/10.1124/JPET.102.046987

Karasawa, J. ichi, Hashimoto, K., and Chaki, S. (2008). D-Serine and a glycine transporter inhibitor improve MK-801-induced cognitive deficits in a novel object recognition test in rats. Behavioural Brain Research, 186(1), 78–83. https://doi.org/10.1016/J.BBR.2007.07.033

Koshiyama, D., Kirihara, K., Tada, M., Nagai, T., Fujioka, M., Usui, K., Koike, S., Suga, M., Araki, T., Hashimoto, K., & Kasai, K. (2019). Gamma-band auditory steady-state response is associated with plasma levels of D-serine in schizophrenia: An exploratory study. Schizophrenia Research, 208, 467–469. https://doi.org/10.1016/j.schres.2019.02.012

Landau, A. N., and Fries, P. (2012). Attention Samples Stimuli Rhythmically. Current Biology, 22(11), 1000–1004. https://doi.org/10.1016/j.cub.2012.03.054

Leucht, S., Cipriani, A., Spineli, L., Mavridis, D., Örey, D., Richter, F., … Davis, J. M. (2013). Comparative efficacy and tolerability of 15 antipsychotic drugs in schizophrenia: a multiple-treatments meta-analysis. Lancet (London, England), 382(9896), 951–962. https://doi.org/10.1016/S0140-6736(13)60733-3

Leucht, S., Corves, C., Arbter, D., Engel, R. R., Li, C., and Davis, J. M. (2009). Second-generation versus first-generation antipsychotic drugs for schizophrenia: a meta-analysis. The Lancet, 373(9657), 31–41. https://doi.org/10.1016/S0140-6736(08)61764-X

Luby, E. D., Gottlieb, J. S., Cohen, B. D., Rosenbaum, G., and Domino, E. F. (1962). Model psychoses and schizophrenia. The American Journal of Psychiatry, 119, 61–67. https://doi.org/10.1176/AJP.119.1.61

Mansbach, R. S., and Geyer, M. A. (1989). Effects of phencyclidine and phencyclidine biologs on sensorimotor gating in the rat. Neuropsychopharmacology, 2(4), 299–308. https://doi.org/10.1016/0893-133X(89)90035-3

Molina, J. L., Thomas, M. L., Joshi, Y. B., Hochberger, W. C., Koshiyama, D., Nungaray, J. A., … Light, G. A. (2020). Gamma oscillations predict pro-cognitive and clinical response to auditory-based cognitive training in schizophrenia. Translational Psychiatry, 10(1), 1–10. https://doi.org/10.1038/s41398-020-01089-6

Murray, T. F., and Horita, A. (1979). Phencyclidine-induced stereotyped behavior in rats: Dose response effects and antagonism by neuroleptics. Life Sciences, 24(24), 2217–2225. https://doi.org/10.1016/0024-3205(79)90097-3

Oh, S., Lee, T. Y., Kim, M., Kim, S. H., Lee, S., Cho, S., … Kwon, J. S. (2020). Effectiveness of antipsychotic drugs in schizophrenia: a 10-year retrospective study in a Korean tertiary hospital. NPJ Schizophrenia, 6(1). https://doi.org/10.1038/S41537-020-00122-3

Pantev, C., Elbert, T., Makeig, S., Hampson, S., Eulitz, C., and Hoke, M. (1993). Relationship of transient and steady-state auditory evoked fields. Electroencephalography and Clinical Neurophysiology, 88(5), 389–396. https://doi.org/10.1016/0168-5597(93)90015-H

Raza, M. U., and Sivarao, D. V. (2021). Test-retest reliability of tone- and 40 Hz train-evoked gamma oscillations in female rats and their sensitivity to low-dose NMDA channel blockade. Psychopharmacology 2021 238:8, 238(8), 2325–2334. https://doi.org/10.1007/S00213-021-05856-1

Sams-Dodd, F. (1995). Distinct effects of d-amphetamine and phencyclidine on the social behaviour of rats. Behavioural Pharmacology, 6(1), 55–65. https://doi.org/10.1097/00008877-199501000-00009

Seeman, P., and Kapur, S. (2000). Schizophrenia: More dopamine, more D2 receptors. Proceedings of the National Academy of Sciences, 97(14), 7673–7675. https://doi.org/10.1073/PNAS.97.14.7673

Siafis, S., Tzachanis, D., Samara, M., & Papazisis, G. (2017). Antipsychotic Drugs: From Receptor-binding Profiles to Metabolic Side Effects. Current Neuropharmacology, 16(8), 1210–1223. https://doi.org/10.2174/1570159X15666170630163616

Singh, S. P., and Singh, V. (2011). Meta-analysis of the efficacy of adjunctive NMDA receptor modulators in chronic schizophrenia. CNS Drugs, 25(10), 859–885. https://doi.org/10.2165/11586650-000000000-00000

Sivarao, D. V., Chen, P., Senapati, A., Yang, Y., Fernandes, A., Benitex, Y., … Ahlijanian, M. K. (2016). 40 Hz Auditory Steady-State Response Is a Pharmacodynamic Biomarker for Cortical NMDA Receptors. Neuropsychopharmacology, 41(9), 2232. https://doi.org/10.1038/NPP.2016.17

Sivarao, D. V., Frenkel, M., Chen, P., Healy, F. L., Lodge, N. J., and Zaczek, R. (2013). MK-801 disrupts and nicotine augments 40 Hz auditory steady state responses in the auditory cortex of the urethane-anesthetized rat. Neuropharmacology, 73, 1–9. https://doi.org/10.1016/j.neuropharm.2013.05.006

Üçok, A., Direk, N., Koyuncu, A., Keskin-Ergen, Y., Yüksel, Ç., Güler, J., … Devrim-Üçok, M. (2013). Cognitive deficits in clinical and familial high risk groups for psychosis are common as in first episode schizophrenia. Schizophrenia Research, 151(1–3), 265–269. https://doi.org/10.1016/J.SCHRES.2013.10.030

Umbricht, D., Javitt, D., Novak, G., Bates, J., Pollack, S., Lieberman, J., and Kane, J. (1998). Effects of clozapine on auditory event-related potentials in schizophrenia. Biological Psychiatry, 44(8), 716–725. https://doi.org/10.1016/S0006-3223(97)00524-6

Venkatasubramanian, G., & Keshavan, M. S. (2016). Biomarkers in Psychiatry - A Critique. Annals of Neurosciences, 23(1), 3. https://doi.org/10.1159/000443549

Voloh, B., & Womelsdorf, T. (2016). A role of phase-resetting in coordinating large scale neural networks during attention and goal-directed behavior. Frontiers in Systems Neuroscience, 10(MAR), 18. https://doi.org/10.3389/FNSYS.2016.00018/BIBTEX

Wadenberg, M. L. G., Soliman, A., VanderSpek, S. C., & Kapur, S. (2001). Dopamine D2 Receptor Occupancy Is a Common Mechanism Underlying Animal Models of Antipsychotics and Their Clinical Effects. Neuropsychopharmacology, 25(5), 633–641. https://doi.org/10.1016/S0893-133X(01)00261-5

Wagner, E., Siafis, S., Fernando, P., Falkai, P., Honer, W. G., Röh, A., … Hasan, A. (2021). Efficacy and safety of clozapine in psychotic disorders—a systematic quantitative meta-review. Translational Psychiatry, 11(1). https://doi.org/10.1038/S41398-021-01613-2

CHAPTER 5. SUMMARY AND DISCUSSION

Currently available antipsychotics have limited efficacy and show many undesirable and even dangerous side effects (Miyamoto et al. 2012). Safer and more efficacious drug development has been hampered by a lack of disease-specific and well-validated preclinical models. On the other hand, clinical development has been hampered by a lack of objective biomarkers and modest effect sizes of treatments that get further diluted by between-subject trial designs with high intersubject variance. Additionally, a lack of objective biomarkers impact meeting drug developmental benchmarks such as target engagement, lead selection, dose selection, and patient stratification, affecting the probability of success for novel treatments (Subramanyam and Goyal 2016). This research outlines a way forward to address some of these challenges.

Due to the unknown etiology and complex nature of schizophrenia, faithfully replicating human symptoms in animals presents a formidable challenge (Hyman 2013). Many currently used animal models rely on behavioral tests like sucrose preference, social withdrawal, Morris water maze, conditional avoidance response, and psychomotor measures like hyperlocomotion and stereotypic behavior, to model the core symptom domains of schizophrenia. How relevant these models are to schizophrenia, an essentially human illness, has been questioned (Nestler and Hyman 2010). In this context, endophenotypes that are specific neurophysiological responses associated with a genetic risk of schizophrenia on one hand and the disease symptoms on the other hand, but are also conserved across mammals, may serve as an alternative strategy to model disease-related circuit dysfunction.

Evoked gamma oscillations in the form of the 40 Hz ASSR are an emerging cortical circuit endophenotype that we chose for this dissertation research. In addition to being translatable, measures like gamma oscillations bring new insight into cortical circuit-level effects of pharmacological intervention, thus providing a clear neurobiological substrate for the drug development process. Moreover, as our research has demonstrated, such tools are especially suitable for within-subject trial design that can curb the high variance associated with psychiatric clinical trials that use a between-subject design (Salkind 2010).

In the present work, we first tested the reliability of tone-evoked gamma oscillations and 40 Hz ASSR from vertex recordings in a repeated measures design. 40 Hz ASSR showed better test-retest reliability as compared to tone evoked gamma response. However, both tone-evoked gamma and 40 Hz ASSR were equally sensitive to the disruption by NMDA antagonist, MK-801's disruption. This might suggest that the repeated measures design may not be as suitable for tone-evoked gamma studies as it is for 40 H ASSR. However, notwithstanding the lower ICC, tone-evoked gamma was just as sensitive to MK801 as 40 Hz ASSR. This is likely due to the large effect size of the treatment. Thus, if the effect size of a drug treatment, for example, as measured by Cohen's d, is large enough, it can overcome the test-retest variability. This is a key message we can draw from these studies.

In preclinical literature, 40 Hz ASSR is recorded from several regions like the midpoint of the skull or the vertex, temporal region, or the frontal region. It remains to be established whether one region is better than the other in terms of response reliability as well as sensitivity to drug treatment. We tested the reliability of 40 Hz ASSR recorded from the vertex and temporal regions. This study confirmed the good test-retest reliability of vertex 40 Hz ASSR as discussed above as well as its high sensitivity to MK801. This is an encouraging finding as assays that are

144

amenable to drug development studies need to be stable and consistent enough in their performance over time, such that leads tested at different times can be compared and prioritized. However, 40 Hz ASSR recording from the temporal area showed poor test-retest reliability as well as a poor sensitivity to MK-801 treatment. Since the temporal cortex represents the auditory primary cortex and the retrosplenial cortex underlying the vertex represents the secondary association cortex, we could speculate that integrative functions such as might occur in the associative cortices may be more vulnerable to NMDA antagonism-mediated disruption, relative to the primary sensory cortex. Indeed, we have previously observed that mismatch negativity was more robust and disrupted more readily at the vertex than at the primary auditory cortex (Sivarao et al. 2014).

Since we have clearly and repeatedly demonstrated that 40 Hz ASSR is highly vulnerable to NMDA antagonism, we asked the question if NMDA channel co-agonists can augment the 40 Hz ASSR response. Despite testing a range of doses of D-serine, a co-agonist at the NMDA receptor, we found no evidence for augmentation. The doses we chose, and the protocol of dosing were previously shown to robustly increase D-serine levels in the brain (Hasegawa et al. 2019). Thus, it is clear from our studies that D-serine had no effect on modulating the ASSR transmission. Previous studies have provided evidence that endogenous D-serine at the NMDA receptors is present at a sub-saturation level and that exogenous increases in D-serine would increase NMDA receptor activation (Bergeron et al. 1998). However, we saw no functional evidence for this as we used a dose range and dosing protocol that was shown to robustly increase D-serine levels in the rat brain (Hasegawa et al. 2019). Of course, we did not directly measure D-serine concentration or NMDA receptor function but only relied on the 40 Hz ASSR measure. Indeed, Matsui and colleagues (1995) observed that in a microdialysis study that D-

serine levels were at saturation vis-a-vis the NMDA receptors in the rat frontal cortex (Matsui et al. 1995).

In the next part of the study, we tested the effects of two prototypical antipsychotics, haloperidol, and clozapine, on the 40 Hz ASSR. In the literature, it is typical to disrupt native neurophysiological processes such as sensory gating or PPI pharmacologically or through genetic manipulation and protect or reverse the deficit through pre- or post-treatment respectively with an antipsychotic (Swerdlow and Geyer 1993). Here, we were more interested in seeing the effect of the antipsychotic drugs by themselves. This is because both clozapine and haloperidol were shown to augment NMDA neurotransmission *in vitro* (Arvanov et al. 1997). Since we have a highly sensitive assay for NMDA blockade, we thought it might also be sensitive to any presumable NMDA augmentation.

In the preclinical literature, it is not unusual to encounter doses of antipsychotic drugs that have little relationship with clinically relevant exposures and therefore therapeutic effects. For example, a commonly used dose of haloperidol in rodents may be as high as 1 mg/kg (Kapur et al. 2000). It is unclear what this dose represents since the D2 occupancy relevant for antipsychotic effect is achieved by a dose that is at least 10 times smaller (ie., <0.1 mg/kg). Moreover, when haloperidol's D2 occupancy exceeds 80%, achieved by a 0.1 mg/kg dose or higher, robust cataleptic effects are seen. When evaluating the in vivo effects of clozapine and haloperidol, we were careful to choose only those doses that are reflective of clinically observed D2 occupancy. This was important since we wanted to know if the potential NMDA mechanism was operational at therapeutically relevant doses.

Clozapine robustly improved the 40 Hz ASSR phase locking, while haloperidol had no effect on the ASSR measures. Additionally, clozapine augmentation was most obvious on the interatrial coherence measure whereas the effect on evoked power was inconsistent, particularly at the low doses. This suggests that clozapine works by causing the phase resetting of the oscillatory signal, rather than increasing the neural recruitment (Canavier 2015), an emerging tool to study information processing in the brain. This is an unprecedented observation and may offer a fundamentally new insight into how clozapine, a drug that stands out from all other antipsychotics in terms of its superior efficacy profile, has a differentiated profile relative to other antipsychotic agents (Nucifora et al. 2017). In future, we plan to test other atypical drugs like olanzapine or risperidone, to see if this feature is shared across other antipsychotic drugs that share a broad-spectrum affinity for neurotransmitter receptors, or it is truly unique to clozapine.

In our current work, we used female Sprague Dawley rats for hypotheses testing. The effect of gender on 40 Hz ASSR has not been studied in detail. Previous studies have shown gender-specific differences in auditory-evoked responses like ABR in humans that are reflective of network responses at the level of the brain stem (Skoe and Kraus 2010). For ABRs, females tend to show stronger responses with shorter latencies as compared to males (Dehan and Jerger 1990; McFadden et al. 2010). In contrast, we are not aware of many studies that documented sex differences for the 40 Hz ASSR. However, we are aware of one study that tested the effects of the menstrual cycle on 40 Hz ASSR in females. It showed that 40 Hz ASSR amplitude was associated with estrogen levels. The amplitude and ITC of 40 Hz increased with increased levels of estrogen (Inga et al. 2014). It has also been reported that 40 Hz ASSR is gender-specific based on handedness. Left-handed females showed significantly lower phase synchrony as compared to left-handed males (Melynyte et al. 2018). However, there is no report of any gender-specific

147

differences in 40 Hz ASSR in rodent studies in the literature. In the current study, we did not see any change in any measures of the 40 Hz ASSR across time in female control rats. Our results from test-reliability studies further support the consistency of 40Hz ASSR over the period of three weeks (i.e., the maximum length of time we recorded). We housed female rats alone in the cages. Although we did not determine the estrous phase or measure estrogen levels, it is possible that single housing induced an anestrous phase in these rats, leading to no obvious observable differences over time. However, this is something that deserves more attention in future studies.

The NMDA receptor hypofunction hypothesis has been proposed as an alternative to the dopamine hypothesis as a pathological model for schizophrenia (Olney and Farber 1995; Goff and Coyle 2001). Consistent with this hypothesis, acute dosing with NMDA antagonists elicits a full spectrum of behavioral changes that are reminiscent of positive, negative, and cognitive symptoms seen in schizophrenia patients (Javitt and Zukin 1991; Krystal et al. 1994). In the current work, we implemented an acute pharmacological model by treating rats with MK-801. Adell and colleagues (2012) have argued that this model has reasonable face, construct, and predictive validity (Adell et al. 2012). Briefly, acute MK-801 administration results in behavioral phenotypes like hyperlocomotion, stereotypic behavior (head weaning, circumambulation), and cognitive deficits of different sorts, which are considered a surrogate for positive and cognitive symptoms in schizophrenia. Furthermore, results from current work have shown that MK-801 dose-dependently reduced 40 Hz ASSR in female rats, consistent with 40 Hz ASSR deficits seen in schizophrenia patients (Thuné et al. 2016). At a cellular level, systemic administration of NMDA antagonists appears to cause a temporary loss of the function of PV+ interneurons as evidenced by an increase in background gamma (disinhibition) and a reduction in evoked gamma (Hakami et al. 2009). Furthermore, behavioral, neurochemical, and neurophysiological

148

(including 40 Hz ASSR, as shown in current work) alterations induced by acute MK-801 administration are responsive to antipsychotics. As compared to other NMDAR blockers like ketamine, and PCP, MK-801 has a substantially higher receptor affinity and duration of the blockade, making it a convenient tool for causing a disruption in NMDA transmission over a period of several hours (Davies et al. 1988; Miyamoto et al. 2000; Pinault 2008; Hakami et al. 2009). Moreover, NMDA antagonists like ketamine show rapid kinetics and as a result, also show a variable response over time (Plourde et al. 1997; Sivarao et al. 2016), making it challenging to use with bolus dosing. However, research groups have used ketamine delivery through intravenous infusion regimens to avoid the rapid change in drug concentrations associated with a bolus injection of ketamine (Haaf et al. 2022).

It is proposed that deficits in information processing lead to the functional impairment experienced in schizophrenia. Thus, neurophysiological biomarkers that can probe the functional integrity of neural structures involved in information processing have gained interest. These include sensory gating, sensorimotor gating (e.g., pre-pulse inhibition (PPI), mismatch negativity (MMN), and others. Abnormalities in the thalamic gating, especially in the corticostriato-thalamocortical circuitry may result in sensory overload and cause cognitive deficits. NMDA antagonists have been shown to cause a reduction in sensory gating as well as sensorimotor gating measures. However, these neurophysiological biomarkers tend to show an all or none effect of the pharmacological intervention, owing to the lack of a robust gradation in response. In contrast, 40 Hz ASSR shows a robust dose-dependent and linear effect of MK-801 treatment, thus highlighting an advantage of this assay over other assays like sensory gating or mismatch negativity.

Moreover, these endophenotypes may each index activity in unique and distinct neural circuits. For example, sensory gating has been attributed to the hippocampal inhibitory mechanism (Bickford et al. 1993), while PPI reflects the activity of a limbic cortex, striatum, pallidum, and pontine tegmentum (CSPP) circuit (Swerdlow et al. 2001). On the other hand, local field potential (LFP) studies have shown layers 2/3 and 4 as the generators of 40 Hz ASSR and mismatch negativity (Javitt and Sweet 2015; Funk et al. 2020). This aligns with the cortical layers that give rise to gamma oscillations (Welle and Contreras 2016). Moreover, molecular disruption of NMDA transmission through NR1 deletion in layers 2/3 specifically affects the ability to entrain at gamma frequencies but not at lower frequencies (Cardin et al. 2009; Carlén et al. 2012; Nakao and Nakazawa 2014). These superficial layers in the cortex play an essential role in sensory processing (Quiquempoix et al. 2018) and cognitive function (e.g., working memory), processes affected in schizophrenia. Moreover, layers 2/3 have centrifugal projections, which play an important role in integrating sensory information across different brain regions (Yamashita et al. 2018). Interestingly, layers 2/3 are also the cortical layers where schizophrenia patients most consistently exhibit GABAergic deficits suggesting that the cellular machinery required for normal cognitive and sensory function including for generating gamma oscillations is damaged (Beneyto et al. 2011). Thus 40 Hz ASSR can be used as a tool to probe the structural and functional integrity of this specific region. From a drug discovery point of view, such endophytopic assays are complementary as they represent neural function in distinct and non-redundant circuits. Additionally, they may underlie distinct phenotypes as well. For example, sensory gating deficits may be a neurophysiological manifestation of the perceptual abnormalities ("sensory inundation"), a common complaint from schizophrenia patients (Scheydt et al. 2017). On the other hand, gamma oscillatory deficits in the prefrontal cortex may be an

endophenotypic manifestation of the working memory deficits that schizophrenia patients and patients with other diagnoses such as bipolar depression, may experience (Singh et al. 2020). Having distinct assays indexing functionally distinct symptoms would also help in identifying patient subgroups and stratifying them according to their specific deficits and symptoms. Such sub-classification is especially relevant for schizophrenia since it is believed that often psychiatric subjects with distinct disease subtypes are clubbed as one due to a lack of specific and discriminating tools (Carpenter et al. 1976). Such subgrouping may be a starting point for more personalized treatments, rather than a "one size fits all" approach that is currently the practice (Donati et al. 2020).

In general, antipsychotics often take several weeks to reach their full therapeutic effect in human patients. Yet, in our rodent studies, we saw robust effects of clozapine on the 40 Hz ASSR within an hour after administration. Are these changes a mere epiphenomenon that have no relationship to therapeutic effect? First, while peak clinical benefit may take weeks, antipsychotic drugs do have a rapid onset (Kapur et al. 2005). This is the reason why they are a staple in every emergency medicine department. However, it was historically thought that the immediate effects are non-specific, and the pharmacological effects take a much longer time to start (Gelder et al. 2012). This perception has been recently challenged using placebo controlled clinical trials. For example, Kapur and colleagues (2005) have shown, using a placebo-controlled multi-center randomized clinical trial that olanzapine showed efficacy within 2 h after administration in acutely psychotic patients while haloperidol's effect was apparent within the first 24 hours (Kapur 2005). Moreover, D2 receptor occupancy of a PET tracer was already at its peak in several subjects, only 3 h after dosing (Nordström et al. 1992). Since 3 h was the earliest time point for evaluation in this study, it is conceivable that the actual peak effect may have been

even earlier. Thus, D2 occupancy and clinical antipsychotic effects can be observed within hours after antipsychotic drug administration. While it is premature to consider 40 Hz ASSR as a measure of efficacy, the time scale for ASSR effects we observed after clozapine administration is not inconsistent with the rapid onset of therapeutic effects outlined above.

Overall, in this work, we have established that vertex recorded 40 Hz ASSR has a good test-retest reliability and that it is exquisitely sensitive to NMDA inhibition. Additionally, we discovered that clozapine augments 40 Hz ASSR and the likely mechanism for this could be through improving phase resetting including how quickly the 40 Hz ASSR entertainment happens, relative to the stimulus onset. By showing that we have a reliable neural synchrony measure in the form of a 40 Hz ASSR that can be bidirectionally altered using pharmacological tools, we believe that we have further fortified the characterization of the 40 Hz ASSR as a pharmacodynamic biomarker of cortical neural synchrony. Translational cortical circuit performance tools such as the 40 Hz ASSR will enable preclinical drug development through identifying and prioritizing molecules based on objective indices (e.g., neural synchrony), that are quantifiable, dose-related, and relevant to higher-order information processing. Clinically, such tools can help in confirming CNS exposure, choosing an appropriate dose, and identifying patient cohorts most likely to benefit from an intervention such as improving evoked gamma response. These are drug development process signposts that can enable the overarching goal of finding more effective and safer treatments for troubling mental illnesses.

REFERENCES

Abi-Dargham A, Horga G. 2016. The search for imaging biomarkers in psychiatric disorders. Nat Med [Internet]. [accessed 2022 Feb 2] 22(11):1248–1255. https://doi.org/10.1038/NM.4190

Abi-Dargham A, Rodenhiser J, Printz D, Zea-Ponce Y, Gil R, Kegeles LS, Weiss R, Cooper TB, Mann JJ, Van Heertum RL, et al. 2000. Increased baseline occupancy of D2 receptors by dopamine in schizophrenia. Proc Natl Acad Sci U S A [Internet]. [accessed 2022 Feb 7] 97(14):8104–8109. https://doi.org/10.1073/PNAS.97.14.8104

Adell A, Jiménez-Sánchez L, López-Gil X, Romón T. 2012. Is the acute NMDA receptor hypofunction a valid model of schizophrenia? Schizophr Bull [Internet]. [accessed 2022 Feb 18] 38(1):9–14. https://doi.org/10.1093/SCHBUL/SBR133

American Psychiatric Association. 2013. The Diagnostic and Statistical Manual of Mental Disorders DSM–5. 5th ed. [place unknown].

Amir A, Headley DB, Lee SC, Haufler D, Paré D. 2018. Vigilance-Associated Gamma Oscillations Coordinate the Ensemble Activity of Basolateral Amygdala Neurons. Neuron [Internet]. [accessed 2022 Mar 26] 97(3):656-669.e7. https://doi.org/10.1016/J.NEURON.2017.12.035/ATTACHMENT/0CE29402-BC3F-4B9E-AA26-B498EFDC837D/MMC1.PDF

Andreasen NC. 1989. The American Concept of Schizophrenia. Schizophr Bull [Internet]. [accessed 2022 Feb 1] 15(4):519–531. https://doi.org/10.1093/SCHBUL/15.4.519

Arvanov VL, Liang X, Schwartz J, Grossman S WR. 1997. Clozapine and haloperidol modulate N-methyl-D-aspartate- and non-N-methyl-D-aspartate receptor-mediated neurotransmission in rat prefrontal cortical neurons in vitro. J Pharmacol Exp Ther [Internet]. 283(1):226–234. https://pubmed.ncbi.nlm.nih.gov/9336328/

Azzena GB, Conti G, Santarelli R, Ottaviani F, Paludetti G, Maurizi M. 1995. Generation of human auditory steadystate responses (SSRs). I: Stimulus rate effects. Hear Res. 83(1–2):1–8. https://doi.org/10.1016/0378-5955(94)00184-R

Backer KC, Kessler AS, Lawyer LA, Corina DP, Miller LM. 2019. A novel EEG paradigm to simultaneously and rapidly assess the functioning of auditory and visual pathways. J Neurophysiol [Internet]. [accessed 2022 Mar 3] 122:1312–1329. https://doi.org/10.1152/jn.00868.2018

Balu DT. 2016. The NMDA Receptor and Schizophrenia. From Pathophysiology to Treatment. In: Adv Pharmacol [Internet]. Vol. 76. [place unknown]: Academic Press Inc.; [accessed 2020 Dec 7]; p. 351–382. https://doi.org/10.1016/bs.apha.2016.01.006

Basar-Eroglu C, Brand A, Hildebrandt H, Karolina Kedzior K, Mathes B, Schmiedt C. 2007. Working memory related gamma oscillations in schizophrenia patients. Int J Psychophysiol [Internet]. [accessed 2022 Mar 2] 64(1):39–45. https://doi.org/10.1016/J.IJPSYCHO.2006.07.007

Başar E, Rosen B, Başar-Eroglu C, Greitschus F. 1987. The associations between 40 Hz-EEG and the middle latency response of the auditory evoked potential. Int J Neurosci [Internet]. [accessed 2022 Mar 3] 33(1–2):103–117. https://doi.org/10.3109/00207458708985933

Beasley CL, Reynolds GP. 1997. Parvalbumin-immunoreactive neurons are reduced in the prefrontal cortex of schizophrenics. Schizophr Res. 24(3):349–355. https://doi.org/10.1016/s0920-9964(96)00122-3

Behrens MM, Ali SS, Dao DN, Lucero J, Shekhtman G, Quick KL, Dugan LL. 2007. Ketamine-induced loss of phenotype of fast-spiking interneurons is mediated by NADPH-oxidase. Science [Internet]. [accessed 2022 Mar 16] 318(5856):1645–1647. https://doi.org/10.1126/SCIENCE.1148045

Bell DS. 1973. The Experimental Reproduction of Amphetamine Psychosis. Arch Gen Psychiatry [Internet]. [accessed 2022 Feb 8] 29(1):35–40. https://doi.org/10.1001/ARCHPSYC.1973.04200010020003

Beneyto M, Abbott A, Hashimoto T, Lewis DA. 2011. Lamina-Specific Alterations in Cortical GABAA Receptor Subunit Expression in Schizophrenia. Cereb Cortex [Internet]. [accessed 2022 Apr 2] 21(5):999–1011. https://doi.org/10.1093/CERCOR/BHQ169

Beppi C, Ribeiro Violante I, Scott G, Sandrone S. 2021. EEG, MEG and neuromodulatory approaches to explore cognition: Current status and future directions. Brain Cogn [Internet]. [accessed 2022 Feb 9] 148. https://doi.org/10.1016/J.BANDC.2020.105677

Bergeron R, Meyer TM, Coyle JT, Greene RW. 1998. Modulation of N-methyl-d-aspartate receptor function by glycine transport. Proc Natl Acad Sci U S A [Internet]. [accessed 2022 Jan 13] 95(26):15730. https://doi.org/10.1073/PNAS.95.26.15730

Bickford PC, Luntz-Leybman V, Freedman R. 1993. Auditory sensory gating in the rat hippocampus: modulation by brainstem activity. Brain Res. 607(1–2):33–38. https://doi.org/10.1016/0006-8993(93)91486-C

Bitzenhofer SH, Ahlbeck J, Wolff A, Wiegert JS, Gee CE, Oertner TG, Hanganu-Opatz IL. 2017. Layer-specific optogenetic activation of pyramidal neurons causes beta–gamma entrainment of neonatal networks. Nat Commun 2017 81 [Internet]. [accessed 2022 Mar 16] 8(1):1–13. https://doi.org/10.1038/ncomms14563

Bleuler E. 1911. Dementia praecox oder Gruppe der Schizophrenien. Vol. 4. [place unknown]: Deuticke.

Bohórquez J, Özdamar Ö. 2008. Generation of the 40-Hz auditory steady-state response (ASSR) explained using convolution. Clin Neurophysiol [Internet]. [accessed 2022 Mar 3] 119(11):2598–2607. https://doi.org/10.1016/j.clinph.2008.08.002

du Bois TM, Huang XF. 2007. Early brain development disruption from NMDA receptor hypofunction: relevance to schizophrenia. Brain Res Rev [Internet]. [accessed 2022 Mar 26] 53(2):260–270. https://doi.org/10.1016/J.BRAINRESREV.2006.09.001

Bora E, Yucel M, Pantelis C. 2009. Cognitive functioning in schizophrenia, schizoaffective disorder and affective psychoses: Meta-analytic study. Br J Psychiatry. 195(6):475–482. https://doi.org/10.1192/BJP.BP.108.055731

Brenner CA, Krishnan GP, Vohs JL, Ahn WY, Hetrick WP, Morzorati SL, O'Donnell BF. 2009. Steady state responses: Electrophysiological assessment of sensory function in schizophrenia. Schizophr Bull [Internet]. [accessed 2020 Nov 22] 35(6):1065–1077. https://doi.org/10.1093/schbul/sbp091

Bromberg-Martin ES, Matsumoto M, Hikosaka O. 2010. Dopamine in motivational control: rewarding, aversive, and alerting. Neuron [Internet]. [accessed 2022 Feb 7] 68(5):815. https://doi.org/10.1016/J.NEURON.2010.11.022

Brown AS. 2011. The environment and susceptibility to schizophrenia. Prog Neurobiol [Internet]. [accessed 2022 Mar 2] 93(1):23. https://doi.org/10.1016/J.PNEUROBIO.2010.09.003

Brown AS, Derkits EJ. 2010. Prenatal infection and schizophrenia: a review of epidemiologic and translational studies. Am J Psychiatry [Internet]. [accessed 2022 Mar 2] 167(3):261–80. https://doi.org/10.1176/appi.ajp.2009.09030361

Bubeníková-Valešová V, Horáček J, Vrajová M, Höschl C. 2008. Models of schizophrenia in humans and animals based on inhibition of NMDA receptors. Neurosci Biobehav Rev [Internet]. [accessed 2022 Mar 26] 32(5):1014–1023. https://doi.org/10.1016/J.NEUBIOREV.2008.03.012

Buckley PF, Miller BJ, Lehrer DS, Castle DJ. 2009. Psychiatric Comorbidities and Schizophrenia. Schizophr Bull [Internet]. [accessed 2022 Feb 9] 35(2):383. https://doi.org/10.1093/SCHBUL/SBN135

Burle B, Spieser L, Roger C, Casini L, Hasbroucq T, Vidal F. 2015. Spatial and temporal resolutions of EEG: Is it really black and white? A scalp current density view. Int J Psychophysiol [Internet]. [accessed 2022 Feb 9] 97(3):210. https://doi.org/10.1016/J.IJPSYCHO.2015.05.004

Buzsáki G. 2006. Rhythms of the Brain [Internet]. [place unknown]: Oxford University Press; [accessed 2022 Feb 9]. https://faculty.washington.edu/seattle/brain-physics/textbooks/buzsaki.pdf

Buzsáki G, Anastassiou CA, Koch C. 2012. The origin of extracellular fields and currents — EEG, ECoG, LFP and spikes. Nat Rev Neurosci 2012 136 [Internet]. [accessed 2022 Feb 9] 13(6):407–420. https://doi.org/10.1038/nrn3241

Buzsáki G, Lai-Wo S. L, Vanderwolf CH. 1983. Cellular bases of hippocampal EEG in the behaving rat. Brain Res [Internet]. [accessed 2022 Mar 2] 287(2):139–171. https://doi.org/10.1016/0165-0173(83)90037-1

Buzsáki G, Logothetis N, Singer W. 2013. Scaling Brain Size, Keeping Timing: Evolutionary Preservation of Brain Rhythms. Neuron. 80(3):751–764. https://doi.org/10.1016/J.NEURON.2013.10.002

Buzsáki G, Wang X-J. 2012. Mechanisms of Gamma Oscillations. Annu Rev Neurosci [Internet]. [accessed 2020 May 11] 35(1):203–225. https://doi.org/10.1146/annurev-neuro-062111-150444

Calvin OL, Redish AD. 2021. Global disruption in excitation-inhibition balance can cause

localized network dysfunction and Schizophrenia-like context-integration deficits. PLOS Comput Biol [Internet]. [accessed 2022 Mar 26] 17(5):e1008985. https://doi.org/10.1371/JOURNAL.PCBI.1008985

Canavier CC. 2015. Phase-resetting as a tool of information transmission. Curr Opin Neurobiol [Internet]. [accessed 2022 Apr 2] 31:206. https://doi.org/10.1016/J.CONB.2014.12.003

Cannon M, Jones PB, Murray RM. 2002. Obstetric complications and schizophrenia: historical and meta-analytic review. Am J Psychiatry [Internet]. [accessed 2022 Apr 4] 159(7):1080–1092. https://doi.org/10.1176/APPI.AJP.159.7.1080

Capilla A, Pazo-Alvarez P, Darriba A, Campo P, Gross J. 2011. Steady-State Visual Evoked Potentials Can Be Explained by Temporal Superposition of Transient Event-Related Responses. PLoS One [Internet]. [accessed 2022 Mar 6] 6(1):e14543. https://doi.org/10.1371/JOURNAL.PONE.0014543

Cardin JA, Carlén M, Meletis K, Knoblich U, Zhang F, Deisseroth K, Tsai LH, Moore CI. 2009. Driving fast-spiking cells induces gamma rhythm and controls sensory responses. Nature [Internet]. [accessed 2020 Dec 21] 459(7247):663–667. https://doi.org/10.1038/nature08002

Cardno AG, Gottesman II. 2000. Twin studies of schizophrenia: From bow-and-arrow concordances to Star Wars Mx and functional genomics. Am J Med Genet [Internet]. 97(1):12–17. https://doi.org/10.1002/(SICI)1096-8628(200021)97:1<12::AID-AJMG3>3.0.CO;2-U

Carlén M, Meletis K, Siegle JH, Cardin JA, Futai K, Vierling-Claassen D, Rühlmann C, Jones SR, Deisseroth K, Sheng M, et al. 2012. A critical role for NMDA receptors in parvalbumin interneurons for gamma rhythm induction and behavior. Mol Psychiatry [Internet]. [accessed 2020 May 14] 17(5):537–548. https://doi.org/10.1038/mp.2011.31

Carlsson A, Lindqvist M. 1963. Effect of chlorpromazine or haloperidol on formation of 3methoxytyramine and normetanephrine in mouse brain. Acta Pharmacol Toxicol (Copenh) [Internet]. [accessed 2022 Feb 8] 20(2):140–144. https://doi.org/10.1111/J.1600-0773.1963.TB01730.X

Carlsson A, Lindqvist M, Magnusson T, Waldeck B. 1958. On the presence of 3-hydroxytyramine in brain. Science [Internet]. [accessed 2022 Feb 7] 127(3296):471. https://doi.org/10.1126/SCIENCE.127.3296.471

Carpenter WT, Bartko JJ, Carpenter CL, Strauss JS. 1976. Another View of Schizophrenia Subtypes: A Report From the International Pilot Study of Schizophrenia. Arch Gen Psychiatry [Internet]. [accessed 2022 Apr 2] 33(4):508–516. https://doi.org/10.1001/ARCHPSYC.1976.01770040068012

Carr MF, Karlsson MP, Frank LM. 2012. Transient Slow Gamma Synchrony Underlies Hippocampal Memory Replay. Neuron. 75(4):700–713. https://doi.org/10.1016/j.neuron.2012.06.014

Carter CS, Barch D, Cohen JD, Braver T. 1997. CNS catecholamines and cognitive dysfunction in schizophrenia. Schizophr Res. 24(1–2):211. https://doi.org/10.1016/S0920-9964(97)82604-7

Catts VS, Derminio DS, Hahn CG, Weickert CS. 2015. Postsynaptic density levels of the NMDA receptor NR1 subunit and PSD-95 protein in prefrontal cortex from people with schizophrenia. npj Schizophr 2015 11 [Internet]. [accessed 2022 Feb 8] 1(1):1–8. https://doi.org/10.1038/npjschz.2015.37

Catts VS, Lai YL, Weickert CS, Weickert TW, Catts S V. 2016. A quantitative review of the postmortem evidence for decreased cortical N-methyl-D-aspartate receptor expression levels in schizophrenia: How can we link molecular abnormalities to mismatch negativity deficits? Biol Psychol [Internet]. [accessed 2022 Feb 8] 116:57–67. https://doi.org/10.1016/J.BIOPSYCHO.2015.10.013

Cheslack-Postava K, Brown AS. 2021. Prenatal infection and schizophrenia: A decade of further progress. Schizophr Res. https://doi.org/10.1016/J.SCHRES.2021.05.014

Cho RY, Konecky RO, Carter CS. 2006. Impairments in frontal cortical γ synchrony and cognitive control in schizophrenia. Proc Natl Acad Sci U S A [Internet]. [accessed 2022 Mar 2] 103(52):19878–19883. https://doi.org/10.1073/PNAS.0609440103/SUPPL_FILE/09440FIG5B.JPG

Christensen CB, Kappel SL, Kidmose P. 2018. Auditory Steady-State Responses Across Chirp Repetition Rates for Ear-EEG and Scalp EEG. Proc Annu Int Conf IEEE Eng Med Biol Soc EMBS. 2018-July:1376–1379. https://doi.org/10.1109/EMBC.2018.8512527

Cleynen I, Engchuan W, Hestand MS, Heung T, Holleman AM, Johnston HR, Monfeuga T, McDonald-McGinn DM, Gur RE, Morrow BE, et al. 2020. Genetic contributors to risk of schizophrenia in the presence of a 22q11.2 deletion. Mol Psychiatry 2020 268 [Internet]. [accessed 2022 Apr 5] 26(8):4496–4510. https://doi.org/10.1038/s41380-020-0654-3

Cochran SM, Kennedy M, McKerchar CE, Steward LJ, Pratt JA, Morris BJ. 2003. Induction of Metabolic Hypofunction and Neurochemical Deficits after Chronic Intermittent Exposure to Phencyclidine: Differential Modulation by Antipsychotic Drugs. Neuropsychopharmacol 2003 282 [Internet]. [accessed 2022 Mar 16] 28(2):265–275. https://doi.org/10.1038/sj.npp.1300031

Cohen BD, Rosenbaum G, Luby ED, Gottlieb JS. 1962. Comparison of Phencyclidine Hydrochloride (Sernyl) with Other Drugs: Simulation of Schizophrenic Performance with Phencyclidine Hydrochloride (Sernyl), Lysergic Acid Diethylamide (LSD-25), and Amobarbital (Amytal) Sodium; II. Symbolic and Sequential Thinking. Arch Gen Psychiatry [Internet]. [accessed 2022 Feb 8] 6(5):395–401. https://doi.org/10.1001/ARCHPSYC.1962.01710230063007

Cohen SM, Tsien RW, Goff DC, Halassa MM. 2015. The impact of NMDA Receptor hypofunction on GABAergic interneurons in the pathophysiology of schizophrenia. Schizophr Res [Internet]. [accessed 2022 Feb 8] 167(0):98. https://doi.org/10.1016/J.SCHRES.2014.12.026

Conti G, Santarelli R, Grassi C, Ottaviani F, Azzena GB. 1999. Auditory steady-state responses to click trains from the rat temporal cortex. Clin Neurophysiol. 110(1):62–70. https://doi.org/10.1016/S0168-5597(98)00045-8

Creese I, Burt DR, Snyder SH. 1976. Dopamine receptor binding predicts clinical and

pharmacological potencies of antischizophrenic drugs. Science [Internet]. [accessed 2022 Feb 8] 192(4238):481–483. https://doi.org/10.1126/SCIENCE.3854

Cromwell HC, Mears RP, Wan L, Boutros NN. 2008. Sensory Gating: A Translational Effort From Basic to Clinical Science. Clin EEG Neurosci [Internet]. [accessed 2022 Apr 3] 39(2):69. https://doi.org/10.1177/155005940803900209

Cryan JF, Mombereau C. 2004. In search of a depressed mouse: utility of models for studying depression-related behavior in genetically modified mice. Mol Psychiatry 2004 94 [Internet]. [accessed 2022 Mar 23] 9(4):326–357. https://doi.org/10.1038/sj.mp.4001457

DAVIES BM, BEECH HR. 1960. The Effect of 1-Arylcyclohexylamine (Sernyl) on Twelve Normal Volunteers. J Ment Sci [Internet]. [accessed 2022 Feb 8] 106(444):912–924. https://doi.org/10.1192/BJP.106.444.912

Davies SN, Martin D, Millar JD, Aram JA, Church J, Lodge D. 1988. Differences in results from in vivo and in vitro studies on the use-dependency of N-methylaspartate antagonism by MK-801 and other phencyclidine receptor ligands. Eur J Pharmacol [Internet]. [accessed 2022 Apr 5] 145(2):141–151. https://doi.org/10.1016/0014-2999(88)90225-7

Dehan CP, Jerger J. 1990. Analysis of gender differences in the auditory brainstem response. Laryngoscope [Internet]. [accessed 2022 Apr 5] 100(1):18–24. https://doi.org/10.1288/00005537-199001000-00005

Demjaha A, MacCabe JH, Murray RM. 2012. How genes and environmental factors determine the different neurodevelopmental trajectories of schizophrenia and bipolar disorder. Schizophr Bull [Internet]. [accessed 2022 Feb 2] 38(2):209–214. https://doi.org/10.1093/SCHBUL/SBR100

Dennison CA, Legge SE, Pardiñas AF, Walters JTR. 2020. Genome-wide association studies in schizophrenia: Recent advances, challenges and future perspective. Schizophr Res. 217:4–12. https://doi.org/10.1016/J.SCHRES.2019.10.048

Donati FL, D'Agostino A, Ferrarelli F. 2020. Neurocognitive and neurophysiological endophenotypes in schizophrenia: An overview. Biomarkers in Neuropsychiatry. 3:100017. https://doi.org/10.1016/J.BIONPS.2020.100017

Dracheva S, Marras SA, Sharif Elhakem ML, Fred Kramer BR, Davis KL, Haroutunian V. 2001. Article N-Methyl-D-Aspartic Acid Receptor Expression in the Dorsolateral Prefrontal Cortex of Elderly Patients With Schizophrenia. Am J Psychiatry. 158(9):1400–1410.

Ellison G, Nielsen EB, Lyon M. 1981. Animal model of psychosis: Hallucinatory behaviors in monkeys during the late stage of continuous amphetamine intoxication. J Psychiatr Res. 16(1):13–22. https://doi.org/10.1016/0022-3956(81)90009-1

Enwright JF, Huo Z, Arion D, Corradi JP, Tseng G, Lewis DA. 2018. Transcriptome alterations of prefrontal cortical parvalbumin neurons in schizophrenia. Mol Psychiatry [Internet]. [accessed 2022 Mar 2] 23(7):1606–1613. https://doi.org/10.1038/MP.2017.216

van Erp TGM, Walton E, Hibar DP, Schmaal L, Jiang W, Glahn DC, Pearlson GD, Yao N, Fukunaga M, Hashimoto R, et al. 2018. Cortical Brain Abnormalities in 4474 Individuals With Schizophrenia and 5098 Control Subjects via the Enhancing Neuro Imaging Genetics

Through Meta Analysis (ENIGMA) Consortium. Biol Psychiatry [Internet]. [accessed 2022 Feb 4] 84(9):644–654. https://doi.org/10.1016/J.BIOPSYCH.2018.04.023

Fabiana D, Silva A, Martijn F, Therese VA, Dick V, Lieuwe DH. 2008. The Revised Dopamine Hypothesis of Schizophrenia: Evidence from Pharmacological MRI Studies with Atypical Antipsychotic Medication. Psycholpharmacology Bull. 41(1):121.

Falkai P, Rossner MJ, Schulze TG, Hasan A, Brzózka MM, Malchow B, Honer WG, Schmitt A. 2015. Kraepelin revisited: schizophrenia from degeneration to failed regeneration. Mol Psychiatry [Internet]. [accessed 2022 Feb 1] 20(6):671–676. https://doi.org/10.1038/mp.2015.35

Farde L, Wiesel FA, Hall Hå, Halldin C, Stone Elander S, Sedvall G. 1987. No D2 Receptor Increase in PET Study of Schizophrenia. Arch Gen Psychiatry [Internet]. [accessed 2022 Feb 7] 44(7):671–672. https://doi.org/10.1001/ARCHPSYC.1987.01800190091013

FDA-NIH Biomarker Working Group. 2016. BEST (Biomarkers, EndpointS, and other Tools) Resource. Silver Spring Food Drug Adm [Internet]. [accessed 2022 Feb 4]. https://www.ncbi.nlm.nih.gov/books/NBK326791/

Featherstone RE, Rizos Z, Kapur S, Fletcher PJ. 2008. A sensitizing regimen of amphetamine that disrupts attentional set-shifting does not disrupt working or long-term memory. Behav Brain Res [Internet]. [accessed 2022 Feb 9] 189(1):170–179. https://doi.org/10.1016/J.BBR.2007.12.032

Fett AKJ, Viechtbauer W, Dominguez M de G, Penn DL, van Os J, Krabbendam L. 2011. The relationship between neurocognition and social cognition with functional outcomes in schizophrenia: A meta-analysis. Neurosci Biobehav Rev. 35(3):573–588. https://doi.org/10.1016/J.NEUBIOREV.2010.07.001

Folmer RL, Billings CJ, Diedesch-Rouse AC, Gallun FJ, Lew HL. 2011. Electrophysiological assessments of cognition and sensory processing in TBI: Applications for diagnosis, prognosis and rehabilitation. Int J Psychophysiol. 82(1):4–15. https://doi.org/10.1016/J.IJPSYCHO.2011.03.005

Fone KCF, Watson DJG, Billiras RI, Sicard DI, Dekeyne A, Rivet J-MM, Gobert A, Millan MJ. 2020. Comparative Pro-cognitive and Neurochemical Profiles of Glycine Modulatory Site Agonists and Glycine Reuptake Inhibitors in the Rat: Potential Relevance to Cognitive Dysfunction and Its Management [Internet]. [accessed 2020 May 11] 57(5):2144–2166. http://link.springer.com/10.1007/s12035-020-01875-9

Freeman WJ. 2007. Definitions of state variables and state space for brain-computer interface : Part 1. Multiple hierarchical levels of brain function. Cogn Neurodyn [Internet]. [accessed 2022 Mar 7] 1(1):3–14. https://doi.org/10.1007/S11571-006-9001-X

Fromer M, Pocklington AJ, Kavanagh DH, Williams HJ, Dwyer S, Gormley P, Georgieva L, Rees E, Palta P, Ruderfer DM, et al. 2014. De novo mutations in schizophrenia implicate synaptic networks. Nat 2014 5067487 [Internet]. [accessed 2022 Feb 8] 506(7487):179–184. https://doi.org/10.1038/nature12929

Funk M, Schuelert N, Jaeger S, Dorner-Ciossek C, Rosenbrock H, Mack V. 2020. Activation of

group II metabotropic receptors attenuates cortical E-I imbalance in a 15q13.3 microdeletion mouse model. bioRxiv [Internet]. [accessed 2022 Apr 5]:2020.09.17.301259. https://doi.org/10.1101/2020.09.17.301259

Fusar-Poli P, Politi P. 2008. Paul Eugen Bleuler and the birth of schizophrenia (1908). Am J Psychiatry [Internet]. [accessed 2022 Mar 16] 165(11):1407. https://doi.org/10.1176/APPI.AJP.2008.08050714

Galambos R. 1982. Tactile and auditory stimuli repeated at high rates (30-50 per sec) produce similar event related potentials. Ann N Y Acad Sci [Internet]. [accessed 2022 Mar 3] 388(1):722–726. https://doi.org/10.1111/J.1749-6632.1982.TB50841.X

Galambos R, Makeig S, Talmachoff PJ. 1981. A 40-Hz auditory potential recorded from the human scalp. Proc Natl Acad Sci [Internet]. [accessed 2020 May 14] 78(4):2643–2647. https://doi.org/10.1073/pnas.78.4.2643

García-Gutiérrez MS, Navarrete F, Sala F, Gasparyan A, Austrich-Olivares A, Manzanares J. 2020. Biomarkers in Psychiatry: Concept, Definition, Types and Relevance to the Clinical Reality. [place unknown]: Frontiers Media S.A.; [accessed 2021 Feb 25]. www.frontiersin.org

Gelder M, Andreasen N, Lopez-Ibor J, Geddes J, editors. 2012. New Oxford Textbook of Psychiatry. 2nd ed. [place unknown]: Oxford University Press. https://doi.org/10.1093/MED/9780199696758.001.0001

Ghiani A, Maniglia M, Battaglini L, Melcher D, Ronconi L. 2021. Binding Mechanisms in Visual Perception and Their Link With Neural Oscillations: A Review of Evidence From tACS. Front Psychol. 12:779. https://doi.org/10.3389/FPSYG.2021.643677/BIBTEX

Goff DC, Coyle JT. 2001. The emerging role of glutamate in the pathophysiology and treatment of schizophrenia. Am J Psychiatry [Internet]. [accessed 2022 Apr 5] 158(9):1367–1377. https://doi.org/10.1176/APPI.AJP.158.9.1367

Gonzalez-Burgos G, Cho RY, Lewis DA. 2015. Alterations in Cortical Network Oscillations and Parvalbumin Neurons in Schizophrenia. Biol Psychiatry [Internet]. [accessed 2022 Mar 17] 77(12):1031. https://doi.org/10.1016/J.BIOPSYCH.2015.03.010

Gonzalez-Burgos G, Lewis DA. 2008. GABA Neurons and the Mechanisms of Network Oscillations: Implications for Understanding Cortical Dysfunction in Schizophrenia. Schizophr Bull [Internet]. [accessed 2020 May 14] 34(5):944–961. https://doi.org/10.1093/schbul/sbn070

Gonzalez-Burgos G, Lewis DA. 2012. NMDA receptor hypofunction, parvalbumin-positive neurons, and cortical gamma oscillations in schizophrenia. Schizophr Bull [Internet]. [accessed 2020 Nov 22] 38(5):950–957. https://doi.org/10.1093/schbul/sbs010

Gottesman II, Gould TD. 2003. The endophenotype concept in psychiatry: etymology and strategic intentions. Am J Psychiatry [Internet]. [accessed 2022 Mar 29] 160(4):636–645. https://doi.org/10.1176/APPI.AJP.160.4.636

Gray CM, König P, Engel AK, Singer W. 1989. Oscillatory responses in cat visual cortex exhibit inter-columnar synchronization which reflects global stimulus properties. Nat 1989

3386213 [Internet]. [accessed 2022 Mar 6] 338(6213):334–337.
https://doi.org/10.1038/338334a0

Green MF, Plaza W. 2016. Impact of Cognitive and Social Cognitive Impairment on Functional
Outcomes in Patients With Schizophrenia. J Clin Psychiatry [Internet]. [accessed 2022 Feb
2] 77(suppl 2):8569. https://doi.org/10.4088/JCP.14074SU1C.02

Grent-'t-Jong T, Gajwani R, Gross J, Gumley A, Krishnadas R, Lawrie S, Schwannauer M,
Schultze-Lutter F, Uhlhaas P. 2021. 40-Hz Auditory Steady-State Responses Characterize
Circuit Dysfunctions and Predict Clinical Outcomes in Clinical High-Risk for Psychosis
Participants: A Magnetoencephalography Study. Biol Psychiatry [Internet]. [accessed 2021
Oct 11] 90(6):419–429. https://doi.org/10.1016/J.BIOPSYCH.2021.03.018

Griskova-Bulanova I, Griksiene R, Korostenskaja M, Ruksenas O. 2014. 40 Hz auditory steady-
state response in females: When is it better to entrain? Acta Neurobiol Exp [Internet].
74(1):91–97. https://pubmed.ncbi.nlm.nih.gov/24718047/#:~:text=The results suggest that
the,comparing patients and healthy subjects.

Gründer G, Cumming P. 2016. The Dopamine Hypothesis of Schizophrenia: Current Status. In:
Neurobiol Schizophr. [place unknown]: Academic Press; p. 109–124.
https://doi.org/10.1016/B978-0-12-801829-3.00015-X

Haaf M, Curic S, Steinmann S, Rauh J, Leicht G, Mulert C. 2022. Glycine attenuates
impairments of stimulus-evoked gamma oscillations in the ketamine model of
schizophrenia. Neuroimage. 251:119004.
https://doi.org/10.1016/J.NEUROIMAGE.2022.119004

Häfner H, Maurer K, Löffler W, An der Heiden W, Hambrecht M, Schultze-Lutter F. 2003.
Modeling the early course of schizophrenia. Schizophr Bull [Internet]. [accessed 2022 Feb
8] 29(2):325–340. https://doi.org/10.1093/OXFORDJOURNALS.SCHBUL.A007008

Haghighi SJ, Komeili M, Hatzinakos D, Beheiry H El. 2018. 40-Hz ASSR for Measuring Depth
of Anaesthesia During Induction Phase. IEEE J Biomed Heal informatics [Internet].
[accessed 2022 Mar 4] 22(6):1871–1882. https://doi.org/10.1109/JBHI.2017.2778140

Hakami T, Jones NC, Tolmacheva EA, Gaudias J, Chaumont J, Salzberg M, O'Brien TJ, Pinault
D. 2009. NMDA receptor hypofunction leads to generalized and persistent aberrant gamma
oscillations independent of hyperlocomotion and the state of consciousness. PLoS One
[Internet]. [accessed 2020 May 11] 4(8):e6755.
https://doi.org/10.1371/journal.pone.0006755

Hamm JP, Gilmore CS, Picchetti NAM, Sponheim SR, Clementz BA. 2011. Abnormalities of
Neuronal Oscillations and Temporal Integration to Low- and High-Frequency Auditory
Stimulation in Schizophrenia. Biol Psychiatry. 69(10):989–996.
https://doi.org/10.1016/j.biopsych.2010.11.021

Harrison PJ, Weinberger DR. 2005. Schizophrenia genes, gene expression, and neuropathology:
on the matter of their convergence. Mol Psychiatry [Internet]. [accessed 2022 Feb 6]
10(1):40–68. https://doi.org/10.1038/SJ.MP.4001558

Harvey PD, Koren D, Reichenberg A, Bowie CR. 2006. Negative Symptoms and Cognitive

Deficits: What Is the Nature of Their Relationship? Schizophr Bull [Internet]. [accessed 2022 Mar 17] 32(2):250–258. https://doi.org/10.1093/SCHBUL/SBJ011

Hasegawa H, Masuda N, Natori H, Shinohara Y, Ichida K. 2019. Pharmacokinetics and toxicokinetics of d-serine in rats. J Pharm Biomed Anal [Internet]. [accessed 2022 Jan 12] 162:264–271. https://doi.org/10.1016/J.JPBA.2018.09.026

Hashimoto T, Volk DW, Eggan SM, Mirnics K, Pierri JN, Sun Z, Sampson AR, Lewis DA. 2003. Gene Expression Deficits in a Subclass of GABA Neurons in the Prefrontal Cortex of Subjects with Schizophrenia. J Neurosci [Internet]. [accessed 2020 May 12] 23(15):6315–6326. https://doi.org/10.1523/JNEUROSCI.23-15-06315.2003

Heinrichs RW, Zakzanis KK. 1998. Neurocognitive deficit in schizophrenia: A quantitative review of the evidence. Neuropsychology. 12(3):426–445. https://doi.org/10.1037/0894-4105.12.3.426

Henssler J, Brandt L, Müller M, Liu S, Montag C, Sterzer P, Heinz A. 2020. Migration and schizophrenia: meta-analysis and explanatory framework. Eur Arch Psychiatry Clin Neurosci [Internet]. [accessed 2022 Apr 4] 270(3):325–335. https://doi.org/10.1007/S00406-019-01028-7

Homayoun H, Moghaddam B. 2007. NMDA Receptor Hypofunction Produces Opposite Effects on Prefrontal Cortex Interneurons and Pyramidal Neurons. J Neurosci [Internet]. [accessed 2020 May 11] 27(43):11496–11500. https://doi.org/10.1523/JNEUROSCI.2213-07.2007

Howard MW, Rizzuto DS, Caplan JB, Madsen JR, Lisman J, Aschenbrenner-Scheibe R, Schulze-Bonhage A, Kahana MJ. 2003. Gamma oscillations correlate with working memory load in humans. Cereb Cortex [Internet]. [accessed 2022 Mar 26] 13(12):1369–1374. https://doi.org/10.1093/CERCOR/BHG084

Hyman SE. 2013. Psychiatric Drug Development: Diagnosing a Crisis. Cerebrum Dana Forum Brain Sci [Internet]. [accessed 2022 Apr 2] 2013:5. /pmc/articles/PMC3662213/

Itil T, Keskiner A, Kiremitci N, Holden JM. 1967. Effect of phencyclidine in chronic schizophrenics. Can Psychiatr Assoc J [Internet]. [accessed 2022 May 7] 12(2):209–212. https://doi.org/10.1177/070674376701200217

Javitt DC. 2009. Sensory processing in schizophrenia: Neither simple nor intact. Schizophr Bull [Internet]. [accessed 2020 Nov 22] 35(6):1059–1064. https://doi.org/10.1093/schbul/sbp110

Javitt DC, Siegel SJ, Spencer KM, Mathalon DH, Hong LE, Martinez A, Ehlers CL, Abbas AI, Teichert T, Lakatos P, Womelsdorf T. 2020. A roadmap for development of neuro-oscillations as translational biomarkers for treatment development in neuropsychopharmacology. Neuropsychopharmacology [Internet]. [accessed 2021 Jan 19] 45(9):1411–1422. https://doi.org/10.1038/s41386-020-0697-9

Javitt DC, Sweet RA. 2015. Auditory dysfunction in schizophrenia: Integrating clinical and basic features. Nat Rev Neurosci [Internet]. [accessed 2020 Dec 7] 16(9):535–550. https://doi.org/10.1038/nrn4002

Javitt DC, Zukin SR. 1991. Recent advances in the phencyclidine model of schizophrenia. Am J Psychiatry [Internet]. [accessed 2022 Jan 11] 148(10):1301–1308.

https://doi.org/10.1176/AJP.148.10.1301

Jewett DL, Williston JS. 1971. Auditory-evoked far fields averaged from the scalp of humans. Brain [Internet]. [accessed 2022 Mar 3] 94(4):681–696. https://doi.org/10.1093/BRAIN/94.4.681

Jones C, Watson D, Fone K. 2011. Animal models of schizophrenia. Br J Pharmacol [Internet]. [accessed 2020 May 19] 164(4):1162. https://doi.org/10.1111/J.1476-5381.2011.01386.X

Kaar SJ, Angelescu I, Marques TR, Howes OD. 2019. Pre-frontal parvalbumin interneurons in schizophrenia: a meta-analysis of post-mortem studies. J Neural Transm [Internet]. [accessed 2022 Mar 2] 126(12):1637–1651. https://doi.org/10.1007/S00702-019-02080-2/FIGURES/3

Kahn RS, Keefe RSE. 2013. Schizophrenia is a cognitive illness: time for a change in focus. JAMA psychiatry [Internet]. [accessed 2022 Feb 2] 70(10):1107–1112. https://doi.org/10.1001/JAMAPSYCHIATRY.2013.155

Kapur S, Arenovich T, Agid O, Zipursky R, Lindborg S, Jones B. 2005. Evidence for onset of antipsychotic effects within the first 24 hours of treatment. Am J Psychiatry [Internet]. [accessed 2022 Jan 12] 162(5):939–946. https://doi.org/10.1176/APPI.AJP.162.5.939

Kapur S, Wadenberg ML, Remington G. 2000. Are animal studies of antipsychotics appropriately dosed? Lessons from the bedside to the bench. Can J Psychiatry [Internet]. [accessed 2022 Apr 2] 45(3):241–246. https://doi.org/10.1177/070674370004500302

Karch S, Leicht G, Giegling I, Lutz J, Kunz J, Buselmeier M, Hey P, Spörl A, Jäger L, Meindl T, et al. 2009. Inefficient neural activity in patients with schizophrenia and nonpsychotic relatives of schizophrenic patients: Evidence from a working memory task. J Psychiatr Res. 43(15):1185–1194. https://doi.org/10.1016/j.jpsychires.2009.04.004

Keavy D, Bristow LJ, Sivarao D V., Batchelder M, King D, Thangathirupathy S, Macor JE, Weed MR. 2016. The qEEG Signature of Selective NMDA NR2B Negative Allosteric Modulators; A Potential Translational Biomarker for Drug Development. PLoS One [Internet]. [accessed 2022 Mar 7] 11(4). https://doi.org/10.1371/JOURNAL.PONE.0152729

Keil J, Romero YR, Balz J, Henjes M, Senkowski D. 2016. Positive and negative symptoms in schizophrenia relate to distinct oscillatory signatures of sensory gating. Front Hum Neurosci. 10(MAR2016):104. https://doi.org/10.3389/FNHUM.2016.00104/BIBTEX

Khuwaja GA, Haghighi SJ, Hatzinakos D. 2015. 40-Hz ASSR fusion classification system for observing sleep patterns. EURASIP J Bioinform Syst Biol [Internet]. [accessed 2022 Mar 4] 2015(1):1–12. https://doi.org/10.1186/S13637-014-0021-2

Kim SW, Cho T, Lee S. 2015. Phospholipase C-β1 hypofunction in the pathogenesis of schizophrenia. Front Psychiatry. 6(NOV):159. https://doi.org/10.3389/FPSYT.2015.00159/BIBTEX

Kirov G, Pocklington AJ, Holmans P, Ivanov D, Ikeda M, Ruderfer D, Moran J, Chambert K, Toncheva D, Georgieva L, et al. 2011. De novo CNV analysis implicates specific abnormalities of postsynaptic signalling complexes in the pathogenesis of schizophrenia. Mol Psychiatry 2012 172 [Internet]. [accessed 2022 Feb 8] 17(2):142–153.

https://doi.org/10.1038/mp.2011.154

Koenig T, van Swam C, Dierks T, Hubl D. 2012. Is gamma band EEG synchronization reduced during auditory driving in schizophrenia patients with auditory verbal hallucinations? Schizophr Res. 141(2–3):266–270. https://doi.org/10.1016/J.SCHRES.2012.07.016

Kostrzewa RM, Nowak P, Brus R, Brown RW. 2016. Perinatal Treatments with the Dopamine D_2-Receptor Agonist Quinpirole Produces Permanent D_2-Receptor Supersensitization: a Model of Schizophrenia. Neurochem Res [Internet]. [accessed 2022 Mar 23] 41(1–2):183–192. https://doi.org/10.1007/S11064-015-1757-0

Kraepelin E. 1899. Psychiatrie: ein Lehrbuch für Studirende und Aertze [Psychiatry: A Textbook for Students and Doctors]. 6th ed. Leipzig: JA Barth.

Kraus N, Özdamar Ö, Hier D, Stein L. 1982. Auditory middle latency responses (MLRs) in patients with cortical lesions. Electroencephalogr Clin Neurophysiol [Internet]. [accessed 2022 Mar 3] 54(3):275–287. https://doi.org/10.1016/0013-4694(82)90177-8

Kristiansen L V, Huerta I, Beneyto M, Meador-Woodruff JH. 2007. NMDA receptors and schizophrenia. Curr Opin Pharmacol [Internet]. [accessed 2020 May 11] 7(1):48–55. https://doi.org/10.1016/j.coph.2006.08.013

Krystal JH, Karper LP, Seibyl JP, Freeman GK, Delaney R, Bremner JD, Heninger GR, Bowers MB, Charney DS. 1994. Subanesthetic Effects of the Noncompetitive NMDA Antagonist, Ketamine, in Humans: Psychotomimetic, Perceptual, Cognitive, and Neuroendocrine Responses. Arch Gen Psychiatry [Internet]. [accessed 2021 Oct 8] 51(3):199–214. https://doi.org/10.1001/ARCHPSYC.1994.03950030035004

Lahti RA, Roberts RC, Conley RR, Cochrane E V., Mutin A, Tamminga CA. 1996. D2-type dopamine receptors in postmortem human brain sections from normal and schizophrenic subjects. Neuroreport [Internet]. [accessed 2022 Feb 7] 7(12):1945–1948. https://doi.org/10.1097/00001756-199608120-00016

LE L, R K, B M, MJ G. 2020. Risk of schizophrenia in relatives of individuals affected by schizophrenia: A meta-analysis. Psychiatry Res [Internet]. [accessed 2022 Feb 4] 286. https://doi.org/10.1016/J.PSYCHRES.2020.112852

Leonhardt BL, Vohs JL, Bartolomeo LA, Visco A, Hetrick WP, Bolbecker AR, Breier A, Lysaker PH, O'Donnell BF. 2020. Relationship of Metacognition and Insight to Neural Synchronization and Cognitive Function in Early Phase Psychosis. Clin EEG Neurosci [Internet]. [accessed 2022 Mar 6] 51(4):259–266. https://doi.org/10.1177/1550059419857971

Lewis DA, Hashimoto T, Volk DW. 2005. Cortical inhibitory neurons and schizophrenia. Nat Rev Neurosci 2005 64 [Internet]. [accessed 2022 Mar 16] 6(4):312–324. https://doi.org/10.1038/nrn1648

Lewis DA, Levitt P. 2002. Schizophrenia as a disorder of neurodevelopment. Annu Rev Neurosci [Internet]. [accessed 2022 Feb 2] 25:409–441. https://doi.org/10.1146/annurev.neuro.25.112701.142754

Lewis DA, Moghaddam B. 2006. Cognitive dysfunction in schizophrenia: convergence of

gamma-aminobutyric acid and glutamate alterations. Arch Neurol [Internet]. [accessed 2020 May 11] 63(10):1372–6. https://doi.org/10.1001/archneur.63.10.1372

Light GA, Hsu JL, Hsieh MH, Meyer-Gomes K, Sprock J, Swerdlow NR, Braff DL. 2006. Gamma Band Oscillations Reveal Neural Network Cortical Coherence Dysfunction in Schizophrenia Patients. 60(11):1231–1240. https://doi.org/10.1016/j.biopsych.2006.03.055

Light GA, Joshi YB, Molina JL, Bhakta SG, Nungaray JA, Cardoso L, Kotz JE, Thomas ML, Swerdlow NR. 2020. Neurophysiological biomarkers for schizophrenia therapeutics. Biomarkers in Neuropsychiatry. 2:100012.

Lim AL, Taylor DA, Malone DT. 2012. Consequences of early life MK-801 administration: long-term behavioural effects and relevance to schizophrenia research. Behav Brain Res [Internet]. [accessed 2022 Mar 26] 227(1):276–286. https://doi.org/10.1016/J.BBR.2011.10.052

Lodge DJ, Grace AA. 2011. Hippocampal dysregulation of dopamine system function and the pathophysiology of schizophrenia. Trends Pharmacol Sci [Internet]. [accessed 2022 Feb 7] 32(9):507–513. https://doi.org/10.1016/J.TIPS.2011.05.001

Lu Y, Truccolo W, Wagner FB, Vargas-Irwin CE, Ozden I, Zimmermann JB, May T, Agha NS, Wang J, Nurmikko A V. 2015. Optogenetically induced spatiotemporal gamma oscillations and neuronal spiking activity in primate motor cortex. J Neurophysiol [Internet]. [accessed 2022 Mar 17] 113(10):3574–3587. https://doi.org/10.1152/JN.00792.2014

Luby ED, Cohen BD, Rosenbaum G, Gottlieb JS, Kelley R. 1959. Study of a New Schizophrenomimetic Drug—Sernyl. AMA Arch Neurol Psychiatry [Internet]. [accessed 2022 Feb 8] 81(3):363–369. https://doi.org/10.1001/ARCHNEURPSYC.1959.02340150095011

Lum JS, Millard SJ, Huang XF, Ooi L, Newell KA. 2018. A postmortem analysis of NMDA ionotropic and group 1 metabotropic glutamate receptors in the nucleus accumbens in schizophrenia. J Psychiatry Neurosci [Internet]. [accessed 2022 Feb 8] 43(2):102. https://doi.org/10.1503/JPN.170077

Lütkenhöner B, Patterson RD. 2015. Disruption of the auditory response to a regular click train by a single, extra click. Exp brain Res [Internet]. [accessed 2022 Mar 3] 233(6):1875–1892. https://doi.org/10.1007/S00221-015-4260-6

Mann EO, Mody I. 2009. Control of hippocampal gamma oscillation frequency by tonic inhibition and excitation of interneurons. Nat Neurosci 2009 132 [Internet]. [accessed 2022 Mar 17] 13(2):205–212. https://doi.org/10.1038/nn.2464

Marcotte ER, Pearson DM, Srivastava LK. 2001. Animal models of schizophrenia: a critical review. J Psychiatry Neurosci [Internet]. [accessed 2022 Mar 7] 26(5):395. /pmc/articles/PMC167198/

Marković D, Brodersen RW, Nanda R, Karkare V. 2012. Time-Frequency Analysis: FFT and Wavelets. In: DSP Archit Des Essentials [Internet]. [place unknown]: Springer, Boston, MA; [accessed 2022 Mar 28]; p. 145–170. https://doi.org/10.1007/978-1-4419-9660-2_8

Mascio A, Stewart R, Botelle R, Williams M, Mirza L, Patel R, Pollak T, Dobson R, Roberts A.

2021. Cognitive Impairments in Schizophrenia: A Study in a Large Clinical Sample Using Natural Language Processing. Front Digit Heal. 0:82. https://doi.org/10.3389/FDGTH.2021.711941

Matsui T, Sekiguchi M, Hashimoto A, Tomita U, Nishikawa T, Wada K. 1995. Functional Comparison of d-Serine and Glycine in Rodents: The Effect on Cloned NMDA Receptors and the Extracellular Concentration. J Neurochem [Internet]. [accessed 2022 Apr 5] 65(1):454–458. https://doi.org/10.1046/J.1471-4159.1995.65010454.X

McCleery A, Nuechterlein KH. 2019. Cognitive impairment in psychotic illness: prevalence, profile of impairment,developmental course, and treatment considerations. Dialogues Clin Neurosci [Internet]. [accessed 2022 Feb 2] 21(3):239. https://doi.org/10.31887/DCNS.2019.21.3/AMCCLEERY

McCutcheon RA, Krystal JH, Howes OD. 2020. Dopamine and glutamate in schizophrenia: biology, symptoms and treatment. World Psychiatry [Internet]. [accessed 2020 May 11] 19(1):15–33. https://doi.org/10.1002/wps.20693

McFadden D, Hsieh MD, Garcia-Sierra A, Champlin CA. 2010. Differences by Sex, Ear, and Sexual Orientation in the Time Intervals between Successive Peaks in Auditory Evoked Potentials. Hear Res [Internet]. [accessed 2022 Apr 5] 270(1–2):56. https://doi.org/10.1016/J.HEARES.2010.09.008

McGee T, Kraus N, Comperatore C, Nicol T. 1991. Subcortical and cortical components of the MLR generating system. Brain Res. 544(2):211–220. https://doi.org/10.1016/0006-8993(91)90056-2

Melcher JR. 2009. Auditory Evoked Potentials. Encycl Neurosci.:715–719. https://doi.org/10.1016/B978-008045046-9.00260-6

Melynyte S, Pipinis E, Genyte V, Voicikas A, Rihs T, Griskova-Bulanova I. 2018. 40 Hz Auditory Steady-State Response: The Impact of Handedness and Gender. Brain Topogr [Internet]. [accessed 2022 Apr 5] 31(3):419–429. https://doi.org/10.1007/S10548-017-0611-X

Minzenberg MJ, Firl AJ, Yoon JH, Gomes GC, Reinking C, Carter CS. 2010. Gamma Oscillatory Power is Impaired During Cognitive Control Independent of Medication Status in First-Episode Schizophrenia. Neuropsychopharmacol 2010 3513 [Internet]. [accessed 2022 Mar 2] 35(13):2590–2599. https://doi.org/10.1038/npp.2010.150

Miyamoto S, Miyake N, Jarskog LF, Fleischhacker WW, Lieberman JA. 2012. Pharmacological treatment of schizophrenia: a critical review of the pharmacology and clinical effects of current and future therapeutic agents. Mol Psychiatry 2012 1712 [Internet]. [accessed 2022 Feb 2] 17(12):1206–1227. https://doi.org/10.1038/mp.2012.47

Molina JL, Thomas ML, Joshi YB, Hochberger WC, Koshiyama D, Nungaray JA, Cardoso L, Sprock J, Braff DL, Swerdlow NR, Light GA. 2020. Gamma oscillations predict pro-cognitive and clinical response to auditory-based cognitive training in schizophrenia. Transl Psychiatry [Internet]. [accessed 2021 Jan 10] 10(1):1–10. https://doi.org/10.1038/s41398-020-01089-6

Moore JK. 1987. The human auditory brain stem as a generator of auditory evoked potentials. Hear Res. 29(1):33–43. https://doi.org/10.1016/0378-5955(87)90203-6

Moskowitz A, Heim G. 2011. Eugen Bleuler's Dementia Praecox or the Group of Schizophrenias (1911): A Centenary Appreciation and Reconsideration. Schizophr Bull [Internet]. [accessed 2022 Feb 1] 37(3):471. https://doi.org/10.1093/SCHBUL/SBR016

Murphy BP, Chung YC, Park TW, McGorry PD. 2006. Pharmacological treatment of primary negative symptoms in schizophrenia: a systematic review. Schizophr Res [Internet]. [accessed 2022 Feb 9] 88(1–3):5–25. https://doi.org/10.1016/J.SCHRES.2006.07.002

Muscat R, Willner P. 1989. Effects of dopamine receptor antagonists on sucrose consumption and preference. Psychopharmacology (Berl) [Internet]. [accessed 2022 Apr 5] 99(1):98–102. https://doi.org/10.1007/BF00634461

Nestler EJ, Hyman SE. 2010. Animal models of neuropsychiatric disorders. Nat Neurosci [Internet]. [accessed 2022 Apr 2] 13(10):1161–1169. https://doi.org/10.1038/NN.2647

Niemelä S, Sourander A, Surcel HM, Hinkka-Yli-Salomäki S, McKeague IW, Cheslack-Postava K, Brown AS. 2016. Prenatal nicotine exposure and risk of schizophrenia among offspring in a national birth cohort. Am J Psychiatry [Internet]. [accessed 2022 Mar 28] 173(8):799–806. https://doi.org/10.1176/APPI.AJP.2016.15060800/ASSET/IMAGES/LARGE/APPI.AJP.2016.15060800F1.JPEG

Nordström AL, Farde L, Halldin C. 1992. Time course of D2-dopamine receptor occupancy examined by PET after single oral doses of haloperidol. Psychopharmacol 1992 1064 [Internet]. [accessed 2022 Apr 2] 106(4):433–438. https://doi.org/10.1007/BF02244811

Nucifora FC, Mihaljevic M, Lee BJ, Sawa A. 2017. Clozapine as a Model for Antipsychotic Development. Neurotherapeutics [Internet]. [accessed 2022 Apr 2] 14(3):750–761. https://doi.org/10.1007/S13311-017-0552-9

Ochoa S, Usall J, Cobo J, Labad X, Kulkarni J. 2012. Gender Differences in Schizophrenia and First-Episode Psychosis: A Comprehensive Literature Review. Schizophr Res Treatment. 2012:1–9. https://doi.org/10.1155/2012/916198

Olney JW, Farber NB. 1995. Glutamate receptor dysfunction and schizophrenia. Arch Gen Psychiatry [Internet]. [accessed 2022 Apr 5] 52(12):998–1007. https://doi.org/10.1001/ARCHPSYC.1995.03950240016004

van Os J, Kapur S. 2009. Schizophrenia. Lancet. 374(9690):635–645. https://doi.org/10.1016/S0140-6736(09)60995-8

Özdamar Ö, Kraus N. 1983. Auditory middle-latency responses in humans. Int J Audiol [Internet]. [accessed 2022 Mar 3] 22(1):34–49. https://doi.org/10.3109/00206098309072768

Pascual-Marqui RD, Michel CM, Lehmann D. 1994. Low resolution electromagnetic tomography: a new method for localizing electrical activity in the brain. Int J Psychophysiol. 18(1):49–65. https://doi.org/10.1016/0167-8760(84)90014-X

Patel NH, Vyas NS, Puri BK, Nijran KS, Al-Nahhas A. 2010. Positron emission tomography in

schizophrenia: a new perspective. J Nucl Med [Internet]. [accessed 2022 Feb 7] 51(4):511–520. https://doi.org/10.2967/JNUMED.109.066076

Perez-Costas E, Melendez-Ferro M, Roberts RC. 2010. Basal ganglia pathology in schizophrenia: dopamine connections and anomalies. J Neurochem [Internet]. [accessed 2022 Feb 7] 113(2):287–302. https://doi.org/10.1111/J.1471-4159.2010.06604.X

Picton T. 2013. Hearing in time: evoked potential studies of temporal processing. Ear Hear [Internet]. [accessed 2022 Mar 4] 34(4):385–401. https://doi.org/10.1097/AUD.0B013E31827ADA02

Pinault D. 2008. N-methyl d-aspartate receptor antagonists ketamine and MK-801 induce wake-related aberrant gamma oscillations in the rat neocortex. Biol Psychiatry [Internet]. [accessed 2020 May 11] 63(8):730–5. https://doi.org/10.1016/j.biopsych.2007.10.006

Plataki ME, Diskos K, Sougklakos C, Velissariou M, Georgilis A, Stavroulaki V, Sidiropoulou K. 2021. Effect of Neonatal Treatment With the NMDA Receptor Antagonist, MK-801, During Different Temporal Windows of Postnatal Period in Adult Prefrontal Cortical and Hippocampal Function. Front Behav Neurosci. 15:111. https://doi.org/10.3389/FNBEH.2021.689193/BIBTEX

Plourde G, Baribeau J, Bonhomme V. 1997. Ketamine increases the amplitude of the 40-Hz auditory steady-state response in humans. Br J Anaesth [Internet]. [accessed 2020 May 12] 78(5):524–529. https://doi.org/10.1093/bja/78.5.524

Ponton C, Eggermont JJ, Khosla D, Kwong B, Don M. 2002. Maturation of human central auditory system activity: separating auditory evoked potentials by dipole source modeling. Clin Neurophysiol. 113(3):407–420. https://doi.org/10.1016/S1388-2457(01)00733-7

Popovic D, Schmitt A, Kaurani L, Senner F, Papiol S, Malchow B, Fischer A, Schulze TG, Koutsouleris N, Falkai P. 2019. Childhood Trauma in Schizophrenia: Current Findings and Research Perspectives. Front Neurosci [Internet]. [accessed 2022 Mar 28] 13. https://doi.org/10.3389/FNINS.2019.00274

Powell CM, Miyakawa T. 2006. Schizophrenia-relevant behavioral testing in rodent models: a uniquely human disorder? Biol Psychiatry [Internet]. [accessed 2022 Feb 9] 59(12):1198–1207. https://doi.org/10.1016/J.BIOPSYCH.2006.05.008

Prado-Gutierrez P, Martínez-Montes E, Weinstein A, Zañartu M. 2019. Estimation of auditory steady-state responses based on the averaging of independent EEG epochs. PLoS One [Internet]. [accessed 2022 Mar 7] 14(1). https://doi.org/10.1371/JOURNAL.PONE.0206018

Presacco A, Bohórquez J, Yavuz E, Özdamar Ö. 2010. Auditory steady-state responses to 40-Hz click trains: Relationship to middle latency, gamma band and beta band responses studied with deconvolution. Clin Neurophysiol. 121(9):1540–1550. https://doi.org/10.1016/J.CLINPH.2010.03.020

Puvvada KC, Summerfelt A, Du X, Krishna N, Kochunov P, Rowland LM, Simon JZ, Hong LE. 2018. Delta Vs Gamma Auditory Steady State Synchrony in Schizophrenia. Schizophr Bull [Internet]. [accessed 2020 May 12] 44(2):378–387. https://doi.org/10.1093/schbul/sbx078

Quiquempoix M, Fayad SL, Boutourlinsky K, Leresche N, Lambert RC, Bessaih T. 2018. Layer

2/3 Pyramidal Neurons Control the Gain of Cortical Output. Cell Rep [Internet]. [accessed 2022 Apr 2] 24(11):2799-2807.e4. https://doi.org/10.1016/J.CELREP.2018.08.038

Rass O, Forsyth JK, Krishnan GP, Hetrick WP, Klaunig MJ, Breier A, O'Donnell BF, Brenner CA. 2012. Auditory steady state response in the schizophrenia, first-degree relatives, and schizotypal personality disorder. Schizophr Res. 136(1–3):143–149. https://doi.org/10.1016/J.SCHRES.2012.01.003

Raza MU, Sivarao D V. 2021. Test-retest reliability of tone- and 40 Hz train-evoked gamma oscillations in female rats and their sensitivity to low-dose NMDA channel blockade. Psychopharmacol 2021 2388 [Internet]. [accessed 2021 Sep 22] 238(8):2325–2334. https://doi.org/10.1007/S00213-021-05856-1

Regan D. 1989. Human Brain Electrophysiology: Evoked Potentials and Evoked Magnetic Fields in Science and Medicine. New York: Elsevier.

van der Reijden CS, Mens LHM, Snik AFM. 2004. Signal-to-noise ratios of the auditory steady-state response from fifty-five EEG derivations in adults. J Am Acad Audiol [Internet]. [accessed 2022 Mar 7] 15(10):692–701. https://doi.org/10.3766/JAAA.15.10.4

Reynolds GP, Beasley CL, Zhang ZJ. 2002. Understanding the neurotransmitter pathology of schizophrenia: selective deficits of subtypes of cortical GABAergic neurons. J Neural Transm 2002 1095 [Internet]. [accessed 2022 Mar 2] 109(5):881–889. https://doi.org/10.1007/S007020200072

Robbins TW, Arnsten AFT. 2009. The Neuropsychopharmacology of Fronto-Executive Function: Monoaminergic Modulation. Annu Rev Neurosci [Internet]. [accessed 2022 Feb 7] 32:267. https://doi.org/10.1146/ANNUREV.NEURO.051508.135535

Roelfsema PR, Engel AK, König P, Singer W. 1997. Visuomotor integration is associated with zero time-lag synchronization among cortical areas. Nat 1997 3856612 [Internet]. [accessed 2022 Feb 9] 385(6612):157–161. https://doi.org/10.1038/385157a0

Ropper AH, Marder SR, Cannon TD. 2019. Schizophrenia.Ropper AH, editor. N Engl J Med [Internet]. [accessed 2022 Feb 2] 381(18):1753–1761. https://doi.org/10.1056/NEJMRA1808803

Ross B, Herdman AT, Pantev C. 2005. Stimulus induced desynchronization of human auditory 40-Hz steady-state responses. J Neurophysiol [Internet]. [accessed 2022 Mar 3] 94(6):4082–4093. https://doi.org/10.1152/JN.00469.2005/ASSET/IMAGES/LARGE/Z9K0120551020007.JPEG

Salkind N. 2010. Encyclopedia of Research Design. 2455 Teller Road, Thousand Oaks California 91320 United States: SAGE Publications, Inc.; [accessed 2021 Jan 10]. https://doi.org/10.4135/9781412961288

Sams-Dodd F. 1998. A Test of the Predictive Validity of Animal Models of Schizophrenia Based on Phencyclidine and D-Amphetamine. Neuropsychopharmacology. 18(4):293–304. https://doi.org/10.1016/S0893-133X(97)00161-9

Scheydt S, Müller Staub M, Frauenfelder F, Nielsen GH, Behrens J, Needham I. 2017. Sensory

overload: A concept analysis. Int J Ment Health Nurs [Internet]. [accessed 2022 Apr 2] 26(2):110–120. https://doi.org/10.1111/INM.12303

Schwartz TL, Sachdeva S, Stahl SM. 2012. Glutamate neurocircuitry: Theoretical underpinnings in: Schizophrenia. Front Pharmacol. 3 NOV:195. https://doi.org/10.3389/FPHAR.2012.00195/BIBTEX

Seeman P, Corbettand R, Van Tol HHM. 1997. Atypical neuroleptics have low affinity for dopamine D2 receptors or are selective for D4 receptors [Internet]. [accessed 2022 Feb 7] 16(2):93–110. https://doi.org/10.1016/S0893-133X(96)00187-X

Seeman P, Kapur S. 2000. Schizophrenia: More dopamine, more D2 receptors. Proc Natl Acad Sci [Internet]. [accessed 2022 Feb 7] 97(14):7673–7675. https://doi.org/10.1073/PNAS.97.14.7673

Seeman P, Lee T, Chau-Wong M, Wong K. 1976. Antipsychotic drug doses and neuroleptic/dopamine receptors. Nat 1976 2615562 [Internet]. [accessed 2022 Feb 8] 261(5562):717–719. https://doi.org/10.1038/261717a0

Shin YW, O'Donnell BF, Youn S, Kwon JS. 2011. Gamma Oscillation in Schizophrenia. Psychiatry Investig [Internet]. [accessed 2022 Mar 2] 8(4):288. https://doi.org/10.4306/PI.2011.8.4.288

Singer W, Gray CM. 1995. Visual feature integration and the temporal correlation hypothesis. Rev Neurosci [Internet]. [accessed 2022 Mar 6] 18:555–561. www.annualreviews.org

Singh F, Shu IW, Hsu SH, Link P, Pineda JA, Granholm E. 2020. Modulation of frontal gamma oscillations improves working memory in schizophrenia. NeuroImage Clin. 27:102339. https://doi.org/10.1016/J.NICL.2020.102339

Sivarao D V., Chen P, Senapati A, Yang Y, Fernandes A, Benitex Y, Whiterock V, Li Y-WW, Ahlijanian MK. 2016. 40 Hz Auditory Steady-State Response Is a Pharmacodynamic Biomarker for Cortical NMDA Receptors. Neuropsychopharmacology [Internet]. [accessed 2020 May 12] 41(9):2232. https://doi.org/10.1038/NPP.2016.17

Sivarao D V., Chen P, Yang Y, Li YW, Pieschl R, Ahlijanian K. MK. 2014. NR2B antagonist CP-101,606 abolishes pitch-mediated deviance detection in awake rats. Front Psychiatry [Internet]. [accessed 2021 Feb 27] 5(AUG):96. https://doi.org/10.3389/fpsyt.2014.00096

Sivarao D V., Frenkel M, Chen P, Healy FL, Lodge NJ, Zaczek R. 2013. MK-801 disrupts and nicotine augments 40 Hz auditory steady state responses in the auditory cortex of the urethane-anesthetized rat. Neuropharmacology [Internet]. [accessed 2020 May 12] 73:1–9. https://doi.org/10.1016/j.neuropharm.2013.05.006

Skoe E, Kraus N. 2010. Auditory brainstem response to complex sounds: a tutorial. Ear Hear [Internet]. [accessed 2022 Apr 2] 31(3):302. https://doi.org/10.1097/AUD.0B013E3181CDB272

Slattery DA, Cryan JF. 2014. The Ups and Downs of Modelling Mood Disorders in Rodents. ILAR J [Internet]. [accessed 2022 Mar 23] 55(2):297–309. https://doi.org/10.1093/ILAR/ILU026

Snyder SH. 1980. Phencyclidine. Nature [Internet]. [accessed 2022 Feb 8] 285(5764):355–356. https://doi.org/10.1038/285355A0

Sohal VS, Zhang F, Yizhar O, Deisseroth K, Zhang F, Deisseroth K, Tsai L, Moore C. 2009. Parvalbumin neurons and gamma rhythms enhance cortical circuit performance. Nature [Internet]. [accessed 2020 May 11] 459(7247):698–702. https://doi.org/10.1038/nature07991

Sørensen HJ, Mortensen EL, Reinisch JM, Mednick SA. 2009. Parental psychiatric hospitalisation and offspring schizophrenia. World J Biol Psychiatry [Internet]. [accessed 2022 Feb 8] 10(4 Pt 2):571–575. https://doi.org/10.1080/15622970701472078

Sörnmo L, Laguna P. 2005. Bioelectrical Signal Processing in Cardiac and Neurological Applications. Bioelectrical Signal Process Card Neurol Appl. https://doi.org/10.1016/B978-0-12-437552-9.X5000-4

Spellman TJ, Gordon JA. 2015. Synchrony in schizophrenia: A window into circuit-level pathophysiology. Curr Opin Neurobiol [Internet]. [accessed 2020 Dec 7] 30:17–23. https://doi.org/10.1016/j.conb.2014.08.009

Spencer KM, Nestor PG, Niznikiewicz MA, Salisbury DF, Shenton ME, McCarley RW. 2003. Abnormal Neural Synchrony in Schizophrenia. J Neurosci [Internet]. [accessed 2021 Oct 7] 23(19):7407–7411. https://doi.org/10.1523/JNEUROSCI.23-19-07407.2003

Spencer KM, Niznikiewicz MA, Nestor PG, Shenton ME, McCarley RW. 2009. Left auditory cortex gamma synchronization and auditory hallucination symptoms in schizophrenia. BMC Neurosci [Internet]. [accessed 2020 May 12] 10(1):85. https://doi.org/10.1186/1471-2202-10-85

Spencer KM, Niznikiewicz MA, Shenton ME, McCarley RW. 2008. Sensory-Evoked Gamma Oscillations in Chronic Schizophrenia. Biol Psychiatry. 63(8):744–747. https://doi.org/10.1016/J.BIOPSYCH.2007.10.017

Srinivasan R. 1999. Methods to Improve the Spatial Resolution of EEG. Int J Bioelectromagn [Internet]. [accessed 2022 Feb 9] 1(1):102–111. www.tut.fi/ijbem/

Stapellst DR, Linden D, Suffield JB, Hamel G, Picton TW. 1984. Human auditory steady state potentials. Ear Hear [Internet]. [accessed 2022 Mar 3] 5(2):105–113. https://doi.org/10.1097/00003446-198403000-00009

Steeds H, Carhart-Harris RL, Stone JM. 2015. Drug models of schizophrenia. Ther Adv Psychopharmacol [Internet]. [accessed 2022 Feb 9] 5(1):43. https://doi.org/10.1177/2045125314557797

Subramanyam M, Goyal J. 2016. Translational biomarkers: from discovery and development to clinical practice. Drug Discov Today Technol. 21–22:3–10. https://doi.org/10.1016/J.DDTEC.2016.10.001

Sullivan PF, Kendler KS, Neale MC. 2003. Schizophrenia as a Complex Trait: Evidence From a Meta-analysis of Twin Studies. Arch Gen Psychiatry [Internet]. [accessed 2022 Feb 4] 60(12):1187–1192. https://doi.org/10.1001/ARCHPSYC.60.12.1187

Sun C, Zhou P, Wang Changming, Fan Y, Tian Q, Dong F, Zhou F, Wang Chuanyue. 2018. Defects of Gamma Oscillations in Auditory Steady-State Evoked Potential of Schizophrenia. Shanghai Arch Psychiatry [Internet]. [accessed 2022 Mar 6] 30(1):27. https://doi.org/10.11919/J.ISSN.1002-0829.217078

Suzuki T, Kobayashi K, Umegaki Y. 1994. Effect of natural sleep on auditory steady state responses in adult subjects with normal hearing. Audiology [Internet]. [accessed 2022 Mar 3] 33(5):274–279. https://doi.org/10.3109/00206099409071887

Swerdlow NR, Geyer MA. 1993. Clozapine and haloperidol in an animal model of sensorimotor gating deficits in schizophrenia. Pharmacol Biochem Behav. 44(3):741–744. https://doi.org/10.1016/0091-3057(93)90193-W

Swerdlow NR, Geyer MA, Braff DL. 2001. Neural circuit regulation of prepulse inhibition of startle in the rat: current knowledge and future challenges. Psychopharmacology (Berl) [Internet]. [accessed 2022 Mar 29] 156(2–3):194–215. https://doi.org/10.1007/S002130100799

Swerdlow NR, Weber M, Qu Y, Light GA, Braff DL. 2008. Realistic expectations of prepulse inhibition in translational models for schizophrenia research. Psychopharmacology (Berl) [Internet]. [accessed 2022 Mar 29] 199(3):331. https://doi.org/10.1007/S00213-008-1072-4

Tada M, Nagai T, Kirihara K, Koike S, Suga M, Araki T, Kobayashi T, Kasai K. 2016. Differential Alterations of Auditory Gamma Oscillatory Responses Between Pre-Onset High-Risk Individuals and First-Episode Schizophrenia. Cereb Cortex [Internet]. [accessed 2022 Mar 6] 26(3):1027–1035. https://doi.org/10.1093/CERCOR/BHU278

Tallon-Baudry C. 1999. Oscillatory gamma activity in humans and its role in object representation. Trends Cogn Sci [Internet]. [accessed 2020 May 20] 3(4):151–162. https://doi.org/10.1016/S1364-6613(99)01299-1

Tandon R, Nasrallah HA, Keshavan MS. 2009. Schizophrenia, "just the facts" 4. Clinical features and conceptualization. Schizophr Res [Internet]. [accessed 2022 Feb 9] 110(1–3):1–23. https://doi.org/10.1016/J.SCHRES.2009.03.005

Tandon R, Nasrallah HA, Keshavan MS. 2010. Schizophrenia, "just the facts" 5. Treatment and prevention. Past, present, and future. Schizophr Res [Internet]. [accessed 2022 Feb 9] 122(1–3):1–23. https://doi.org/10.1016/J.SCHRES.2010.05.025

Teale P, Carlson J, Rojas D, Reite M. 2003. Reduced laterality of the source locations for generators of the auditory steady-state field in schizophrenia. Biol Psychiatry [Internet]. [accessed 2022 Mar 6] 54(11):1149–1153. https://doi.org/10.1016/S0006-3223(03)00411-6

Thuné H, Recasens M, Uhlhaas PJ. 2016. The 40-Hz Auditory Steady-State Response in Patients With Schizophrenia: A Meta-analysis. JAMA Psychiatry [Internet]. [accessed 2022 Feb 10] 73(11):1145–1153. https://doi.org/10.1001/JAMAPSYCHIATRY.2016.2619

Thut G, Schyns PG, Gross J. 2011. Entrainment of perceptually relevant brain oscillations by non-invasive rhythmic stimulation of the human brain. Front Psychol. 2(JUL):170. https://doi.org/10.3389/FPSYG.2011.00170/BIBTEX

Tremblay R, Lee S, Rudy B. 2016. GABAergic Interneurons in the Neocortex: From Cellular

Properties to Circuits. Neuron. https://doi.org/10.1016/j.neuron.2016.06.033

Tripathi A, Kar SK, Shukla R. 2018. Cognitive deficits in schizophrenia: Understanding the biological correlates and remediation strategies. Clin Psychopharmacol Neurosci. 16(1):7–17. https://doi.org/10.9758/CPN.2018.16.1.7

Üçok A, Direk N, Koyuncu A, Keskin-Ergen Y, Yüksel Ç, Güler J, Karadayi G, Akturan E, Devrim-Üçok M. 2013. Cognitive deficits in clinical and familial high risk groups for psychosis are common as in first episode schizophrenia. Schizophr Res. 151(1–3):265–269. https://doi.org/10.1016/J.SCHRES.2013.10.030

Umbricht D, Vyssotky D, Latanov A, Nitsch R, Brambilla R, D'Adamo P, Lipp HP. 2004. Midlatency auditory event-related potentials in mice: comparison to midlatency auditory ERPs in humans. Brain Res. 1019(1–2):189–200. https://doi.org/10.1016/J.BRAINRES.2004.05.097

Varese F, Smeets F, Drukker M, Lieverse R, Lataster T, Viechtbauer W, Read J, Van Os J, Bentall RP. 2012. Childhood Adversities Increase the Risk of Psychosis: A Meta-analysis of Patient-Control, Prospective- and Cross-sectional Cohort Studies. Schizophr Bull [Internet]. [accessed 2022 Apr 4] 38(4):661–671. https://doi.org/10.1093/SCHBUL/SBS050

Wahbeh MH, Avramopoulos D. 2021. Gene-Environment Interactions in Schizophrenia: A Literature Review. Genes 2021, Vol 12, Page 1850 [Internet]. [accessed 2022 Feb 2] 12(12):1850. https://doi.org/10.3390/GENES12121850

Wainberg M, Jacobs GR, di Forti M, Tripathy SJ. 2021. Cannabis, schizophrenia genetic risk, and psychotic experiences: a cross-sectional study of 109,308 participants from the UK Biobank. Transl Psychiatry 2021 111 [Internet]. [accessed 2022 Apr 4] 11(1):1–9. https://doi.org/10.1038/s41398-021-01330-w

Wang XJ, Buzsáki G. 1996. Gamma Oscillation by Synaptic Inhibition in a Hippocampal Interneuronal Network Model. J Neurosci [Internet]. [accessed 2022 Mar 23] 16(20):6402–6413. https://doi.org/10.1523/JNEUROSCI.16-20-06402.1996

Weickert CS, Fung SJ, Catts VS, Schofield PR, Allen KM, Moore LT, Newell KA, Pellen D, Huang XF, Catts S V., Weickert TW. 2012. Molecular evidence of N-methyl-D-aspartate receptor hypofunction in schizophrenia. Mol Psychiatry 2012 1811 [Internet]. [accessed 2022 Feb 8] 18(11):1185–1192. https://doi.org/10.1038/mp.2012.137

Weickert CS, Weickert TW, Pillai A, Buckley PF. 2013. Biomarkers in Schizophrenia: A Brief Conceptual Consideration. Dis Markers [Internet]. [accessed 2022 Feb 2] 35(1):3. https://doi.org/10.1155/2013/510402

Welle CG, Contreras D. 2016. Sensory-driven and spontaneous gamma oscillations engage distinctcortical circuitry. J Neurophysiol [Internet]. [accessed 2021 Oct 7] 115(4):1821. https://doi.org/10.1152/JN.00137.2015

Whittington MA, Traub RD, Jefferys JGR. 1995. Synchronized oscillations in interneuron networks driven by metabotropic glutamate receptor activation. Nature [Internet]. [accessed 2022 Mar 2] 373(6515):612–615. https://doi.org/10.1038/373612A0

Woo TU, Miller JL, Lewis DA. 2006. Schizophrenia and the parvalbumin-containing class of

cortical local circuit neurons. https://doi.org/101176/ajp15471013 [Internet]. [accessed 2022 Mar 2] 154(7):1013–1015. https://doi.org/10.1176/AJP.154.7.1013

Yamashita T, Vavladeli A, Pala A, Galan K, Crochet S, Petersen SSA, Petersen CCH. 2018. Diverse long-range axonal projections of excitatory layer 2/3 neurons in mouse barrel cortex. Front Neuroanat. 12:33. https://doi.org/10.3389/FNANA.2018.00033/BIBTEX

Yang AC, Tsai SJ. 2017. New Targets for Schizophrenia Treatment beyond the Dopamine Hypothesis. Int J Mol Sci [Internet]. [accessed 2022 Feb 8] 18(8). https://doi.org/10.3390/IJMS18081689

Yang Z, Lee SH, Abdul Rashid NA, See YM, Dauwels J, Tan BL, Lee J. 2021. Predicting Real-World Functioning in Schizophrenia: The Relative Contributions of Neurocognition, Functional Capacity, and Negative Symptoms. Front Psychiatry. 12:219. https://doi.org/10.3389/FPSYT.2021.639536/BIBTEX

Yizhar O, Fenno LE, Prigge M, Schneider F, Davidson TJ, Ogshea DJ, Sohal VS, Goshen I, Finkelstein J, Paz JT, et al. 2011. Neocortical excitation/inhibition balance in information processing and social dysfunction. Nat 2011 4777363 [Internet]. [accessed 2022 Mar 2] 477(7363):171–178. https://doi.org/10.1038/nature10360

Yokota Y, Naruse Y. 2015. Phase coherence of auditory steady-state response reflects the amount of cognitive workload in a modified N-back task. Neurosci Res. 100:39–45. https://doi.org/10.1016/J.NEURES.2015.06.010

Yoon JH, Minzenberg MJ, Raouf S, D'Esposito M, Carter CS. 2013. Impaired Prefrontal-Basal Ganglia Functional Connectivity and Substantia Nigra Hyperactivity in Schizophrenia. Biol Psychiatry [Internet]. [accessed 2022 Feb 7] 74(2):122–129. https://doi.org/10.1016/J.BIOPSYCH.2012.11.018

Young A, Cornejo J, Spinner A. 2022. Auditory Brainstem Response. [place unknown]: StatPearls Publishing; [accessed 2022 Mar 3]. https://www.ncbi.nlm.nih.gov/books/NBK564321/

Zhou T-H, Mueller NE, Spencer KM, Mallya SG, Lewandowski KE, Norris LA, Levy DL, Cohen BM, Öngür D, Hall M-H. 2018. Auditory steady state response deficits are associated with symptom severity and poor functioning in patients with psychotic disorder. Schizophr Res. 201:278–286. https://doi.org/10.1016/j.schres.2018.05.027

Zorumski CF, Izumi Y, Mennerick S. 2016. Ketamine: NMDA Receptors and Beyond. J Neurosci [Internet]. [accessed 2022 Feb 8] 36(44):11158. https://doi.org/10.1523/JNEUROSCI.1547-16.2016
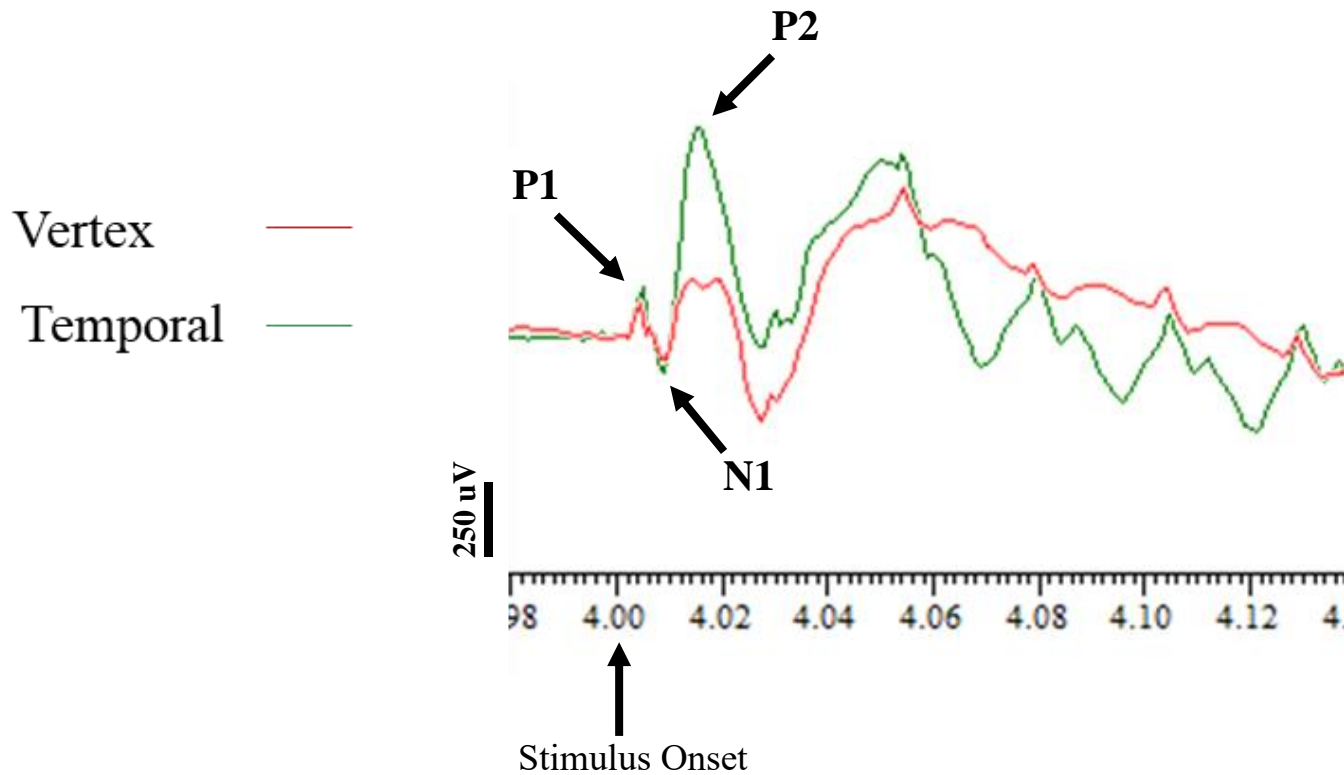
Appendix A: Supplementary Figure 1

Line plots showing the mean RMS-amplitude value for tone-evoked response (left panel) and 40 Hz ASSR (right panel) for each animal, across six sessions (N=12). Notice a greater variability in tone-evoked gamma vs. 40 Hz ASSR.
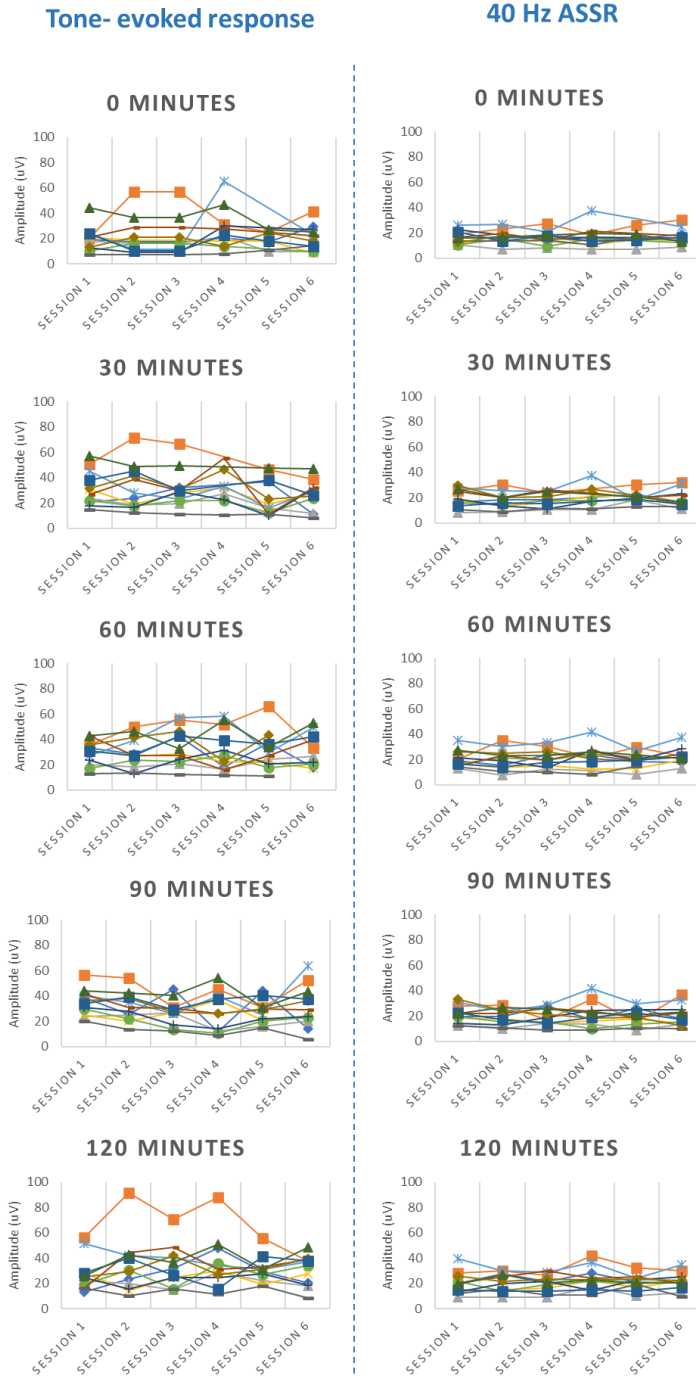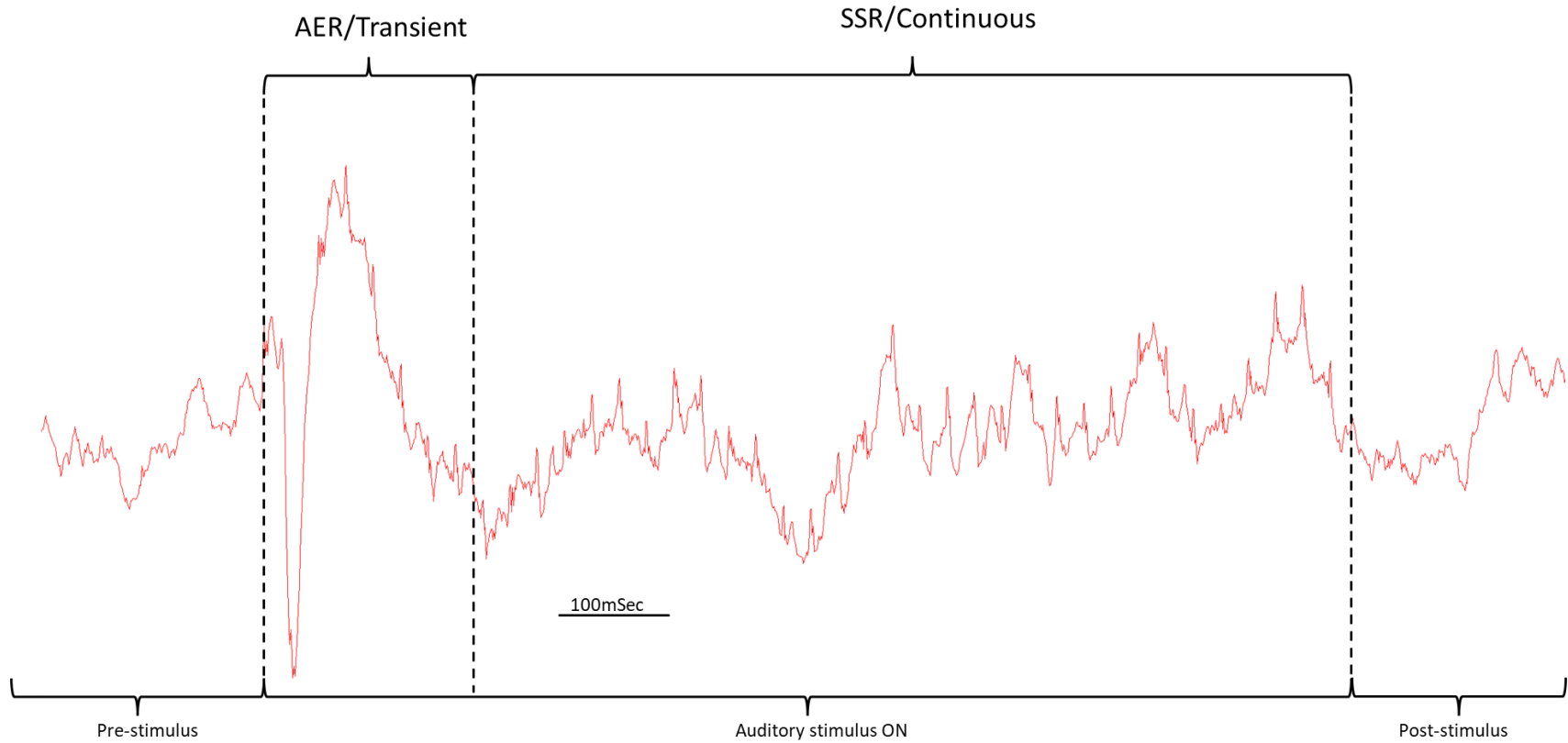
Appendix B: Supplementary Figure 2

Comparison of latencies for P1, N1, and P2 in unfiltered 40 Hz ASSR recordings from vertex and temporal regions. The waveforms depict a grand average of 12 rats. Both vertex and temporal ERP responses show similar latencies for P1, N1 and P2, as shown below, indicating that they may represent two parallel rather than serial sources.

Appendix C: Supplementary Figure 3

Breakdown of averaged 40 Hz click train-evoked response into AER (auditory-evoked response), and an SSR (steady-state response).

AER/Transient

SSR/Continuous

100mSec

Pre-stimulus

Auditory stimulus ON

Post-stimulus

Narrow band filtered (35-45 Hz) overlay of 40 Hz ASSR averages from 10 rats from the frontal lead, after vehicle or 5 mg/kg clozapine treatment. Left panel shows random/asynchronous activity during a 200 msec period (boxed) in vehicle group, whereas the clozapine group shows robust and early onset entrainment. Inset demonstrates the same at an enhanced temporal resolution. This neurophysiological evidence for clozapine-mediated phase resetting is unprecedented in literature.
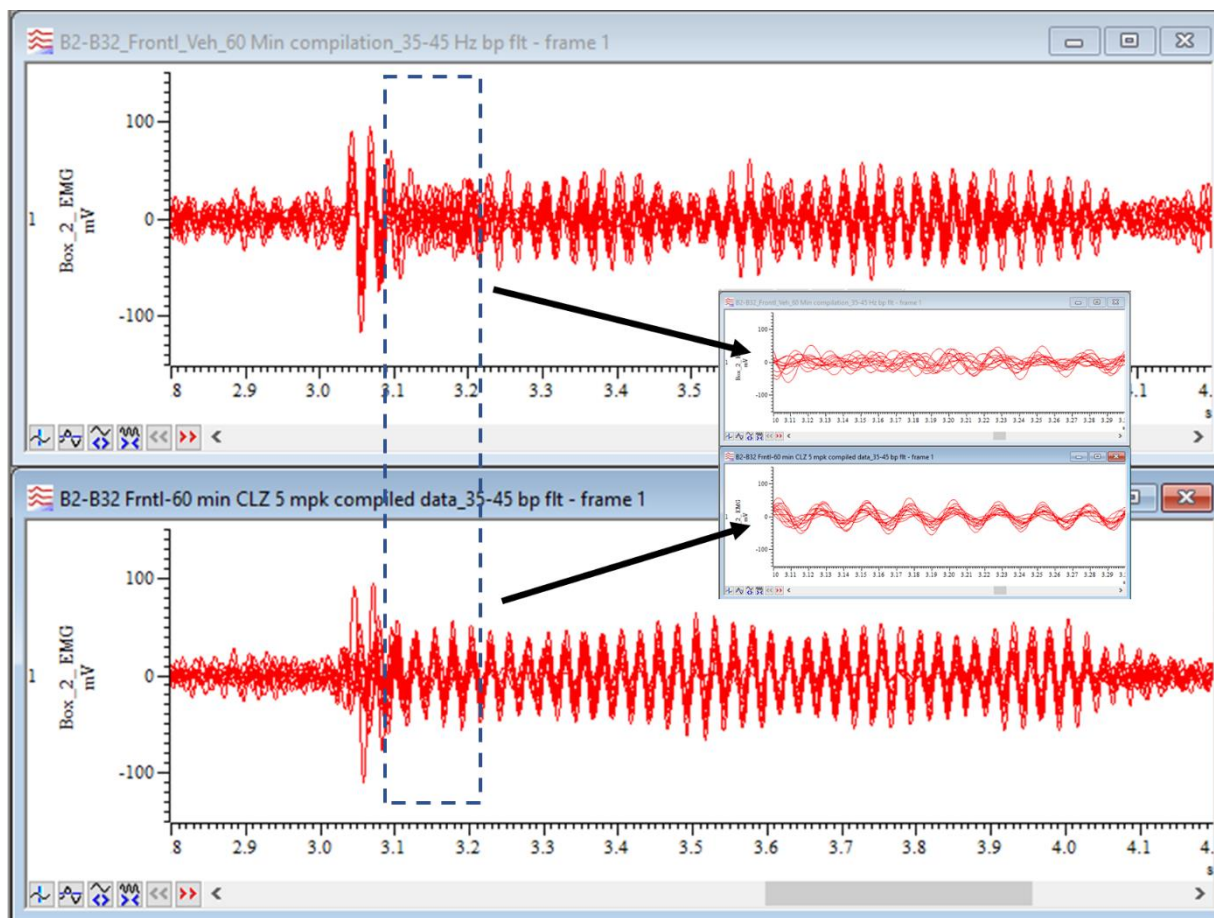
VITA

MUHAMMAD UMMEAR RAZA

Education:	PhD (Biomedical Sciences); Concentration (Pharmacology) East Tennessee State University, Johnson City, Tennessee, 2022
	M.Phil. (Human Genetics); Concentration (Genetic epidemiology) Quaid-I- Azam University, Islamabad 2014
Professional Experience:	Graduate Research Assistant, Biomedical Sciences PhD program, James H. Quillen College of Medicine, Bill Gatton College of Pharmacy, East Tennessee State University, Tennessee, 2017-2022
	Visiting Research Scholar, James H. Quillen College of Medicine, East Tennessee State University, Tennessee, 2015-2017
Publications:	Raza, M. U., Rorie, D., Sivarao, D. V. Clozapine dose-dependently improves 40 Hz auditory steady-state response and protects against MK-801-induced disruption in female rats, while haloperidol shows no effect. (In progress)

Raza, M. U., and Sivarao, D. V. (2021). Test-retest reliability of tone- and 40 Hz train-evoked gamma oscillations in female rats and their sensitivity to low-dose NMDA channel blockade. Psychopharmacology, doi.org/10.1007/s00213 021-05856-1

Cui, K., Yang, F., Tufan, T., Raza, M. U., Zhan, Y., Fan, Y., Zeng, F., Brown, R. W., Price, J. B., Jones, T. C., Miller, G. W., and Zhu, M. Y. (2021). Restoration of Noradrenergic Function in Parkinson's Disease Model Mice. ASN neuro, 13, doi.org/10.1177/17590914211009730

Zhan, Y., Raza M.U.*, Yuan L., Zhu M.Y., (2019). Critical role of oxidatively damaged DNA in selective noradrenergic vulnerability, Neuroscience, 422,184-201.

doi.org/10.1016/j.neuroscience.2019.09.036

Zhu, M.Y., Raza, M.U., Zhan, Y., Fan, Y., (2019). Norepinephrine upregulates the expression of tyrosine hydroxylase and protects dopaminergic neurons against 6-hydrodopamine toxicity, Neurochem. Intern. 131: 104549. doi.org/10.1016/j.neuint.2019.104549

Fan, Y., Chen, P., Raza, M.U., Szebeni, A., Szebeni, K., Ordway, G. A., Zhu, M.-Y. (2018). Altered expression of phox2 transcription factors in the locus coeruleus in major depressive disorder mimicked by chronic stress and corticosterone treatment in vivo and in vitro. Neuroscience, 393, 123–137. doi.org/10.1016/J.NEUROSCIENCE.2018.09.038

Zhang, J., Fan, Y., Raza, M.U., Zhan, Y., Du, X.D., Patel, P.D., Zhu, M.Y. (2017). The regulation of corticosteroid receptors in response to chronic social defeat. Neurochem. Intern. doi.org/10.1016/j.neuint.2017.05.021

Raza, M.U., Tufan, T., Wang, Y., Hill, C., Zhu, M.-Y. (2016). DNA damage in major psychiatric diseases, Neurotox. Res., 30: 251. doi:10.1007/s12640-016-9621-9

Deng, M., Tufan, T., Raza, M.U., Jones, T.C., Zhu, M.-Y. (2016). MicroRNAs 29b and 181a down regulate the expression of the norepinephrine transporter and glucocorticoid receptors in PC12 cells. J. Neurochem., 139: 197–207. doi:10.1111/jnc.13761

Honors and Awards: Dissertation research award ($1000), East Tennessee State University. (2021)